# USE OF SIMULATED STRONG GROUND MOTION RECORDS IN EARTHQUAKE ENGINEERING APPLICATIONS

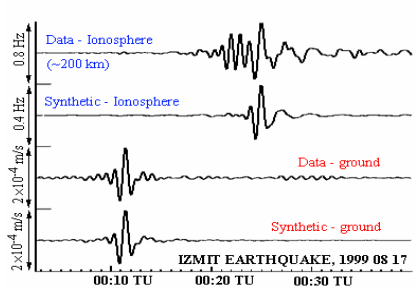


Dr. Shaghayegh Karimzadeh Naghshineh
(Postdoctoral researcher at METU)

**Ph.D. Supervisor:** Prof. Dr. Ayşegül Askan Gündoğan

**October 6, 2017 D-Learning**

# Outline

- Introduction, Problem statement and objectives
- Ground motion simulation methodology
- Part 1: Use of simulated records for seismic loss estimation: A case study for Erzincan (Turkey)
- Part 2: Application of simulated records in nonlinear time history analysis of MDOF structures
  - First case study: The 1999 Duzce Earthquake (Mw=7.1)
  - Second case study: The 2009 L'Aquila Earthquake (Mw=6.3)
- Part 3: Distribution of seismic intensity maps (MMI) for the eastern part of the NAFZ (Turkey) using simulated records
- Summary and what is next?

# Introduction, Problem statement and objectives

- Full time histories are required for engineering purposes like seismic design and analysis of special structures (e.g.: tall buildings, dams, bridges etc), fragility analysis and vulnerability assessment.

- Use of nonlinear time history analysis, which requires full time series of ground acceleration, is common tool to assess the post-elastic dynamic response of a structure.

- In regions with sparse ground motion data, and also events with long return periods: simulations provide alternative acceleration time series

- One important task is to investigate the ability of using simulated records for estimation of structural demands in earthquake engineering practice.

Three main issues (by Seismo. Soc. of Amer. 1906):

1. the physical earthquake event itself (when, where, how)
2. the associated ground motions
3. the effect on the structures

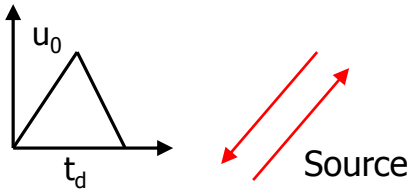


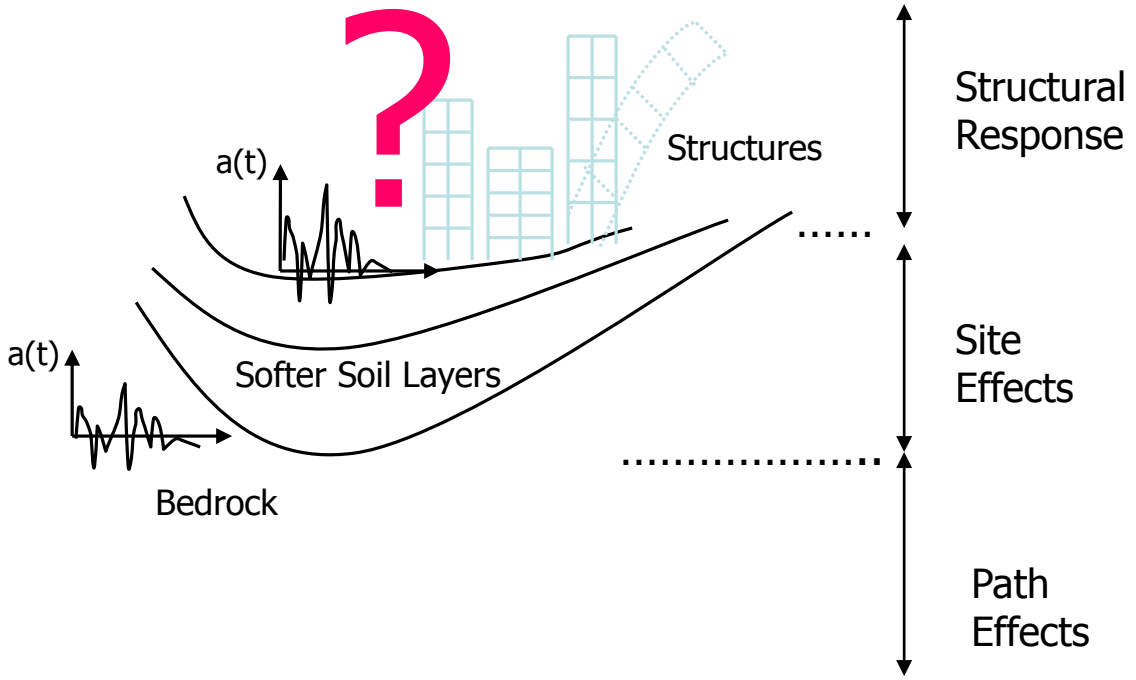

**The objective is to investigate the efficiency of simulated ground motions for earthquake engineering purposes**

To fulfill this objective:

Different approaches :

1. Seismic loss estimation using simulated records for a case study: Comparison against the results with real records
1. Prediction of the dynamic responses of detailed MDOF models for different case studies: Comparison against the results with real records
2. Distribution of seismic intensity maps based on simulated records: Comparison against the results with real records

# Ground motion simulation methodology

## Objective of Ground Motion Simulations (in General):

- To generate realistic ground motions in regions of sparse or no networks
- To study regional parameters through simulations

## Methods Existing in the Literature:

- Deterministic Methods: Numerical Solutions of Seismic Wave Propagation, Green's functions
- Stochastic Methods: Point Source and Finite Fault
- Hybrid methods

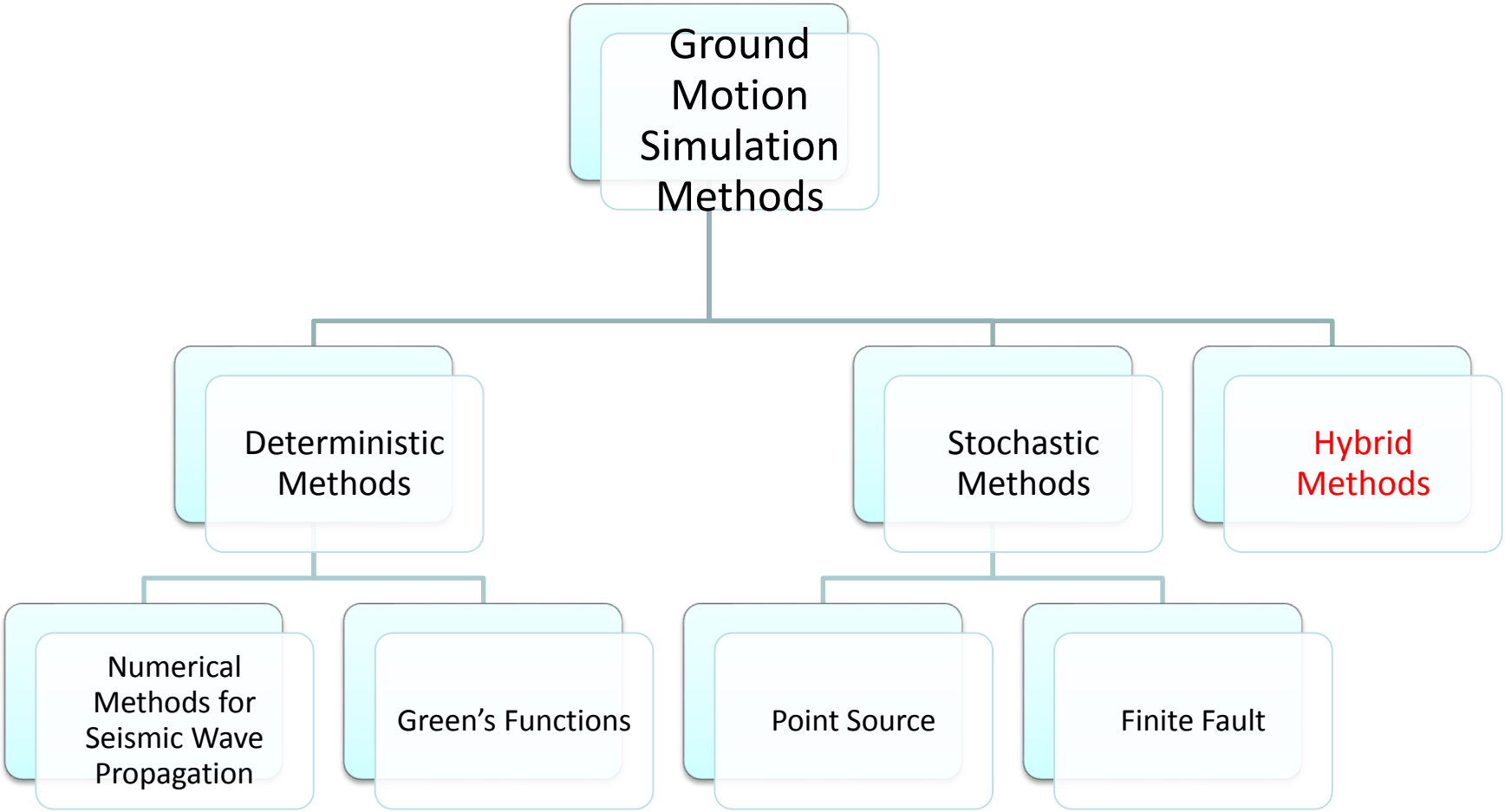
Ground Motion Simulation Methods
Deterministic Methods
Stochastic Methods
Hybrid Methods
Numerical Methods for Seismic Wave Propagation
Green's Functions
Point Source
Finite Fault

# Stochastic Point-Source Modeling

## (Descriptions by Atkinson et al., 2009, BSSA and Boore, 2003)

The shear wave amplitude spectrum in frequency domain is the product of filter functions representing the source, propagation and site effects.

$$\mathrm{Acc}(M_0, R, f) = \mathrm{Source}(M_0, f)\mathrm{Path}(R, f)\mathrm{Site}(f)$$

- The stochastic point-source model assumes that the earthquake source is concentrated at a point.
- Acceleration time series generated at a site carry both deterministic and random aspects of ground-motion shaking.

# Finite-Fault Source Models

Figure is adapted from Hisada, 2008, Journal of Seismology

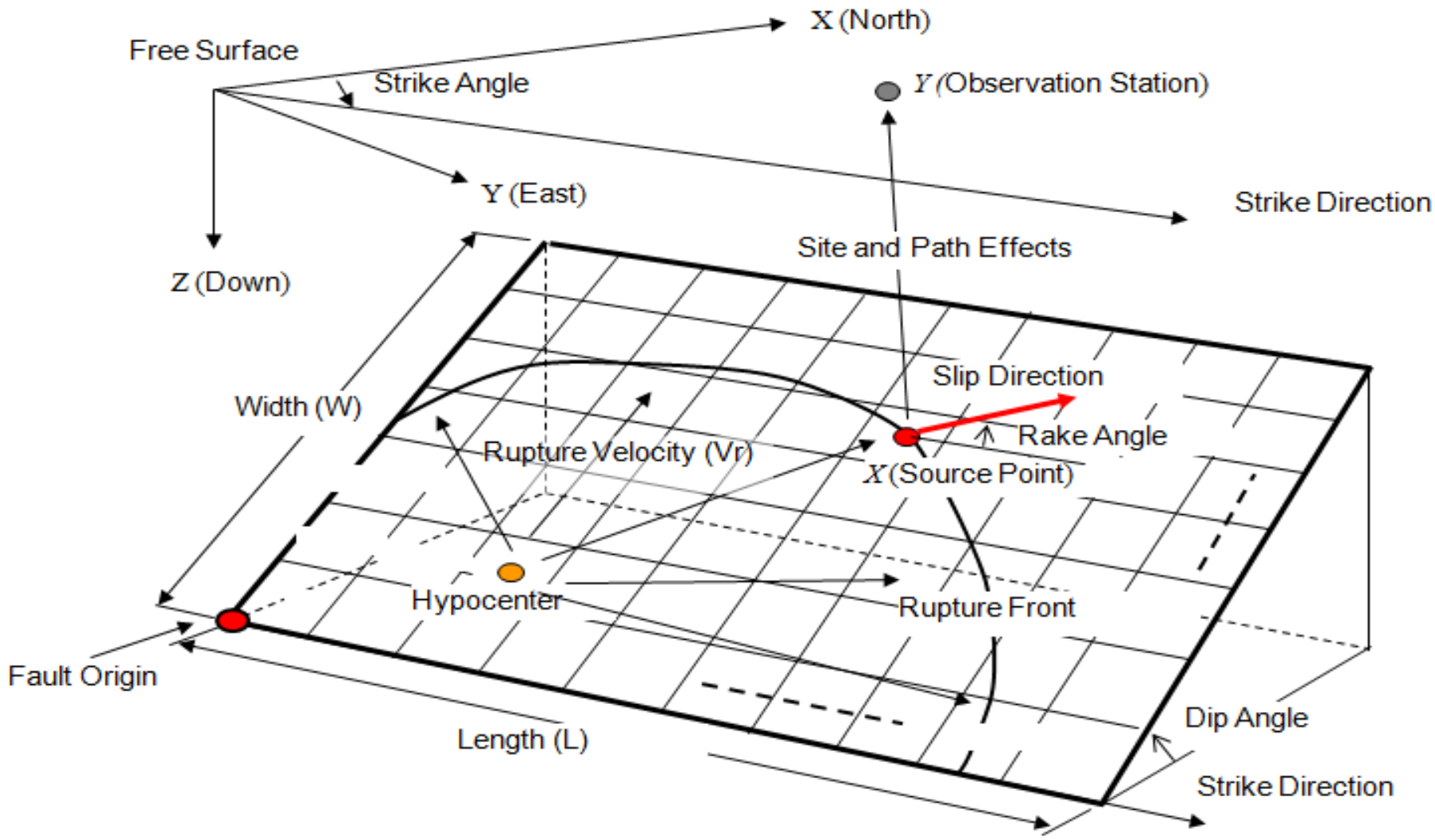

# Stochastic finite-fault (SFF) methodology using Exsim program

(Introduced by Motazedian and Atkinson, 2005)

- Fault is assumed to be a finite rectangular plane and divided into subfaults
- Each subfault
- Each subfault is assumed to be a point source with an $\omega^2$ spectrum
- Ground motions from each subfault are summed with a time delay in order to obtain the ground motion acceleration from the entire fault as rupture starts from the hypocenter

$$a(t) = \sum_{i=1}^{nl} \sum_{j=1}^{nw} a_{ij}\,(t + \Delta t_{ij})$$

- Corner frequency of the ij$^{th}$ subfault at any time is a function of the total number of ruptured subfaults at that time

# Part 1:

# Use of simulated records for seismic loss estimation: A case study for Erzincan (Turkey)

# Objective

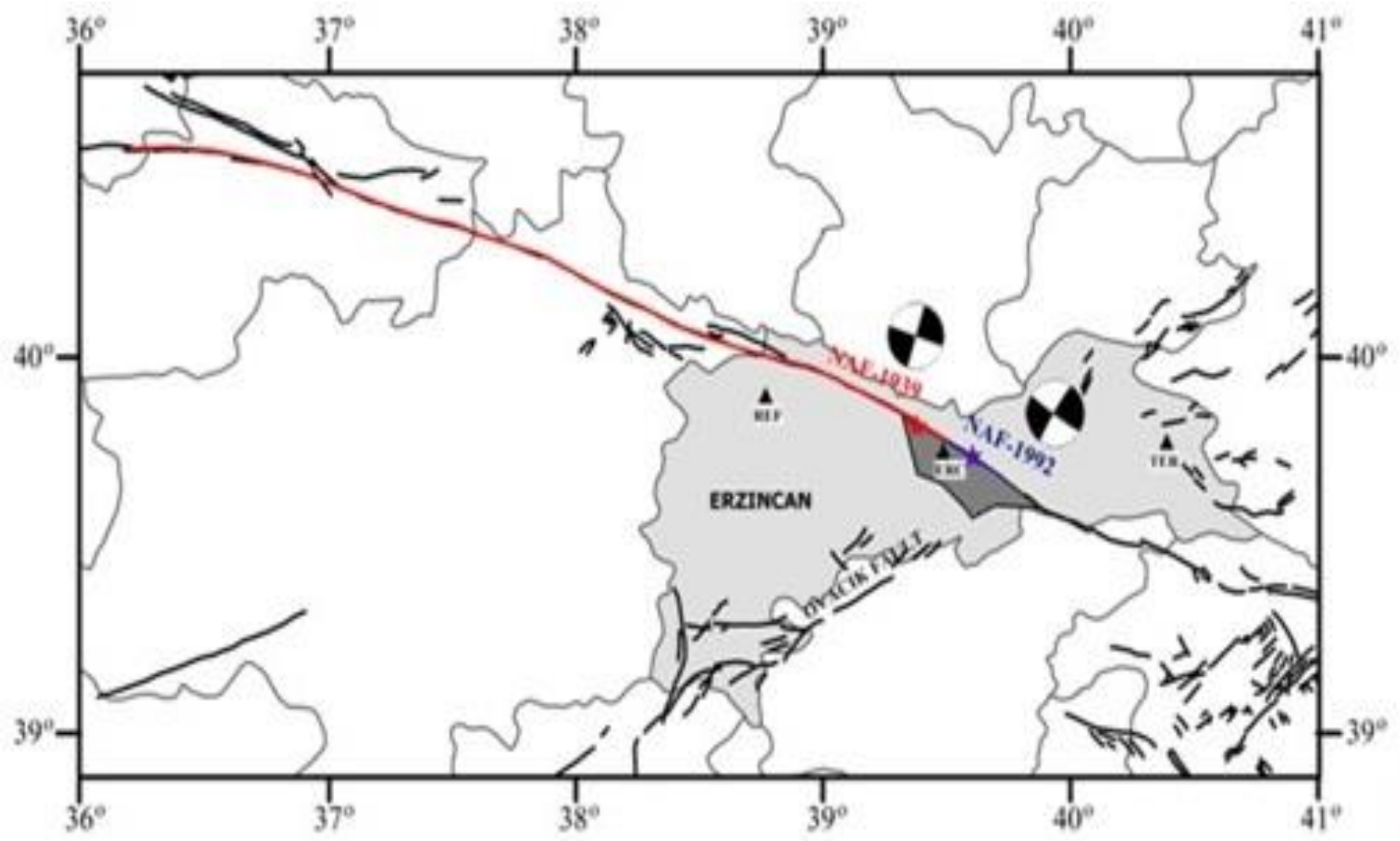

**What are the main steps:**

- Ground motion simulations
- Classification of local building stock
- Selection of regional ground motion database
- Generation of fragility curves using simulated GMs
- Estimation of damage
- Results and main findings

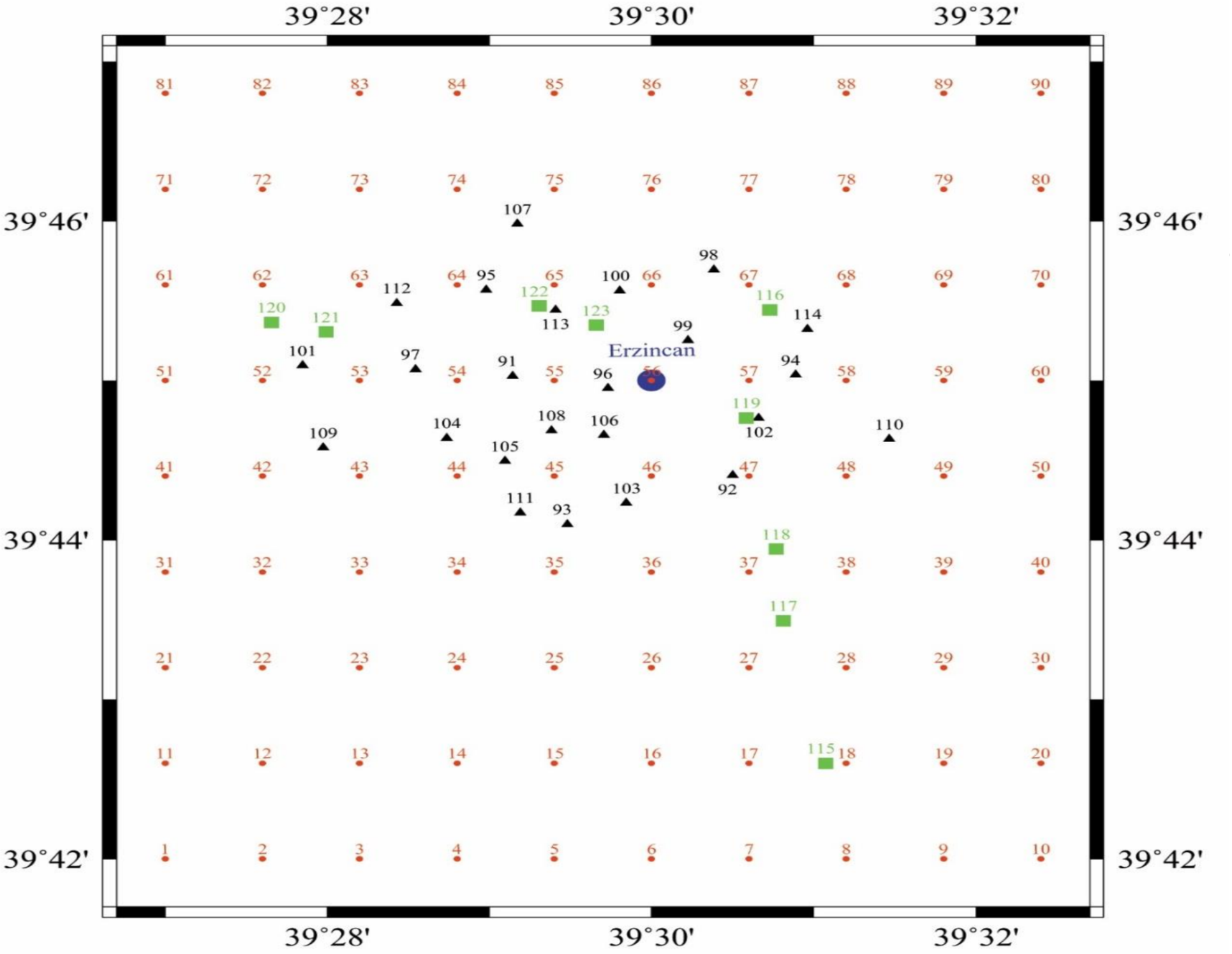
39°28'
39°30'
39°32'
39°46'
39°44'
39°42'
Erzincan
81 82 83 84 85 86 87 88 89 90
71 72 73 74 75 76 77 78 79 80
61 62 63 64 65 66 67 68 69 70
51 52 53 54 55 56 57 58 59 60
41 42 43 44 45 46 47 48 49 50
31 32 33 34 35 36 37 38 39 40
21 22 23 24 25 26 27 28 29 30
11 12 13 14 15 16 17 18 19 20
1 2 3 4 5 6 7 8 9 10
107
98
95
100
112
122
116
120
121
123
114
113
99
101
97
91
94
96
119
108
106
110
104
109
102
105
92
103
111
93
118
117
115

# Spatial distribution of the simulated (a) PGA, (b) PGV values of the 1992 Erzincan earthquake

(a)

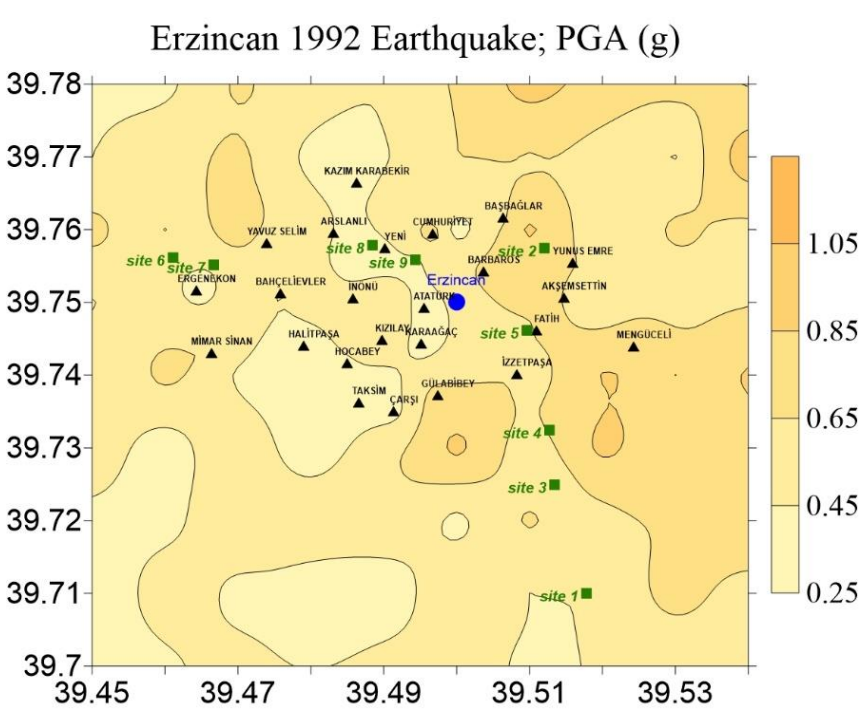


(b)

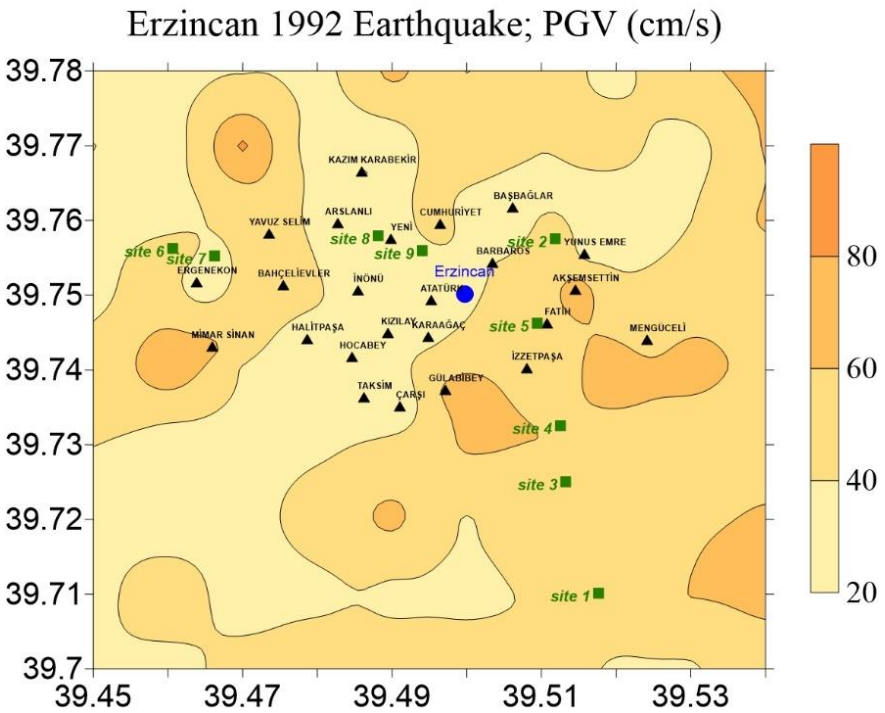

# Spatial distribution of the simulated (a) PGA, (b) PGV values of the scenario event Mw=7.0

(a)

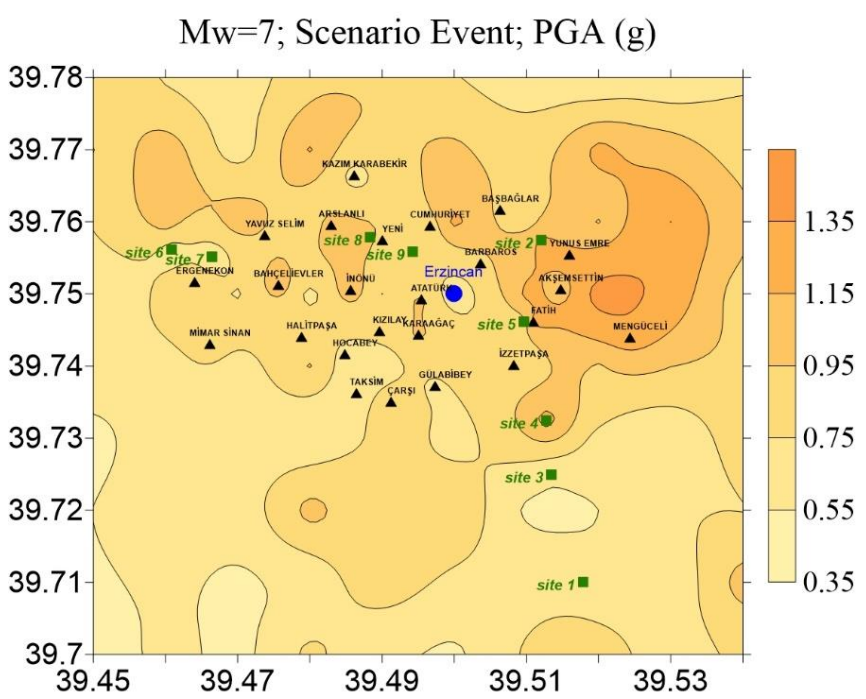


(b)

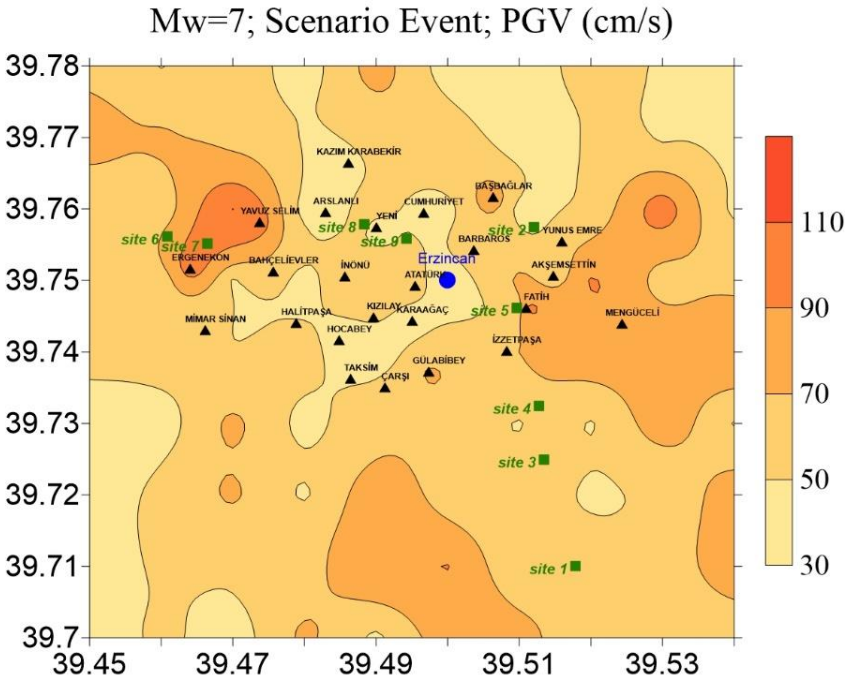

# Classification of regional building stock

- On site structural classification: 21 groups, (12 RC and 9 Masonry).
- Structu

1. Type o
2. Numbe
3. The lev

- MDOF s
- Latin H
- Detaile

platform

Modified Ibarra-Medina-Krawinkler Deterioration Model

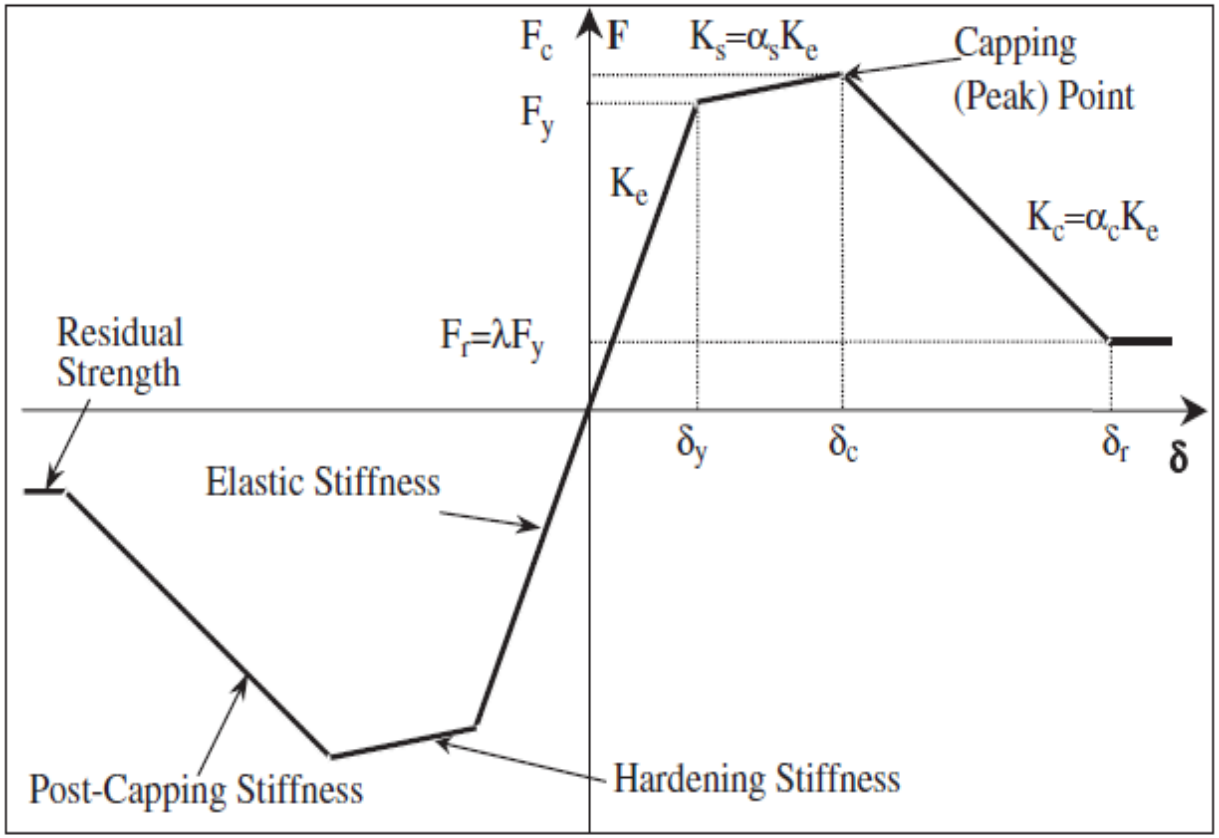

# Spatial distribution of the RC buildings in the districts

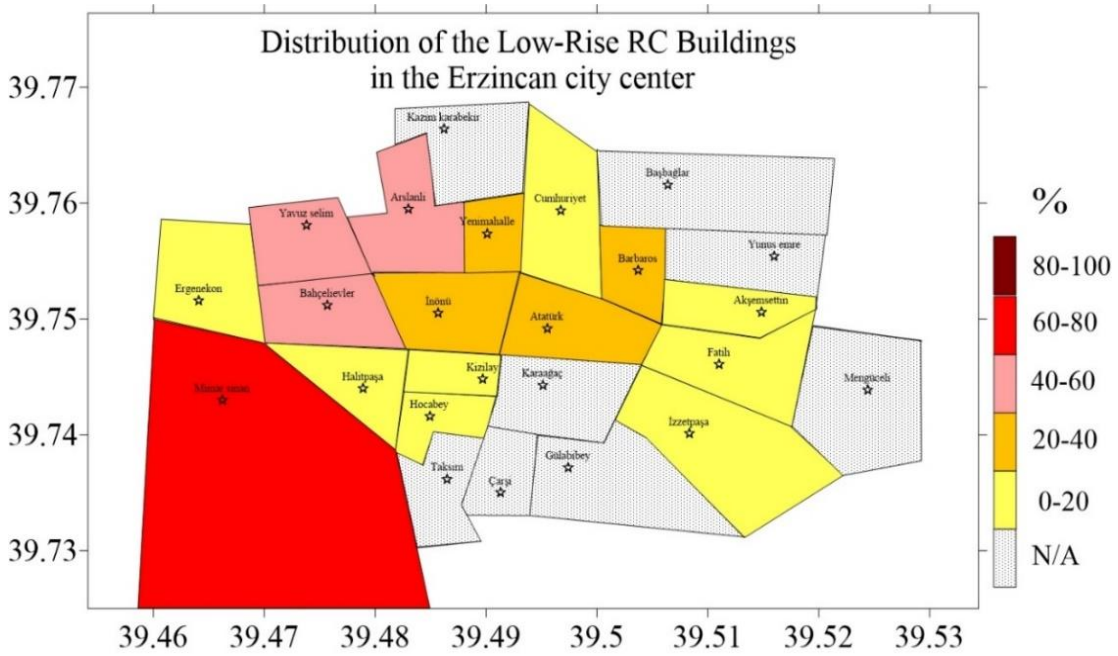


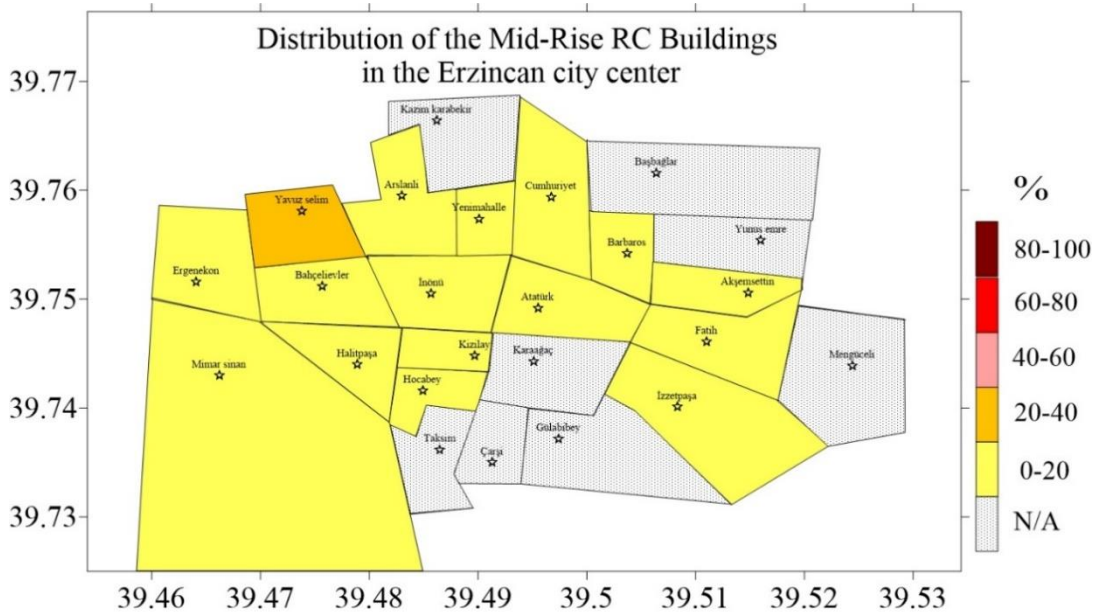

# Spatial distribution of the masonry buildings in the districts

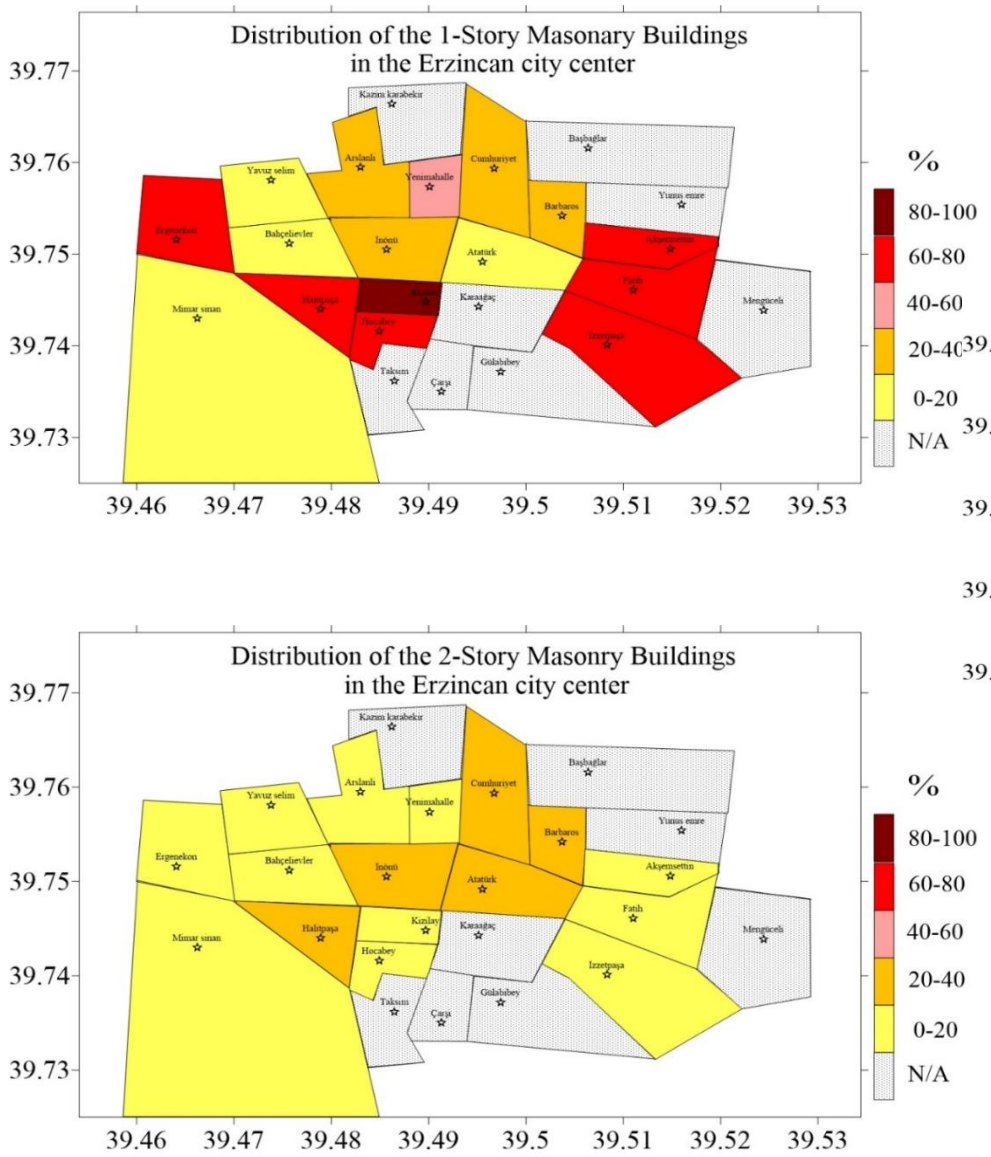


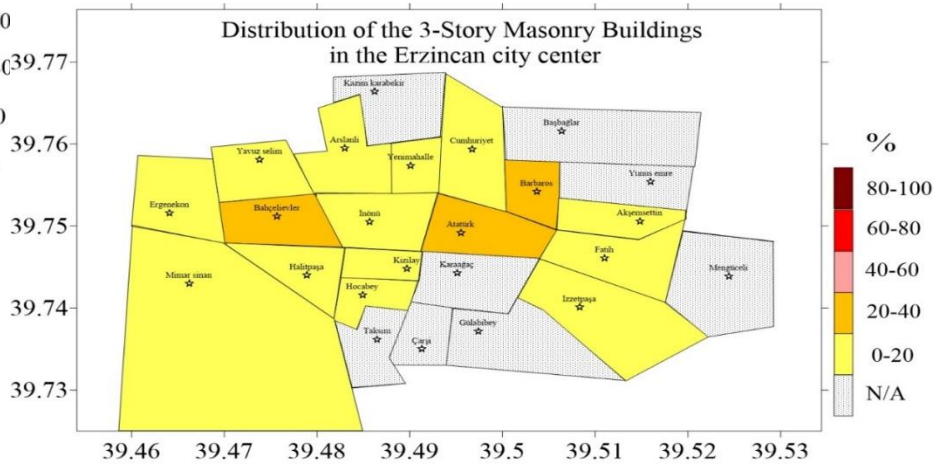

# Selection of ground motions for fragility analyses

- Input to fragility analyses: a set from the synthetic GM database
- Ground motions are separated into two groups:

(a) Categorized according to PGV (for RC buildings)

(b) Categorized according to PGA (for Masonry buildings)

- The ground motion intensity levels are subdivided into 20 groups, ($\Delta$PGV=5 cm/s and $\Delta$PGA=0.05g)
- To account for the variability in seismic demand: for each intensity level, selection of 10 time histories with different soil conditions, distance, and magnitude values

# Generation of fragility curves

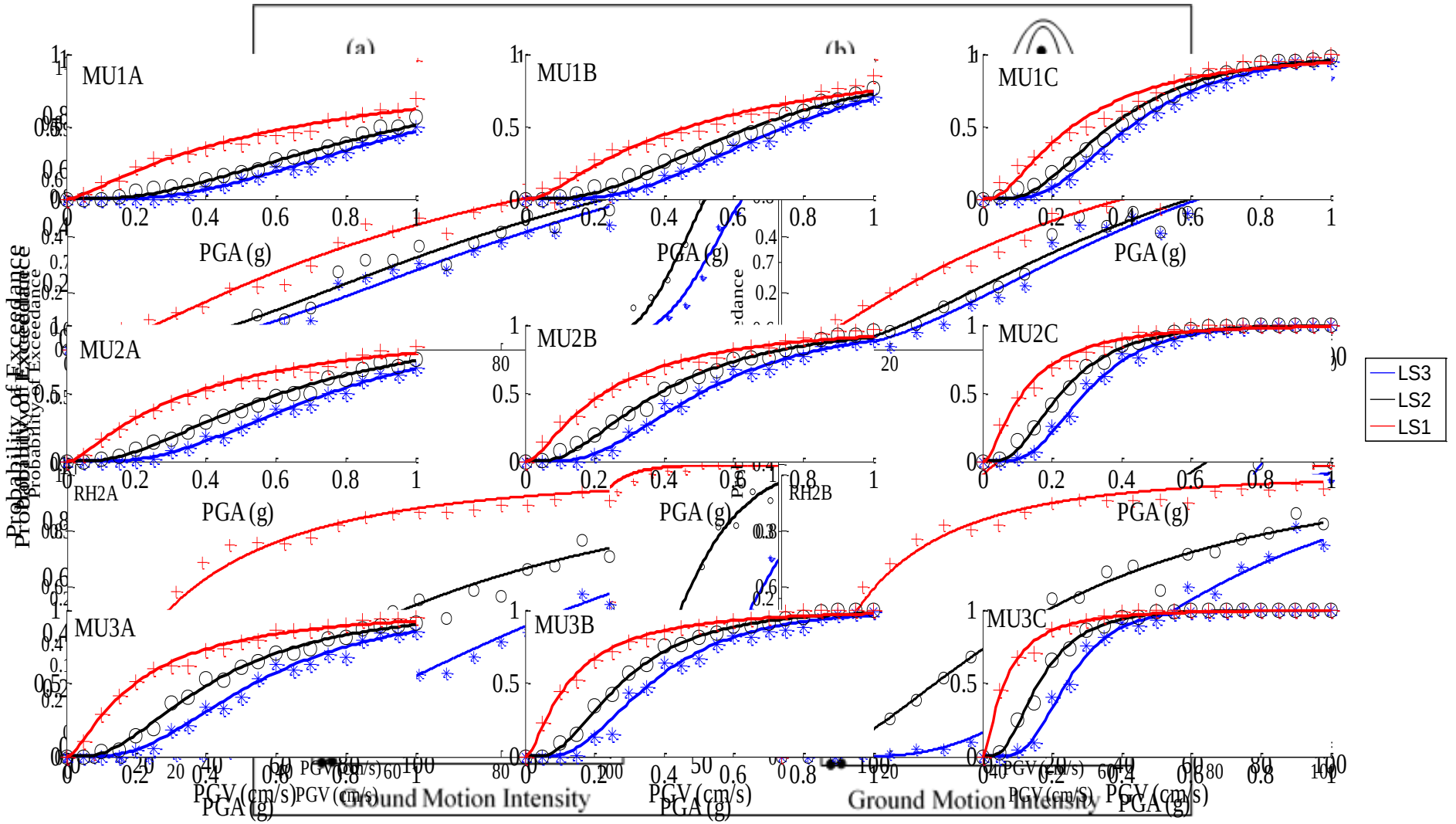

# Spatial distribution of the (a) simulated PGA, (b) simulated PGV, (c) Observed MDR and (d) Estimated MDR values of the 1992 Erzincan earthquake in the districts

(a)

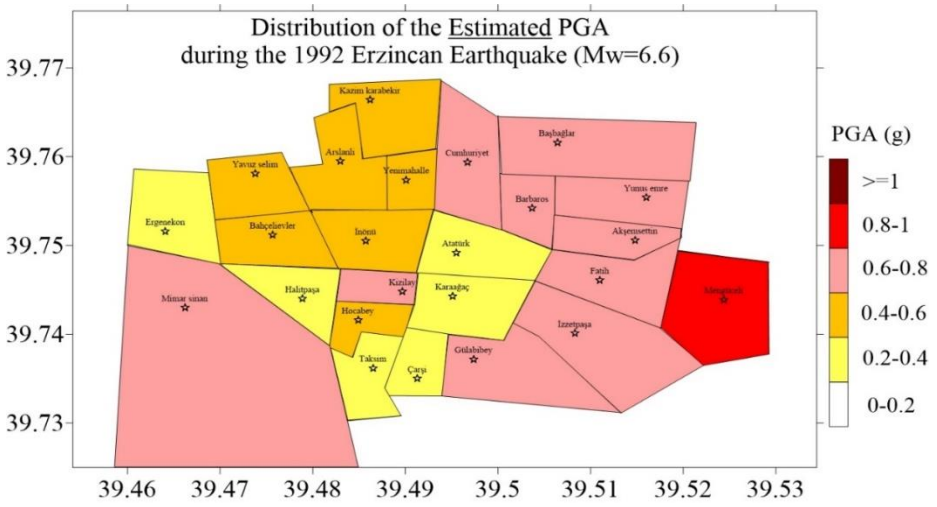


(b)

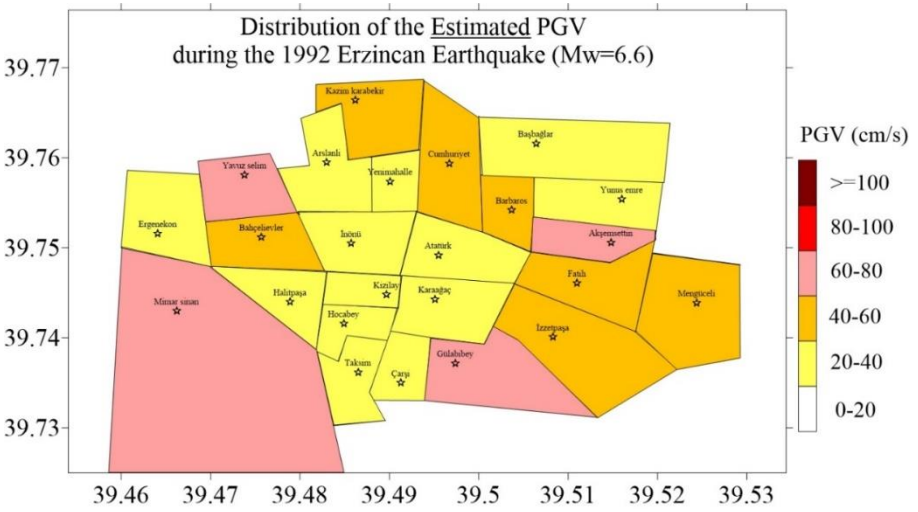


(c)

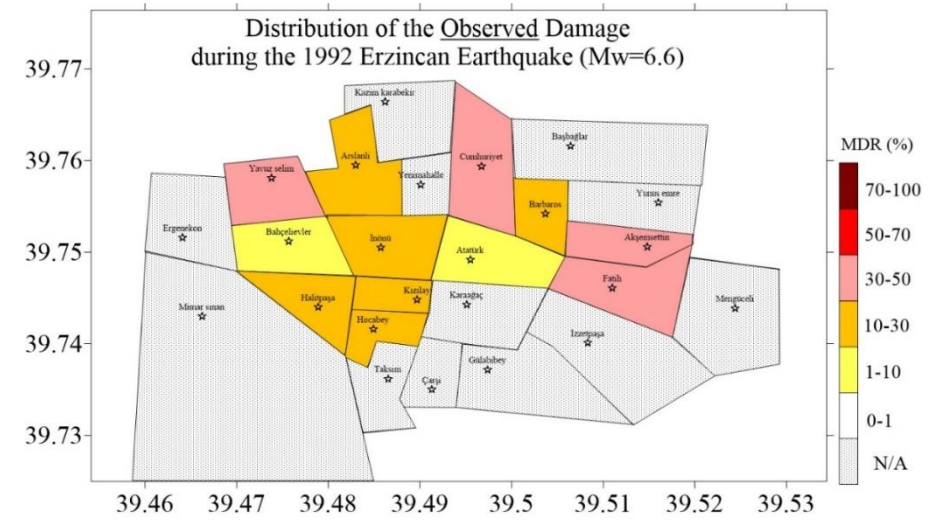


(d)

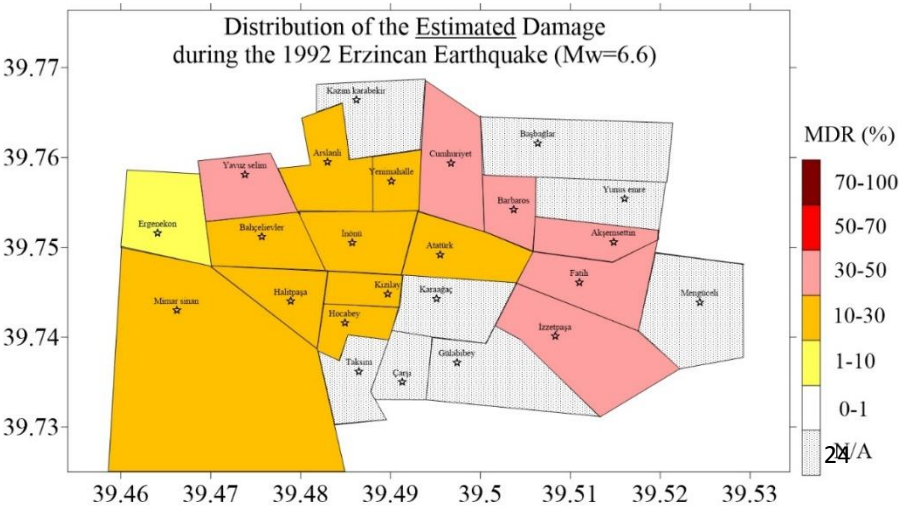

# Spatial distribution of the (a) simulated PGA, (b) simulated PGV and (c) Estimated MDR values for scenario event of Mw=7.0 in the districts

(a)

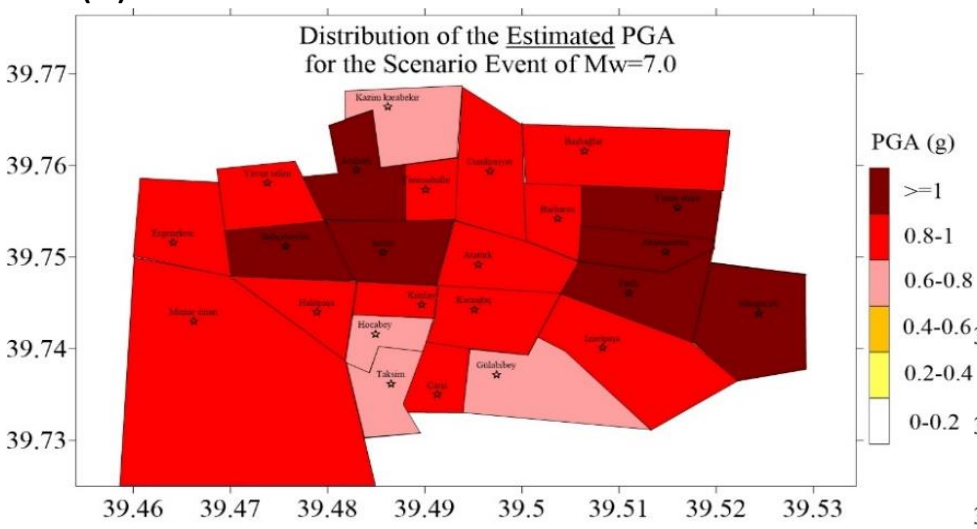


(b)

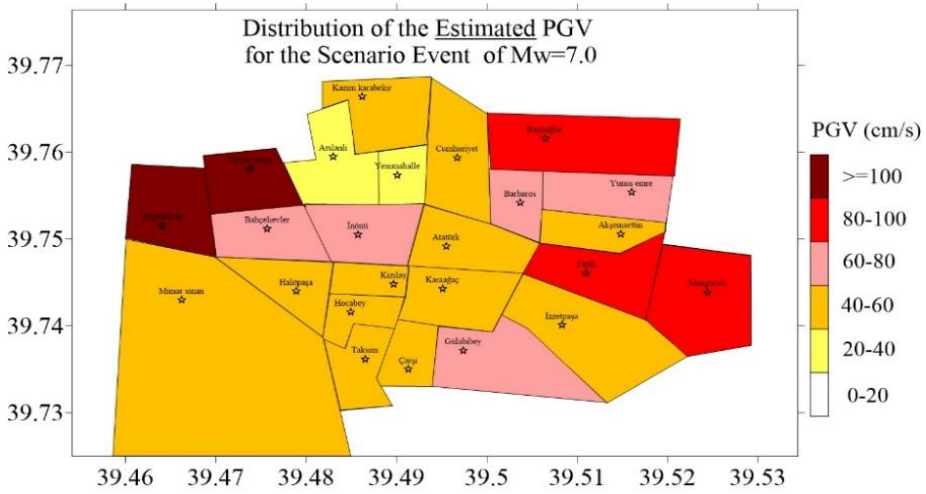


(c)

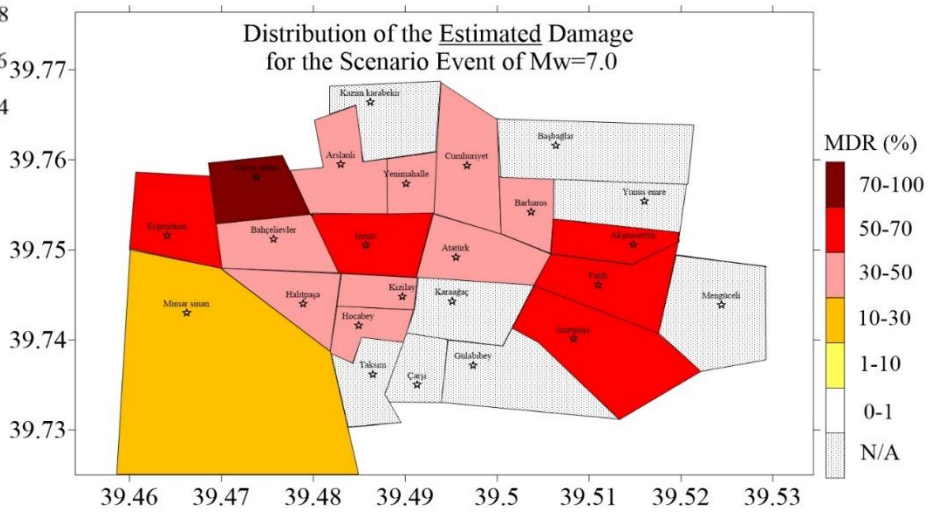

# Part 2:

# Application of simulated records in nonlinear time history analysis of MDOF structures

# Objective

- The dynamic response of typical MDOF structures to simulated records of a particular earthquake in comparison with the response due to the real records of the same event

- To investigate the efficiency of the simulated records in prediction of nonlinear demands of typical MDOF structures:

- Let's define goodness of fit in terms of engineering demand parameters (story displacements)

- Examination through simulation of :

a. The 1999 Duzce (Turkey) Earthquake (Mw=7.1)
b. The 2009 L'Aquila (Italy) earthquake (Mw=6.3)

# Nonlinear time history analyses of MDOF structures

- Time history analysis is a step-by-step analysis of the dynamic response of a structure under a loading which is a function of time
- linear / nonlinear

$$[M]\frac{\partial^2 u}{\partial t^2}+[C]\frac{\partial u}{\partial t}+[K(u)]u=f(t)$$

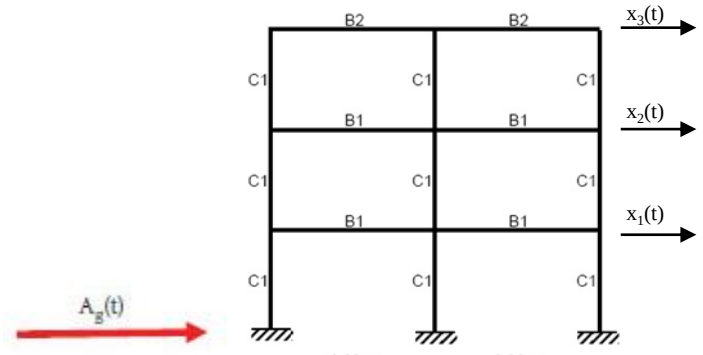


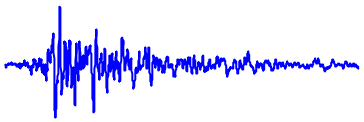

# MDOF structures

- Pick 3 model R/C structures (3-5-8 stories)
- Structural Analysis Software: OPENSEES

(Finite Element in space and Newmark-integration in time)

- Fiber based nonlinear beam-column elements

| Frame ID | Total Mass (Tons) | Fundamental Period (s) |
|---|---|---|
| F2-3S2B | 226.5 | 0.71 |
| F6-5S2B | 260.2 | 0.78 |
| F9-8S3B | 1816.1 | 1.3 |

# Model Frames

Existing structure located in the city of Bursa in Turkey

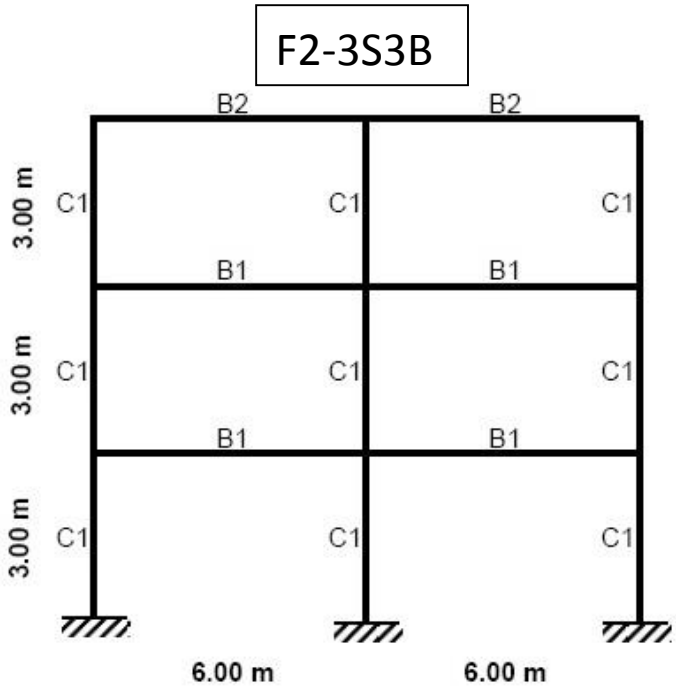


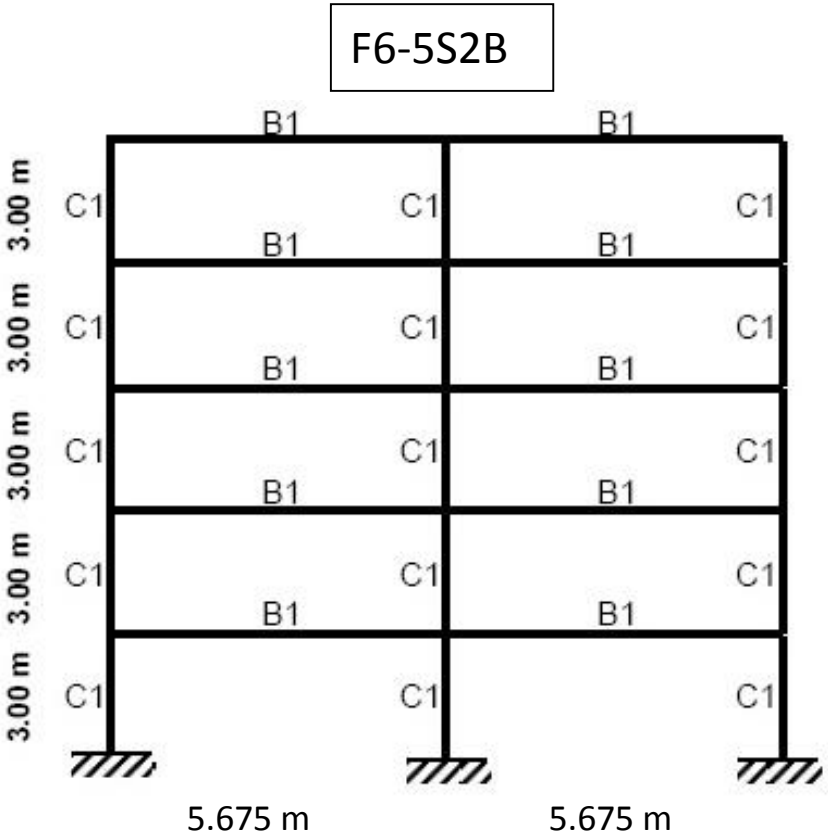

# Model Frames

Designed in California complying with the Uniform Building Code-1982

F9-8S3B

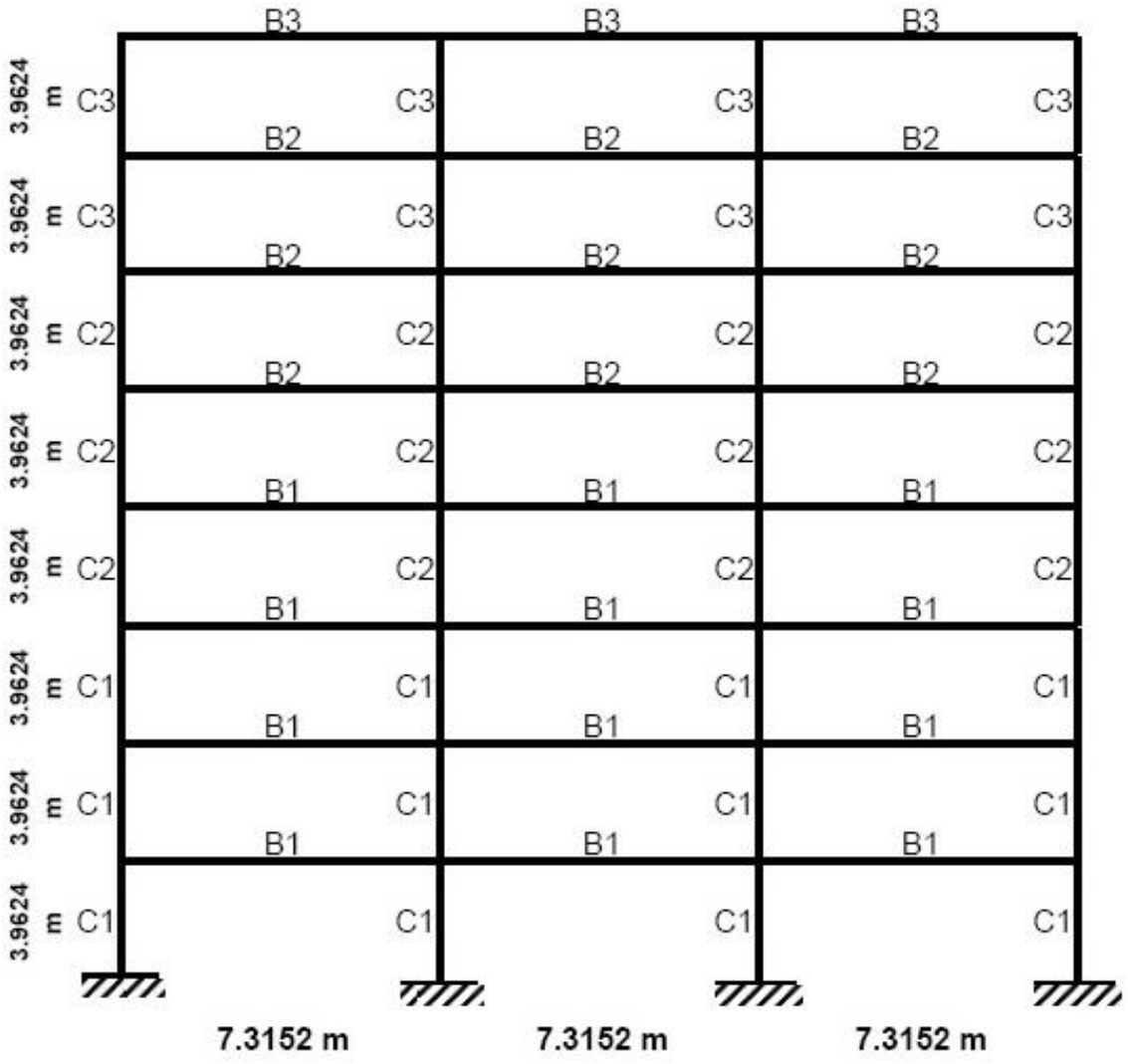

# MDOF structures

- Concrete Model (Kent-Scott-Park):

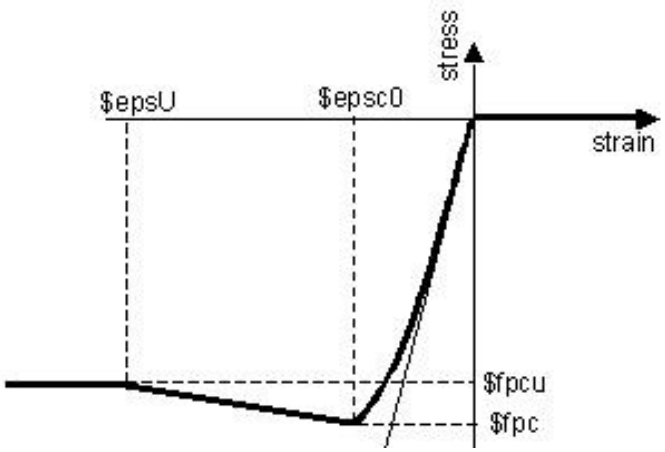


- Geometric nonlinearity
- Material nonlinearity

- Steel Model:

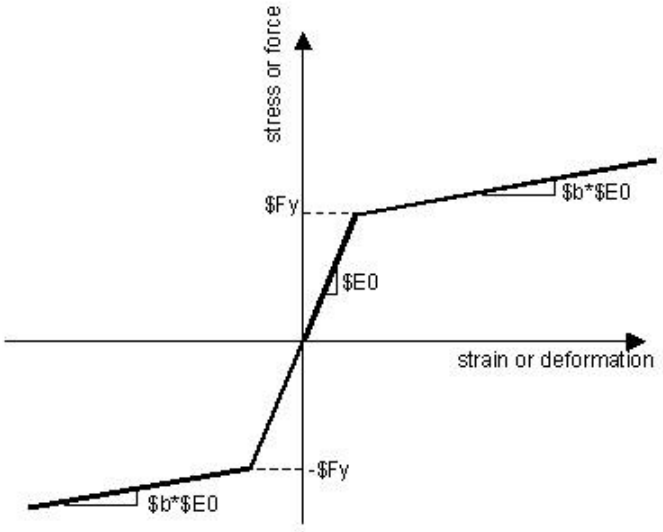

# Comparison of seismological misfits vs. NR misfits

$$Misfit_{FAS} = \frac{1}{n_f}\sum_{f}\log\frac{FAS_{syn}}{FAS_{obs}}$$

$$Misfit_{RS} = \frac{1}{n_T}\sum_{T}\left|\log\frac{RS_{syn}}{RS_{obs}}\right|$$

0.2Tn<T<1.2Tn

$$Misfit_{NR} = \frac{1}{n_s}\sum_{s=1}^{n_S}\left|\log\frac{NR(s)_{syn}}{NR(s)_{obs}}\right|$$

$n_s$: Number of stories

# a. The 1999 Duzce (Turkey) earthquake

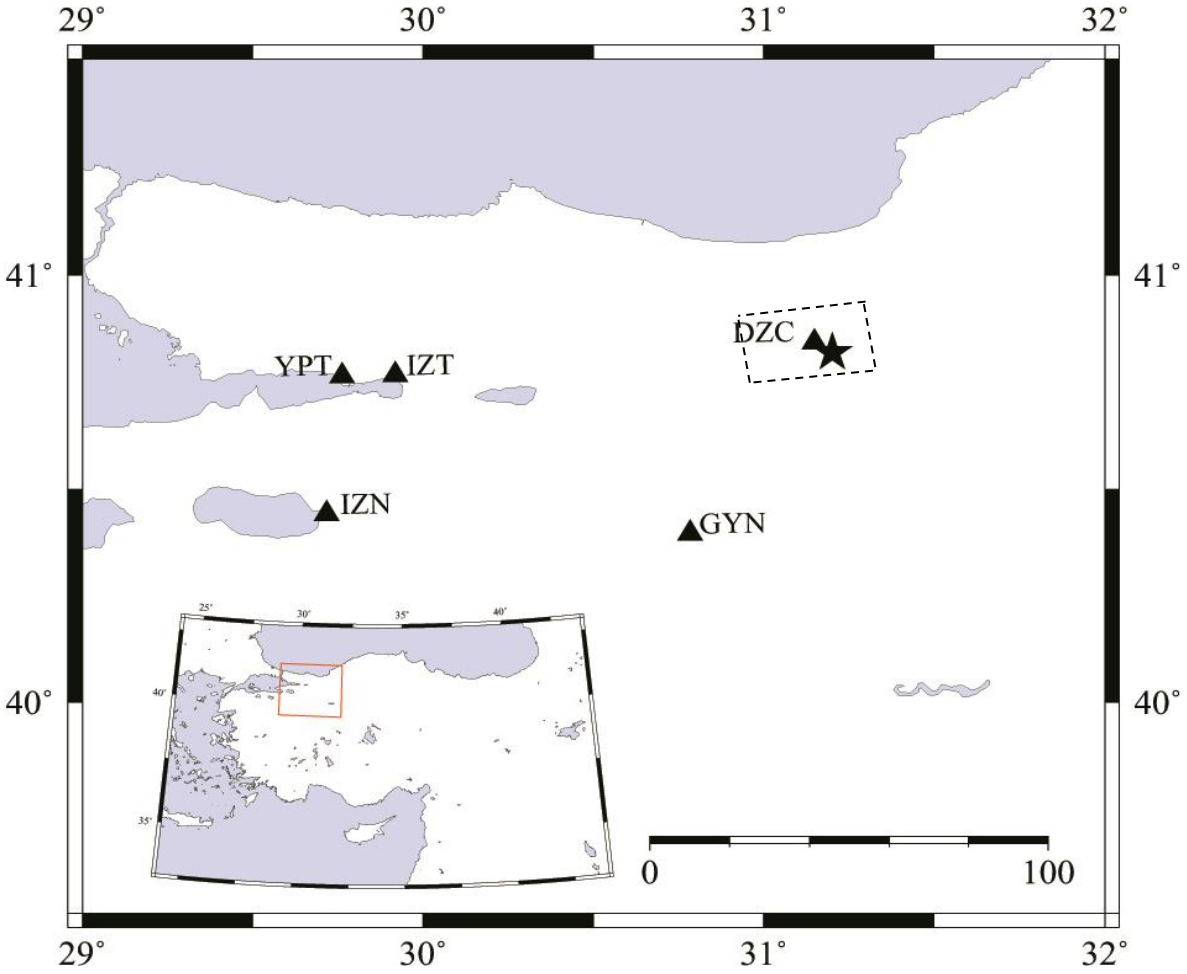


- Mw=7.1
- Strike-slip fault
- Led to destructive damages of the city with 900 deaths and 3000 injuries
- 5 records with epicentral distances less than 125 Km are selected

# Selected stations and their properties for Duzce

| Station | Code | Latitude (N) | Longitude(E) | Site Class (EC08) | $R_{epi}$ (Km) | PGA-EW ($cm/s^2$) | PGA-NS ($cm/s^2$) | PGV-EW (cm/s) | PGV-NS (cm/s) |
|---|---|---|---|---|---|---|---|---|---|
| Düzce | DZC | 40.8436 | 31.1488 | D | 9.314 | 520.41 | 328.03 | 86.54 | 54.53 |
| Göynük | GYN | 40.3965 | 30.7830 | D | 55.163 | 22.17 | 25.79 | 5.84 | 4.49 |
| İznik | IZN | 40.4416 | 29.7168 | D | 123.67 | 20.06 | 21.25 | 1.97 | 2.27 |
| İzmit | IZT | 40.7665 | 29.9172 | C | 100.7 | 16.41 | 18.73 | 2.27 | 1.73 |
| Yarımca Petkim | YPT | 40.7639 | 29.7620 | D | 116.85 | 16.15 | 23.47 | 4.08 | 8.38 |

# Results

Station DZC

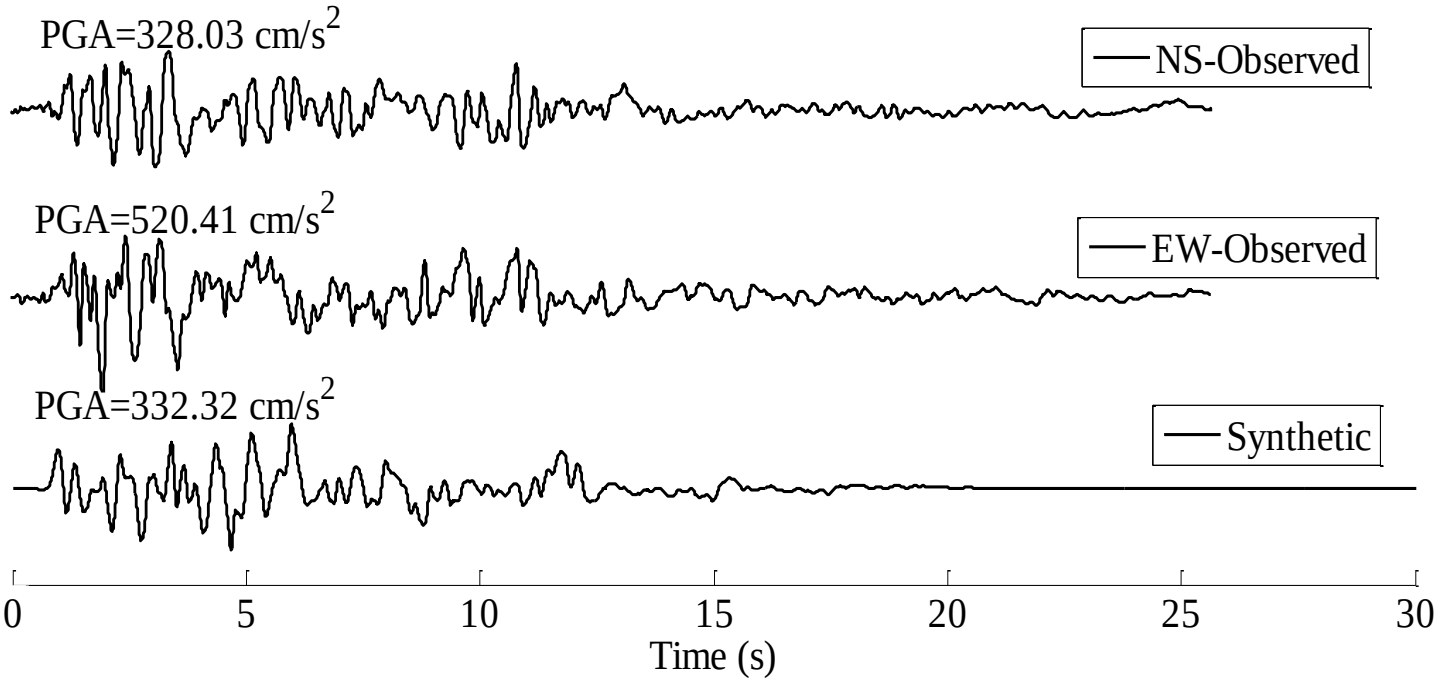

## Station GYN

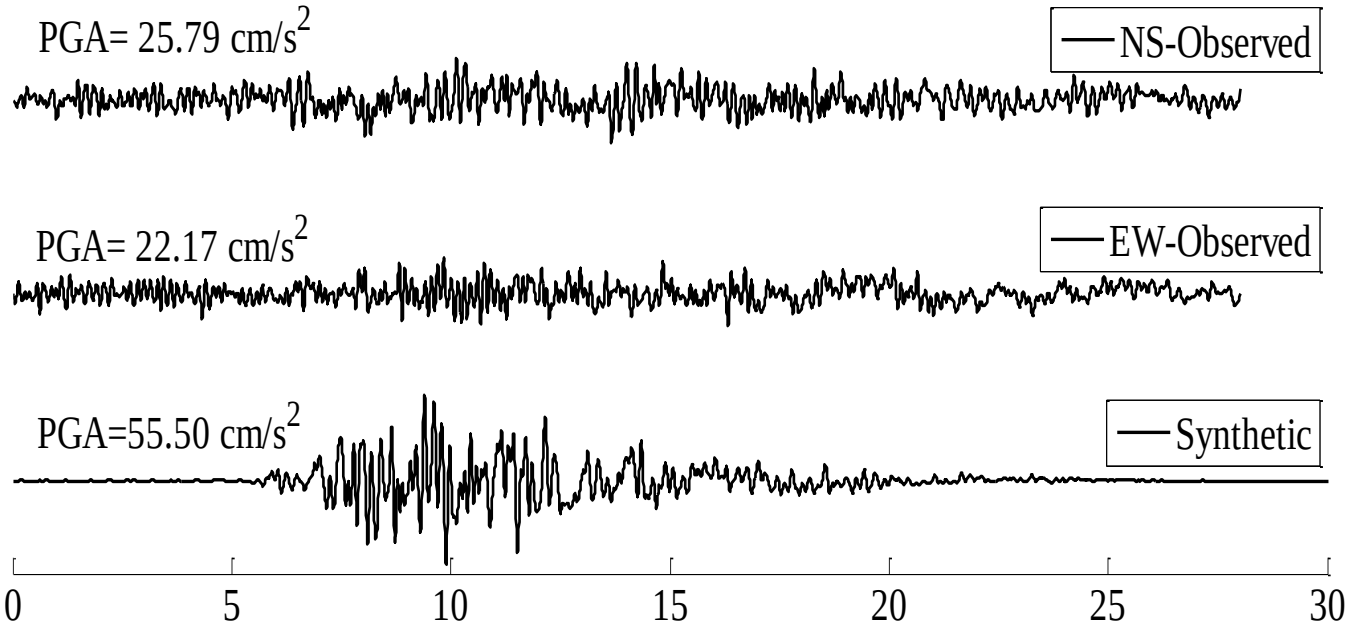
PGA= 25.79 cm/s2
NS-Observed
PGA= 22.17 cm/s2
EW-Observed
PGA=55.50 cm/s2
Synthetic
0
5
10
15
20
25
30

# Station IZN

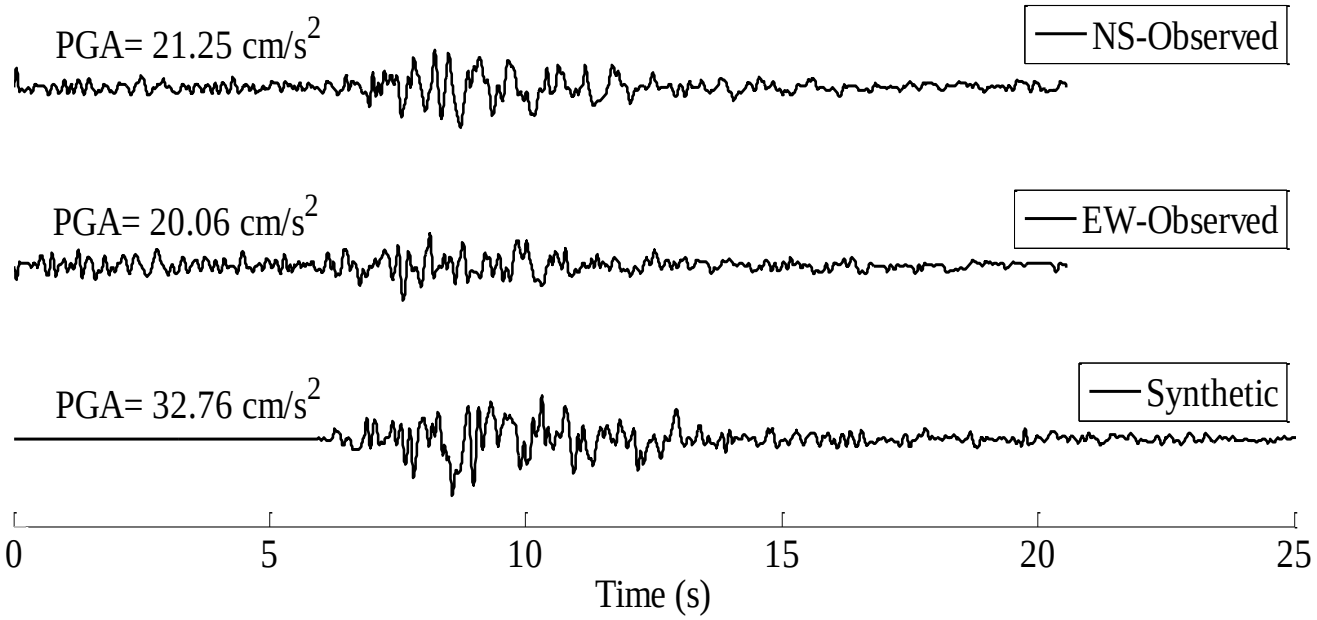
PGA= 21.25 cm/s2
NS-Observed
PGA= 20.06 cm/s2
EW-Observed
PGA= 32.76 cm/s2
Synthetic
0
5
10
15
20
25
Time (s)

# Station IZT

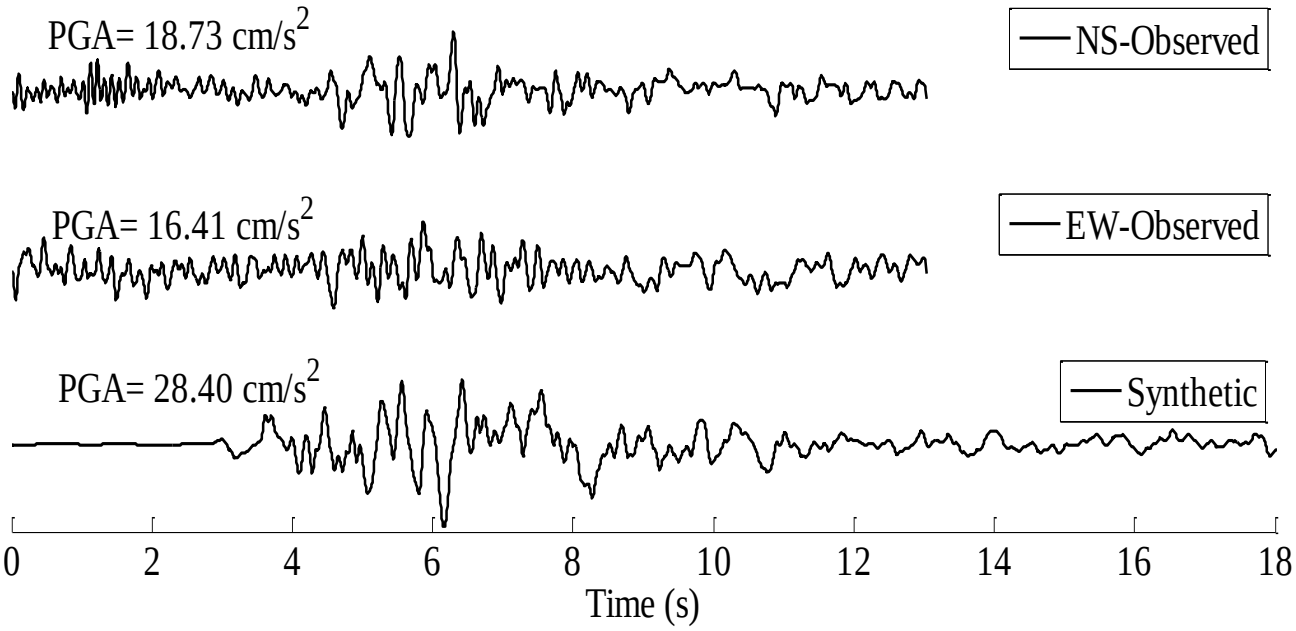
PGA= 18.73 cm/s2
NS-Observed
PGA= 16.41 cm/s2
EW-Observed
PGA= 28.40 cm/s2
Synthetic
0
2
4
6
8
10
12
14
16
18
Time (s)

## Station YPT

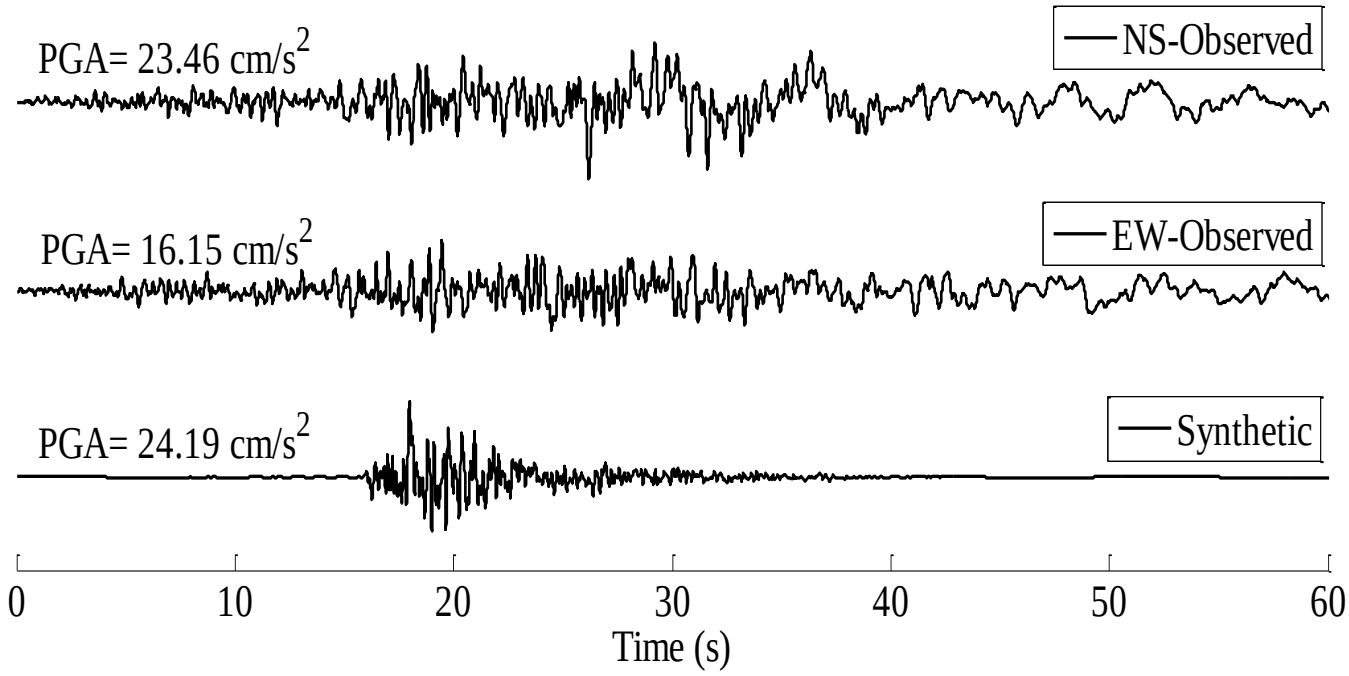
PGA= 23.46 cm/s2
NS-Observed
PGA= 16.15 cm/s2
EW-Observed
PGA= 24.19 cm/s2
Synthetic
0
10
20
30
40
50
60
Time (s)

# Comparison of observed vs. simulated GMs (FAS)

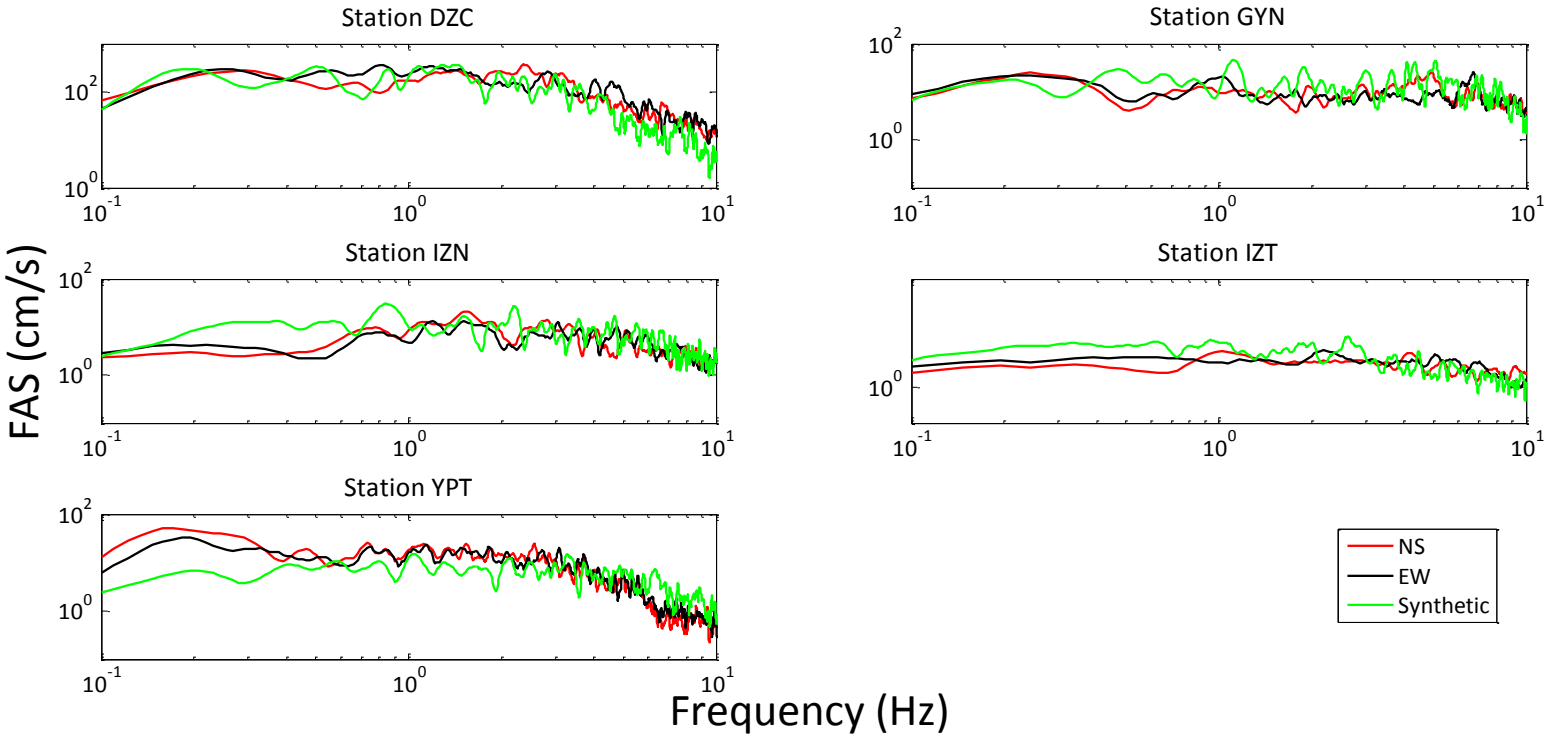


$$\text{Residual} = \log \frac{\text{FAS}_{\text{syn}}}{\text{FAS}_{\text{obs}}}$$

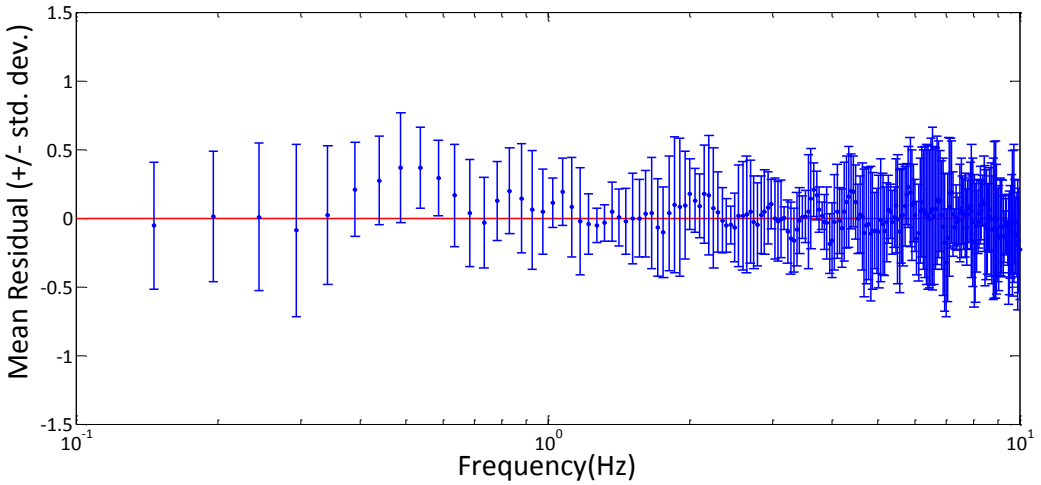

# Comparison of observed vs. simulated GMs (SDOF RS)

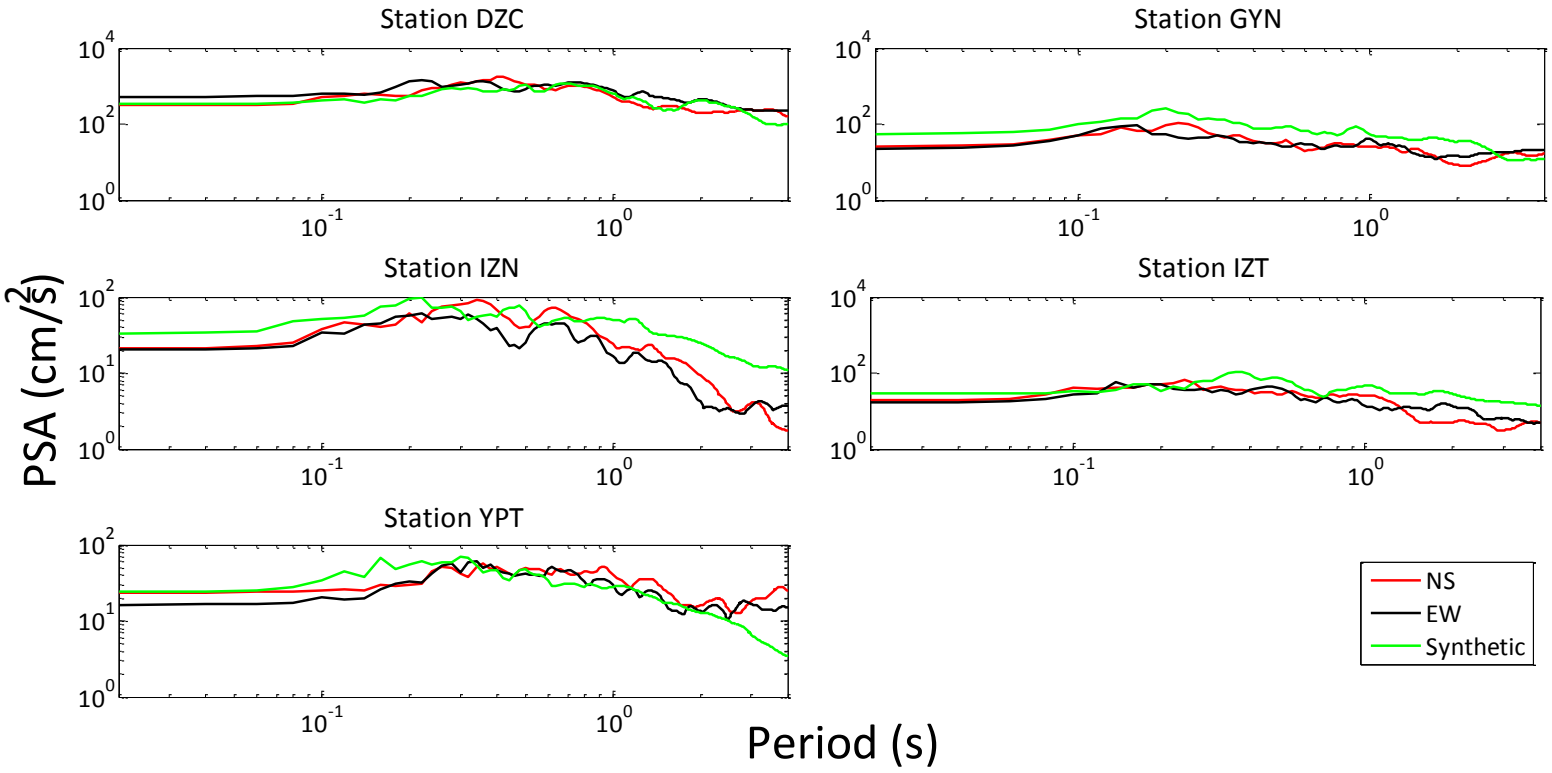


$$\text{Residual} = \log \frac{\text{RS}_{\text{syn}}}{\text{RS}_{\text{obs}}}$$

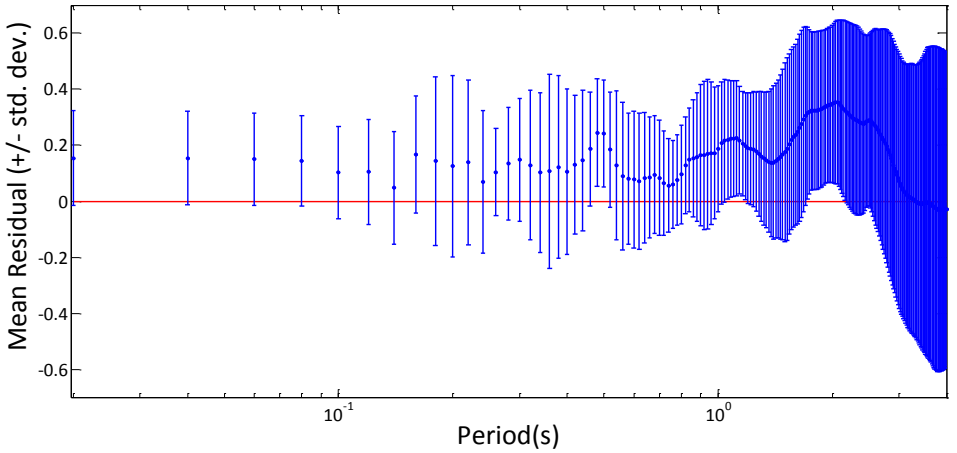

# Distribution of maximum story displacements due to the real and simulated records– F2-3S2B

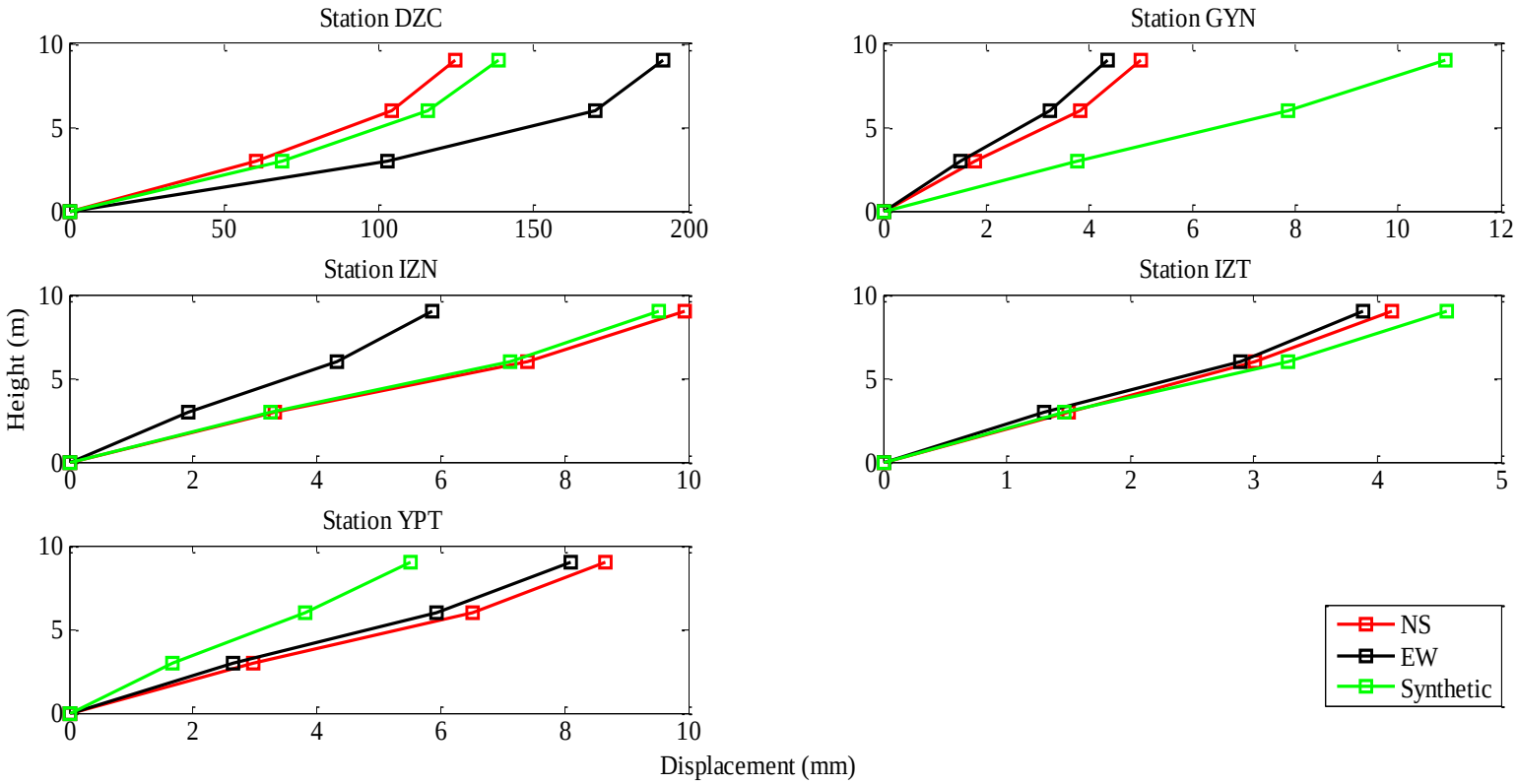


| Station | Real (mm) | $NR(roof)_{syn}$ / $NR(roof)_{obs}$ |
|---|---|---|
| DZC | 154.7119 | 0.8950 |
| GYN | 4.6696 | 2.3382 |
| IZN | 7.6369 | 1.2454 |
| IZT | 4.0036 | 1.1392 |
| YPT | 8.3841 | 0.6570 |

# Distribution of maximum story displacements due to the real and simulated records– F6-5S2B

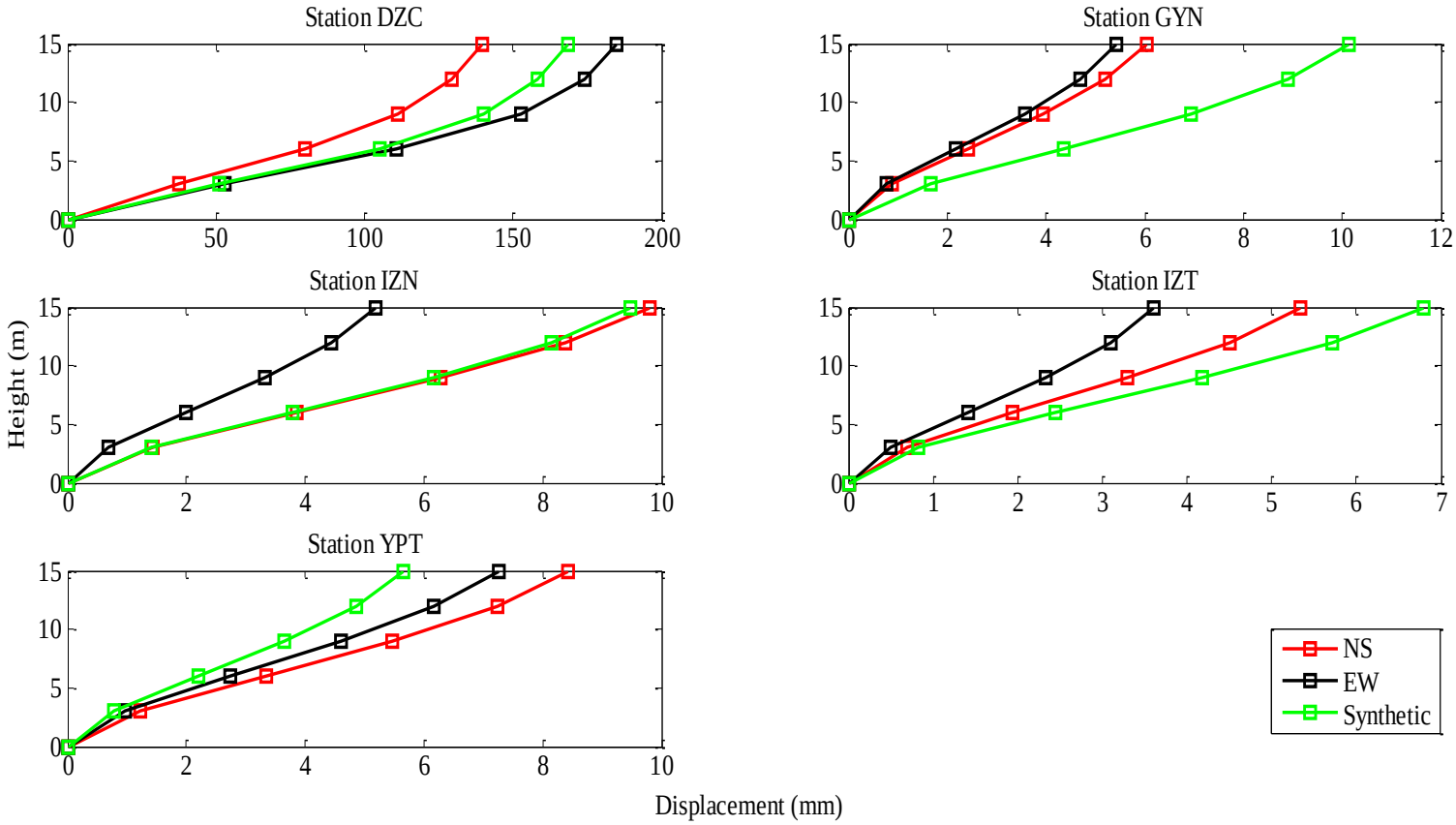


| Station | Real (mm) | $NR(roof)_{syn}$ / $NR(roof)_{obs}$ |
|---|---|---|
| DZC | 160.5637 | 1.0482 |
| GYN | 5.7227 | 1.7715 |
| IZN | 7.1243 | 1.4230 |
| IZT | 4.3898 | 1.5463 |
| YPT | 7.8122 | 0.7249 |

# Distribution of maximum story displacements due to the real and simulated records– F9-8S3B

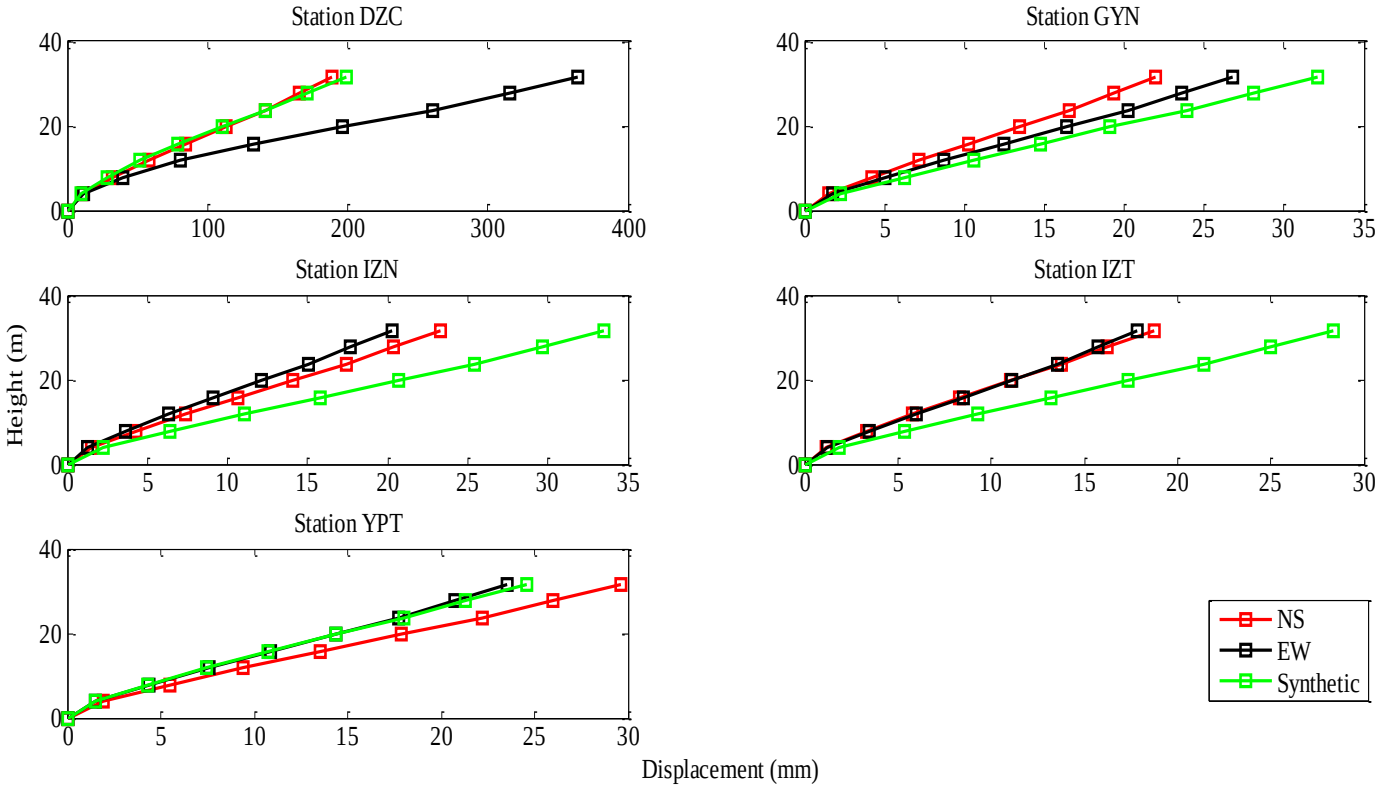


| Station | Real (mm) | $NR(roof)_{syn}$ / $NR(roof)_{obs}$ |
|---|---|---|
| DZC | 262.2008 | 0.7606 |
| GYN | 24.2472 | 1.3244 |
| IZN | 21.7067 | 1.5437 |
| IZT | 18.3138 | 1.5469 |
| YPT | 26.3956 | 0.9304 |

# F2-3S2B

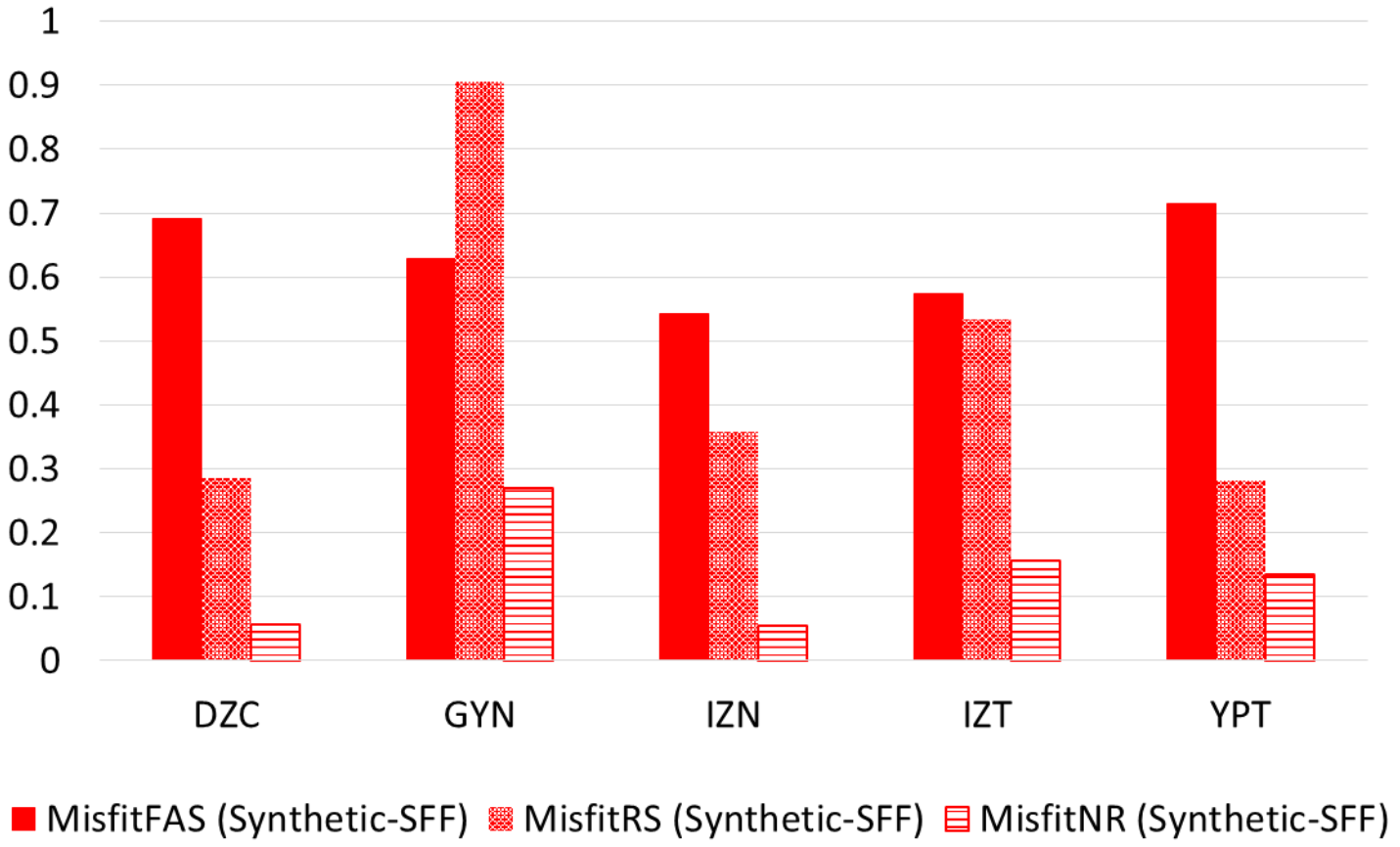
1
0.9
0.8
0.7
0.6
0.5
0.4
0.3
0.2
0.1
0
DZC
GYN
IZN
IZT
YPT
MisfitFAS (Synthetic-SFF)
MisfitRS (Synthetic-SFF)
MisfitNR (Synthetic-SFF)

# F6-5S2B

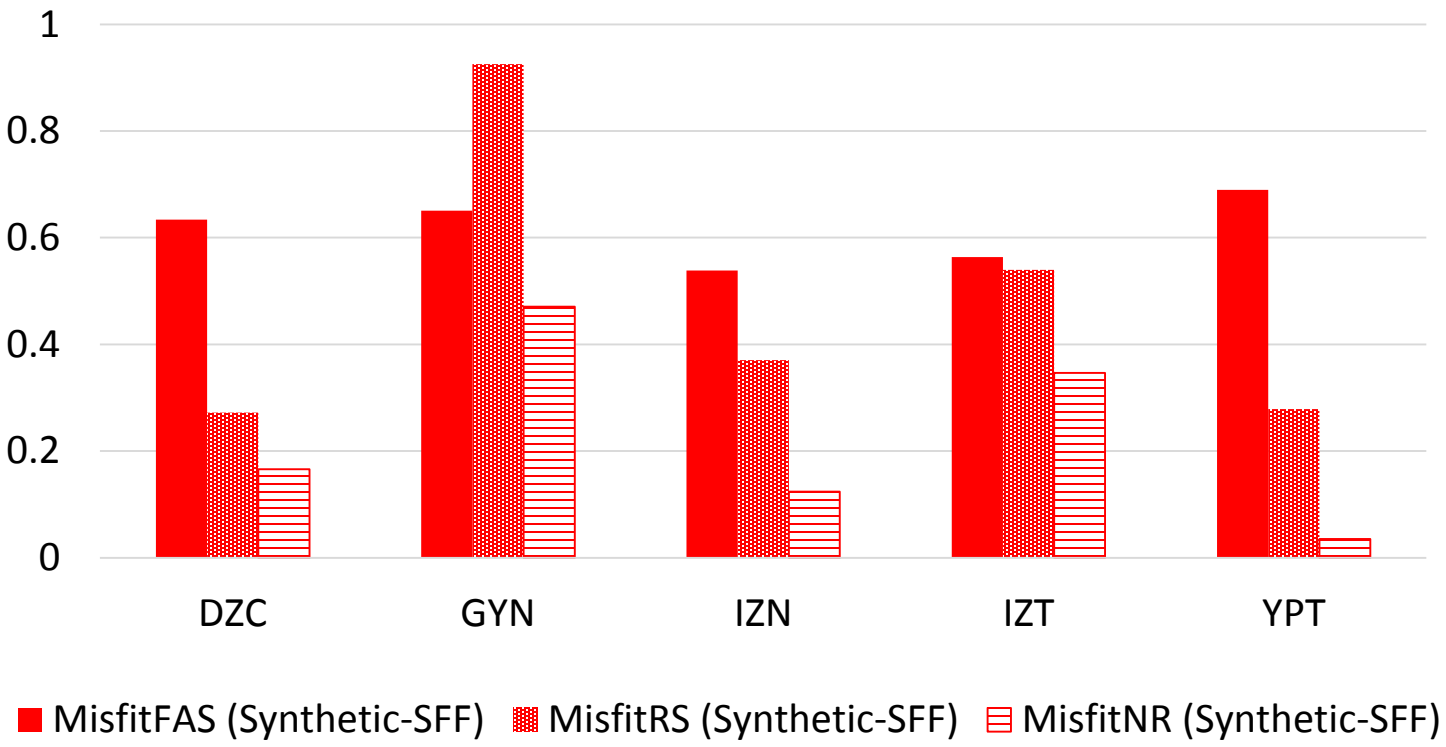
1
0.8
0.6
0.4
0.2
0
DZC
GYN
IZN
IZT
YPT
MisfitFAS (Synthetic-SFF)
MisfitRS (Synthetic-SFF)
MisfitNR (Synthetic-SFF)

# F9-8S3B

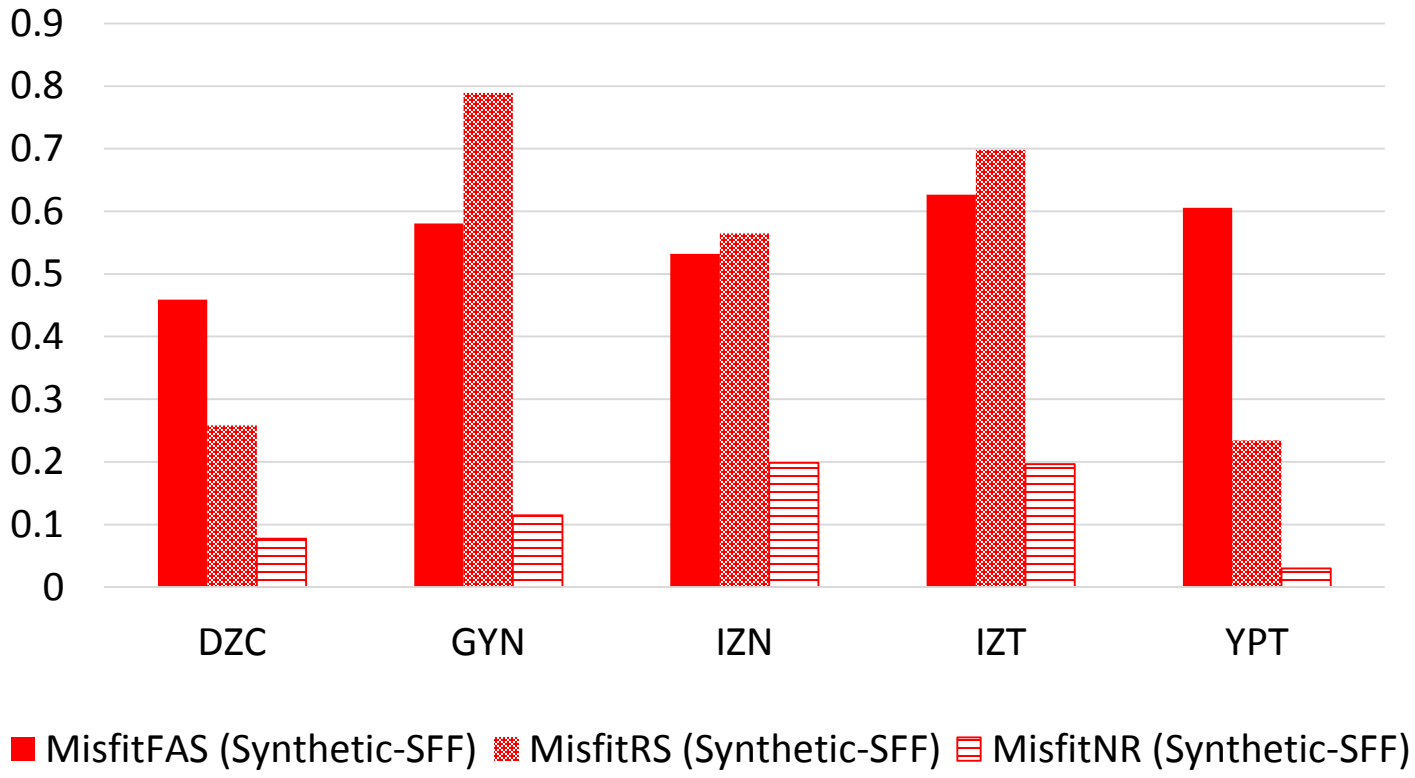
0.9
0.8
0.7
0.6
0.5
0.4
0.3
0.2
0.1
0
DZC
GYN
IZN
IZT
YPT
MisfitFAS (Synthetic-SFF)
MisfitRS (Synthetic-SFF)
MisfitNR (Synthetic-SFF)

# b. The 2009 L'Aquila (Italy) earthquake

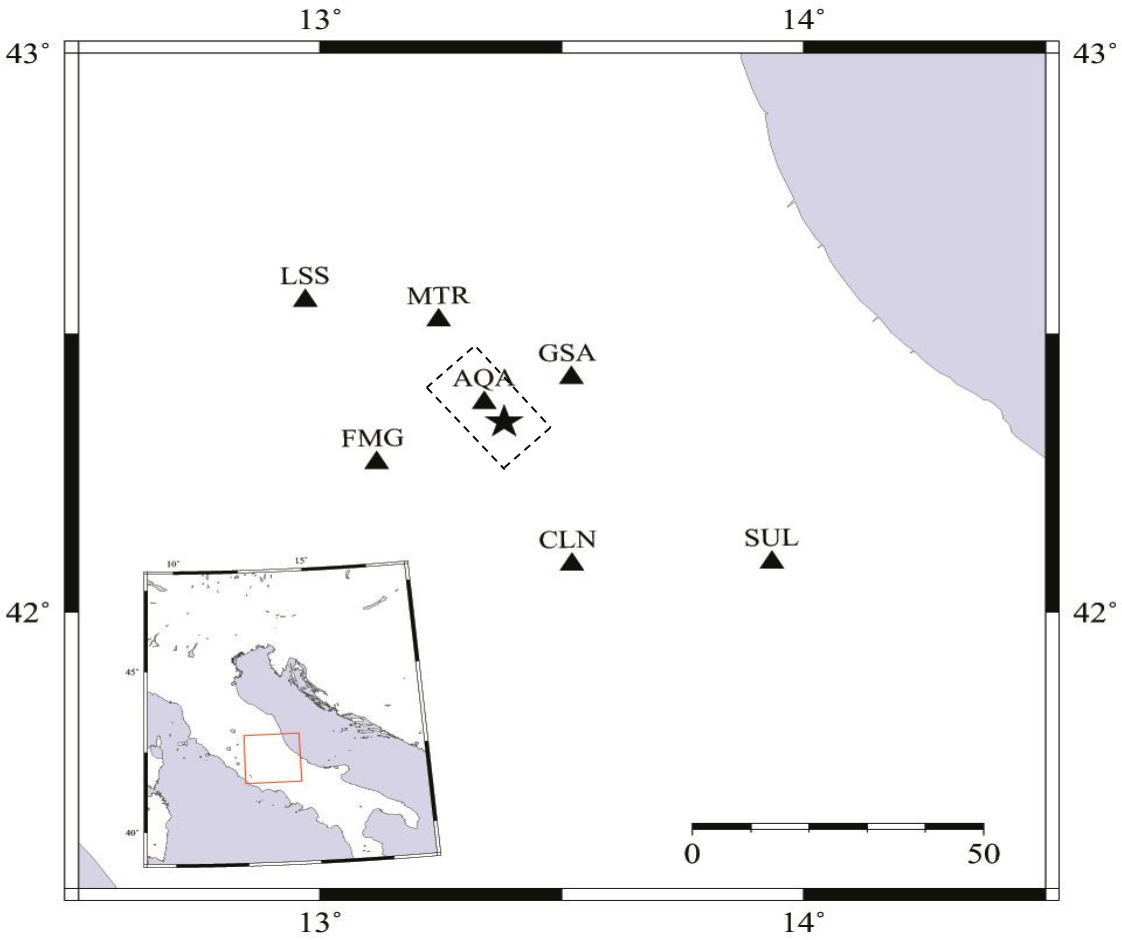


Karimzadeh, Askan, Yakut and Ameri (2017)
Soil Dynamics and Earthquake Engineering

- Mw=6.3
- Normal fault
- Caused severe damage in epicentral area with approximately 300 casualties and total damage cost of 2–3 billion Euros
- 7 near-fault records are selected

# Selected stations and their properties for L'Aquila

| Station | Code | Latitude (N) | Longitude (E) | Site Class (EC08) | $R_{epi}$ (Km) | PGA-EW ($cm/s^2$) | PGA-NS ($cm/s^2$) | PGV-EW (cm/s) | PGV-NS (cm/s) |
|---|---|---|---|---|---|---|---|---|---|
| V. Aterno-F. Aterno | AQA | 42.376 | 13.339 | B | 4.2 | 350.46 | 347.59 | 29.86 | 24.07 |
| Celano | CLN | 42.085 | 13.5207 | A | 31.79 | 73.49 | 76.57 | 4.61 | 6.56 |
| Fiamignano | FMG | 42.268 | 13.1172 | A | 23.17 | 20.12 | 24.53 | 2.52 | 1.67 |
| Gran Sasso | GSA | 42.421 | 13.5194 | B | 14.15 | 131.88 | 139.02 | 9.63 | 7.41 |
| Leonessa | LSS | 42.558 | 12.9689 | A | 40.62 | 9.21 | 7.61 | 0.71 | 0.72 |
| Montereale | MTR | 42.524 | 13.2448 | A | 22.13 | 42.17 | 51.65 | 3.25 | 3.09 |
| Sulmona | SUL | 42.09 | 13.9343 | C | 54.29 | 27.04 | 24.53 | 2.69 | 2.82 |

# Simulated ground motions in region of interest

Using two alternative ground motion simulation methods:

a) Stochastic Finite-Fault Method: (Motazedian and Atkinson, 2005)

(Ugurhan et al. 2012, BSSA) Synthetic-SFF

b) Hybrid-Integral Composite Method: (Gallovič and Brokešová, 2007)

- Broadband synthetics
- k-square kinematic rupture model, combining low frequency coherent and high-frequency incoherent, Brune's source radiation

(Ameri et. al, 2012, JGR) Synthetic-HIC

# Results

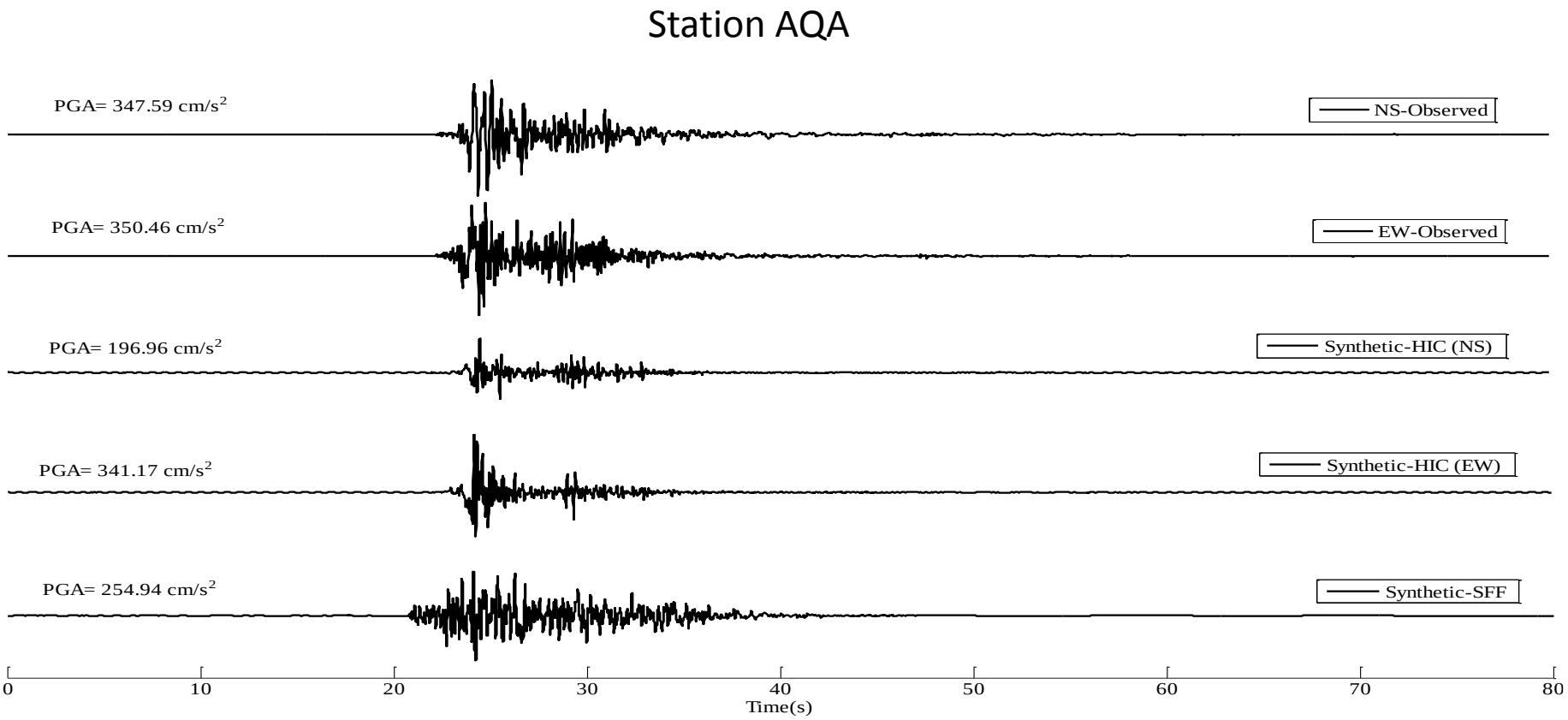
Station AQA
PGA= 347.59 cm/s$^2$
NS-Observed
PGA= 350.46 cm/s$^2$
EW-Observed
PGA= 196.96 cm/s$^2$
Synthetic-HIC (NS)
PGA= 341.17 cm/s$^2$
Synthetic-HIC (EW)
PGA= 254.94 cm/s$^2$
Synthetic-SFF
0
10
20
30
40
50
60
70
80
Time(s)

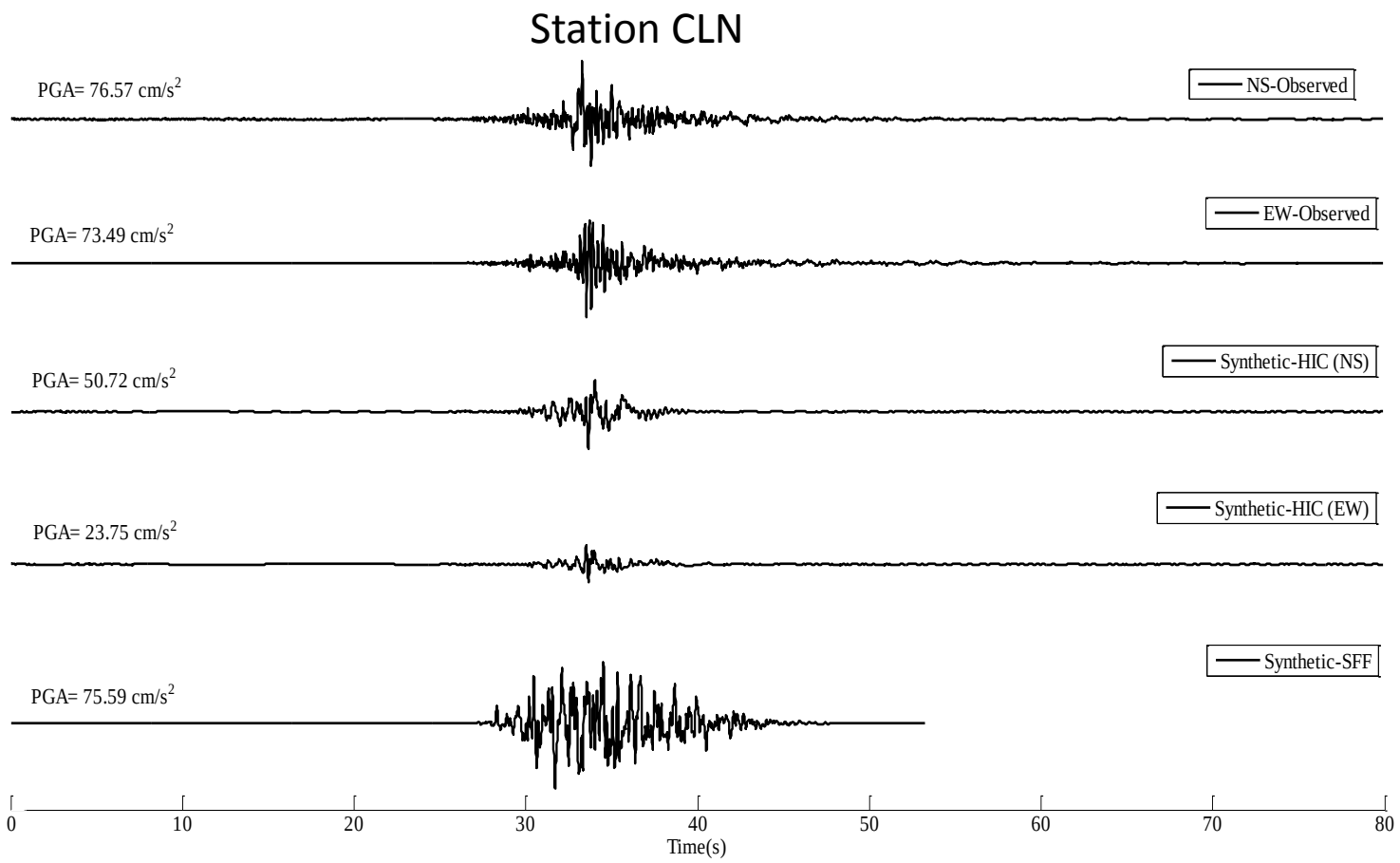
Station CLN
PGA= 76.57 cm/s2
NS-Observed
PGA= 73.49 cm/s2
EW-Observed
PGA= 50.72 cm/s2
Synthetic-HIC (NS)
PGA= 23.75 cm/s2
Synthetic-HIC (EW)
PGA= 75.59 cm/s2
Synthetic-SFF
0
10
20
30
40
50
60
70
80
Time(s)

# Station FMG

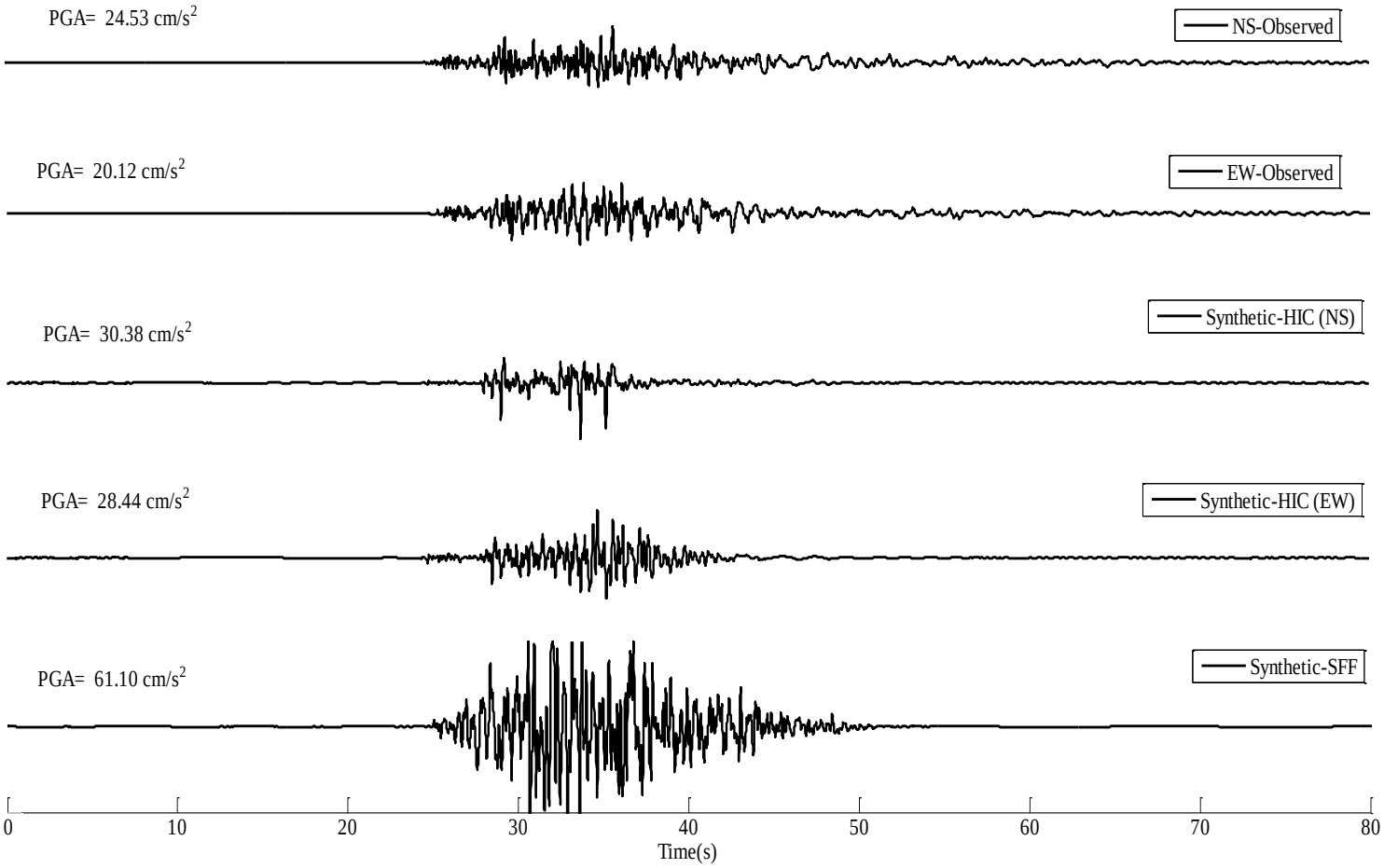
PGA= 24.53 cm/s2
NS-Observed
PGA= 20.12 cm/s2
EW-Observed
PGA= 30.38 cm/s2
Synthetic-HIC (NS)
PGA= 28.44 cm/s2
Synthetic-HIC (EW)
PGA= 61.10 cm/s2
Synthetic-SFF
0
10
20
30
40
50
60
70
80
Time(s)

# Station GSA

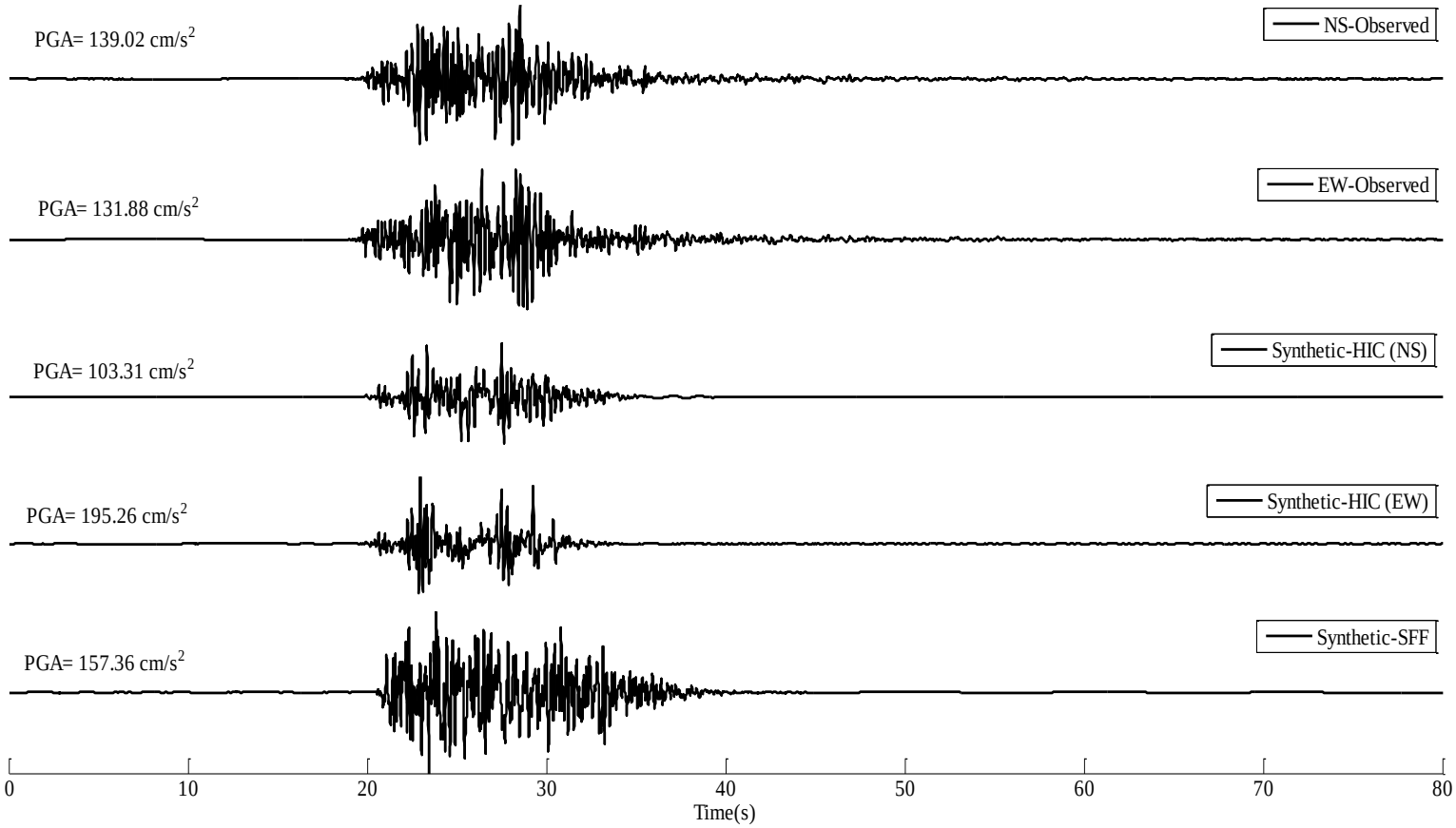
PGA= 139.02 cm/s2
NS-Observed
PGA= 131.88 cm/s2
EW-Observed
PGA= 103.31 cm/s2
Synthetic-HIC (NS)
PGA= 195.26 cm/s2
Synthetic-HIC (EW)
PGA= 157.36 cm/s2
Synthetic-SFF
0
10
20
30
40
50
60
70
80
Time(s)

# Station LSS

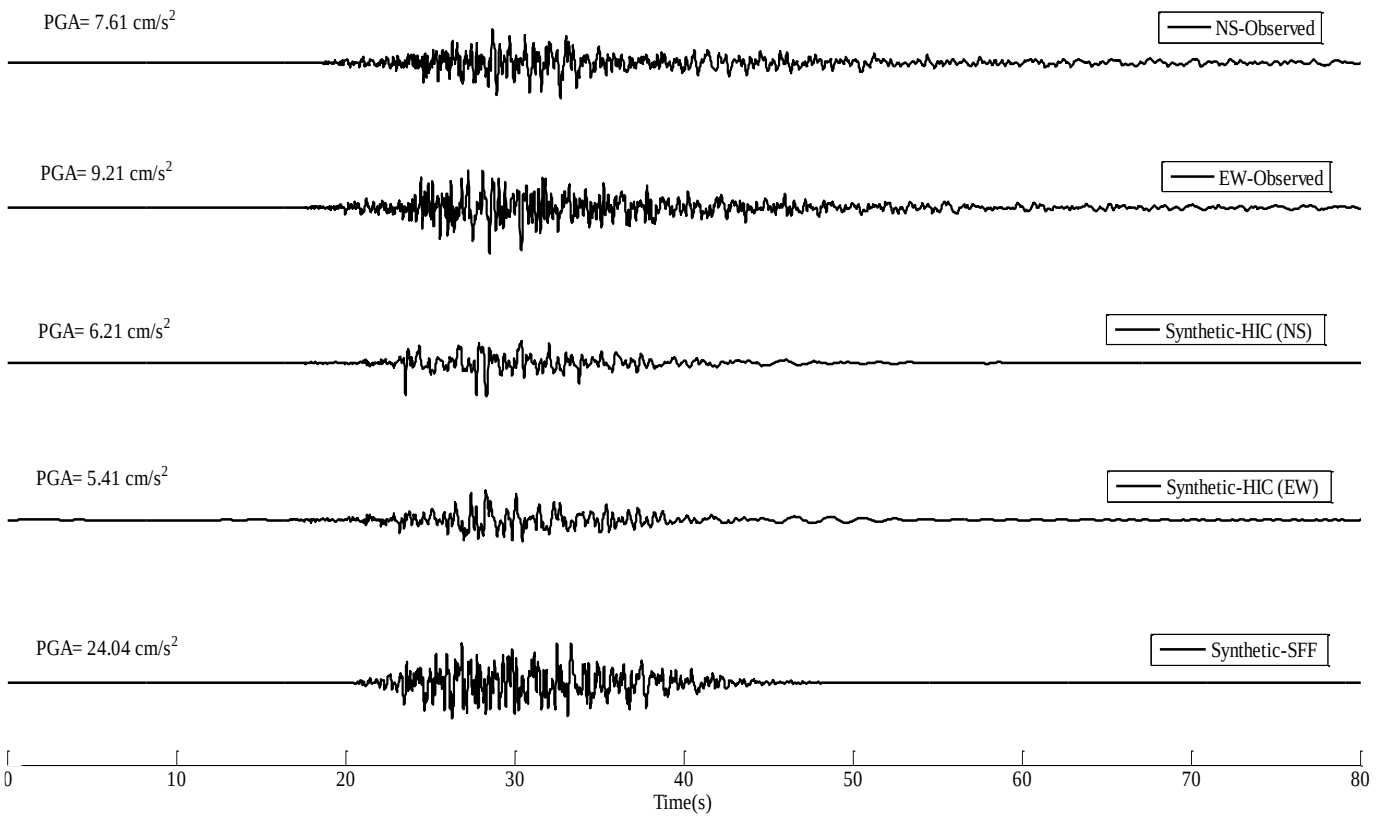
PGA= 7.61 cm/s2
NS-Observed
PGA= 9.21 cm/s2
EW-Observed
PGA= 6.21 cm/s2
Synthetic-HIC (NS)
PGA= 5.41 cm/s2
Synthetic-HIC (EW)
PGA= 24.04 cm/s2
Synthetic-SFF
0
10
20
30
40
50
60
70
80
Time(s)

# Station MTR

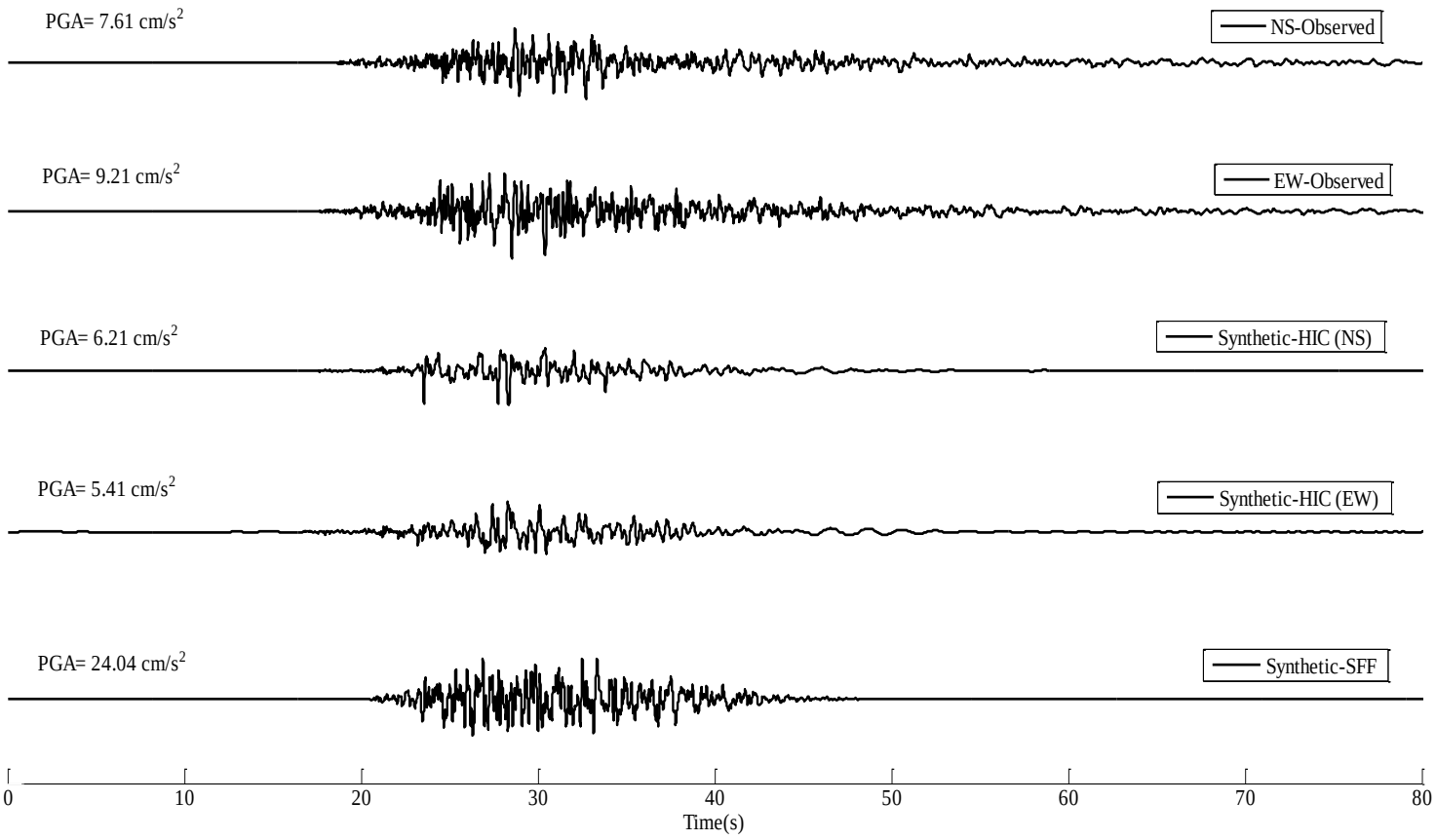
PGA= 7.61 cm/s2
NS-Observed
PGA= 9.21 cm/s2
EW-Observed
PGA= 6.21 cm/s2
Synthetic-HIC (NS)
PGA= 5.41 cm/s2
Synthetic-HIC (EW)
PGA= 24.04 cm/s2
Synthetic-SFF
0
10
20
30
40
50
60
70
80
Time(s)

# Station SUL

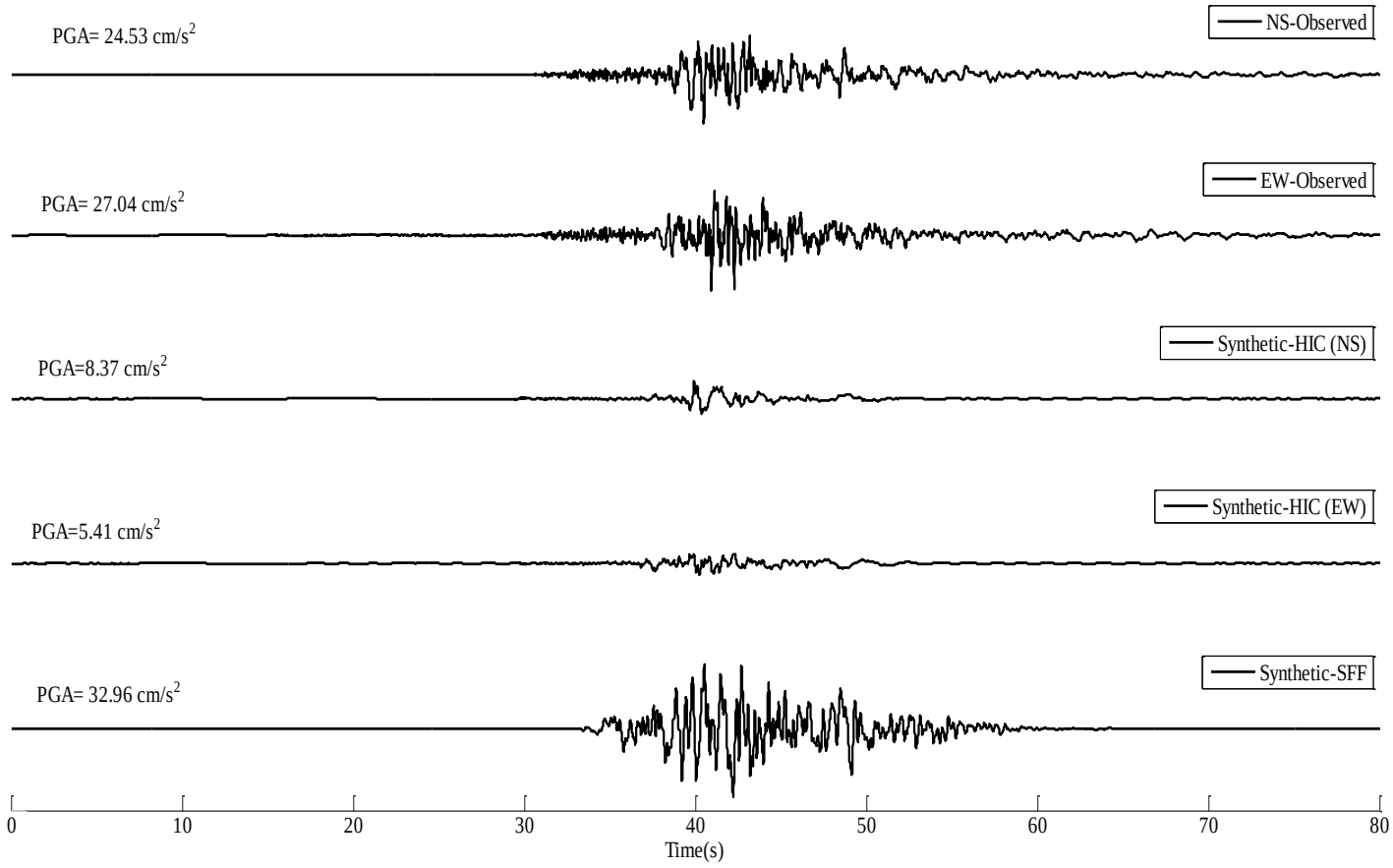
PGA= 24.53 cm/s2
NS-Observed
PGA= 27.04 cm/s2
EW-Observed
PGA=8.37 cm/s2
Synthetic-HIC (NS)
PGA=5.41 cm/s2
Synthetic-HIC (EW)
PGA= 32.96 cm/s2
Synthetic-SFF
0
10
20
30
40
50
60
70
80
Time(s)

# Comparison of observed vs. simulated GMs (FAS)

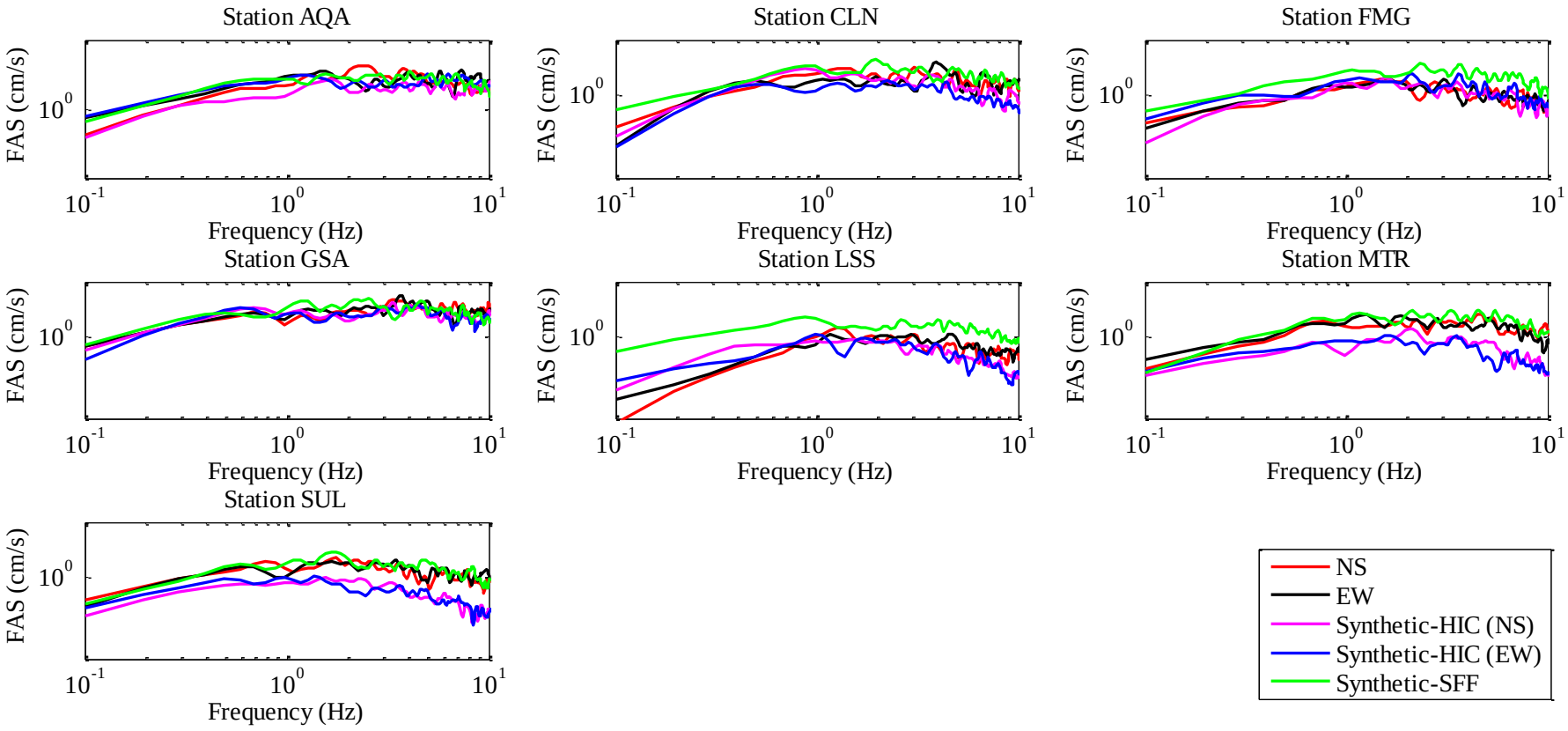

# Comparison of observed vs. simulated GMs (FAS)

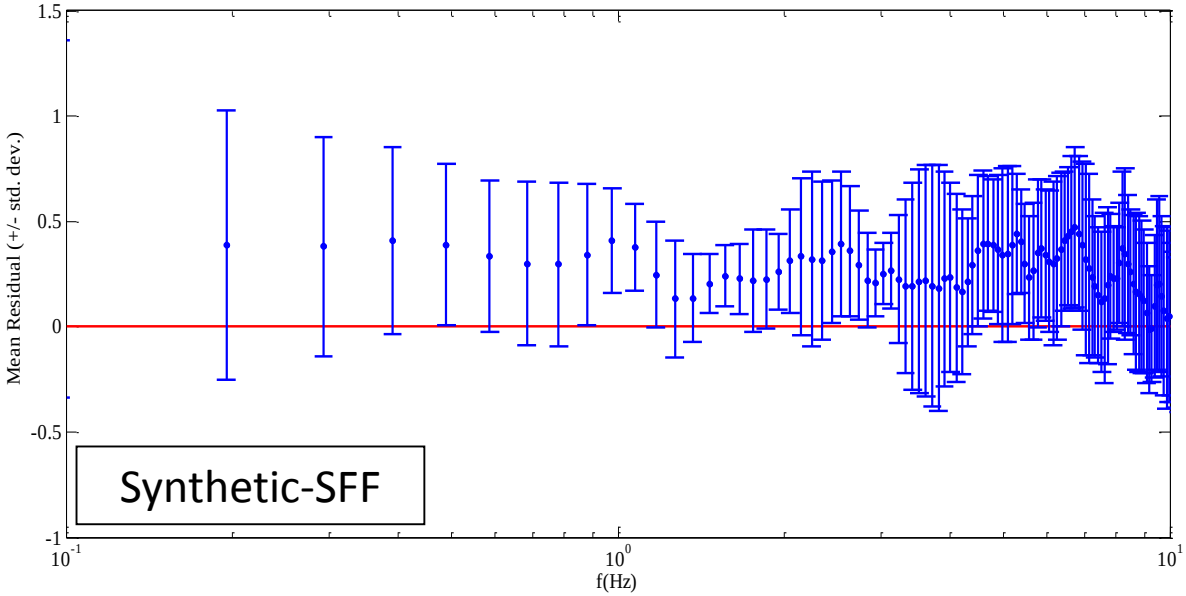


$$\text{Residual} = \log \frac{\text{FAS}_{\text{syn}}}{\text{FAS}_{\text{obs}}}$$

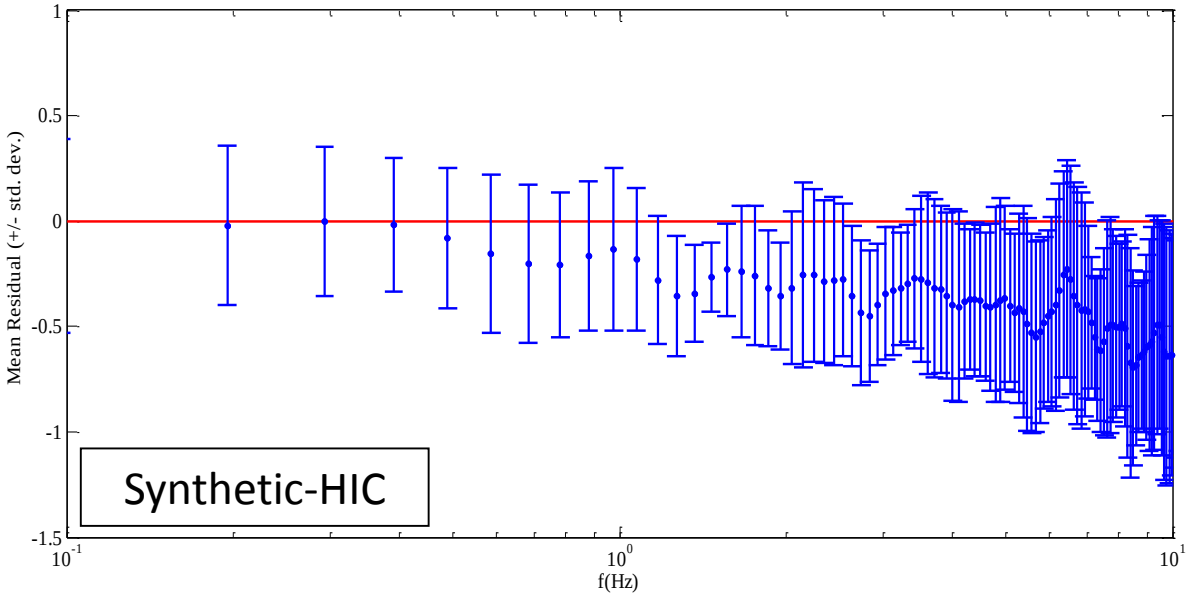

# Comparison of observed vs. simulated GMs (SDOF RS)

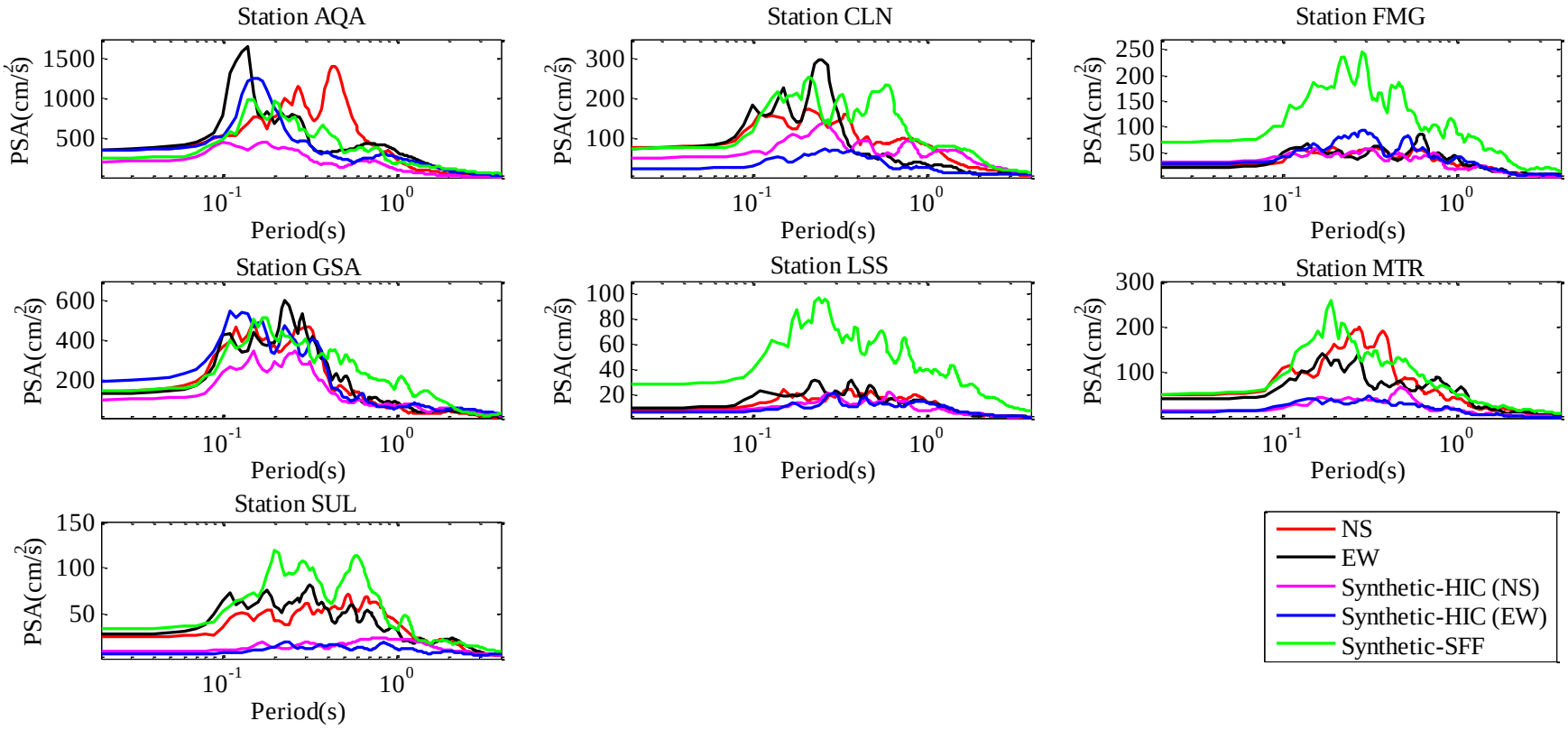

# Comparison of observed vs. simulated GMs (SDOF RS)

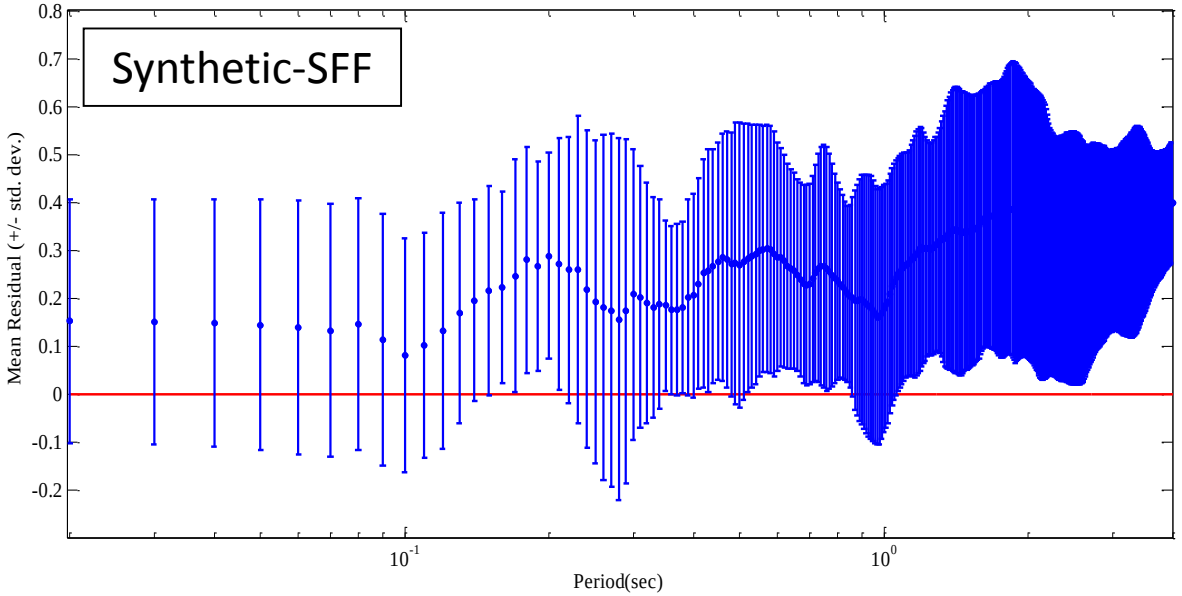


$$\text{Residual} = \log \frac{\text{RS}_{\text{syn}}}{\text{RS}_{\text{obs}}}$$

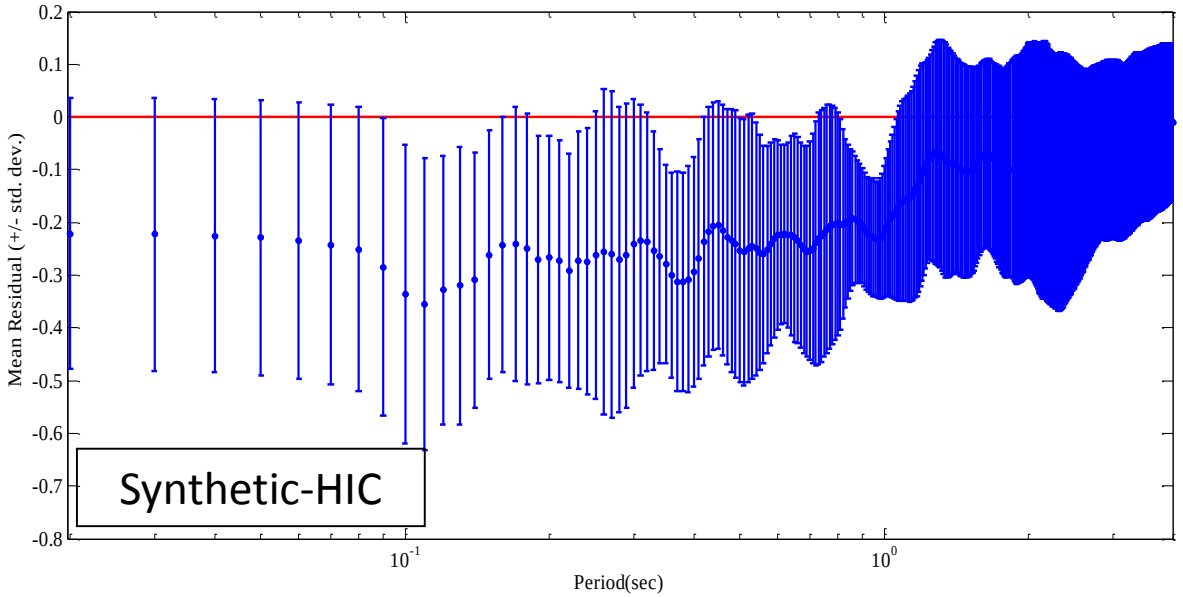

# Distribution of maximum story displacements due to the real and simulated records– F2-3S2B

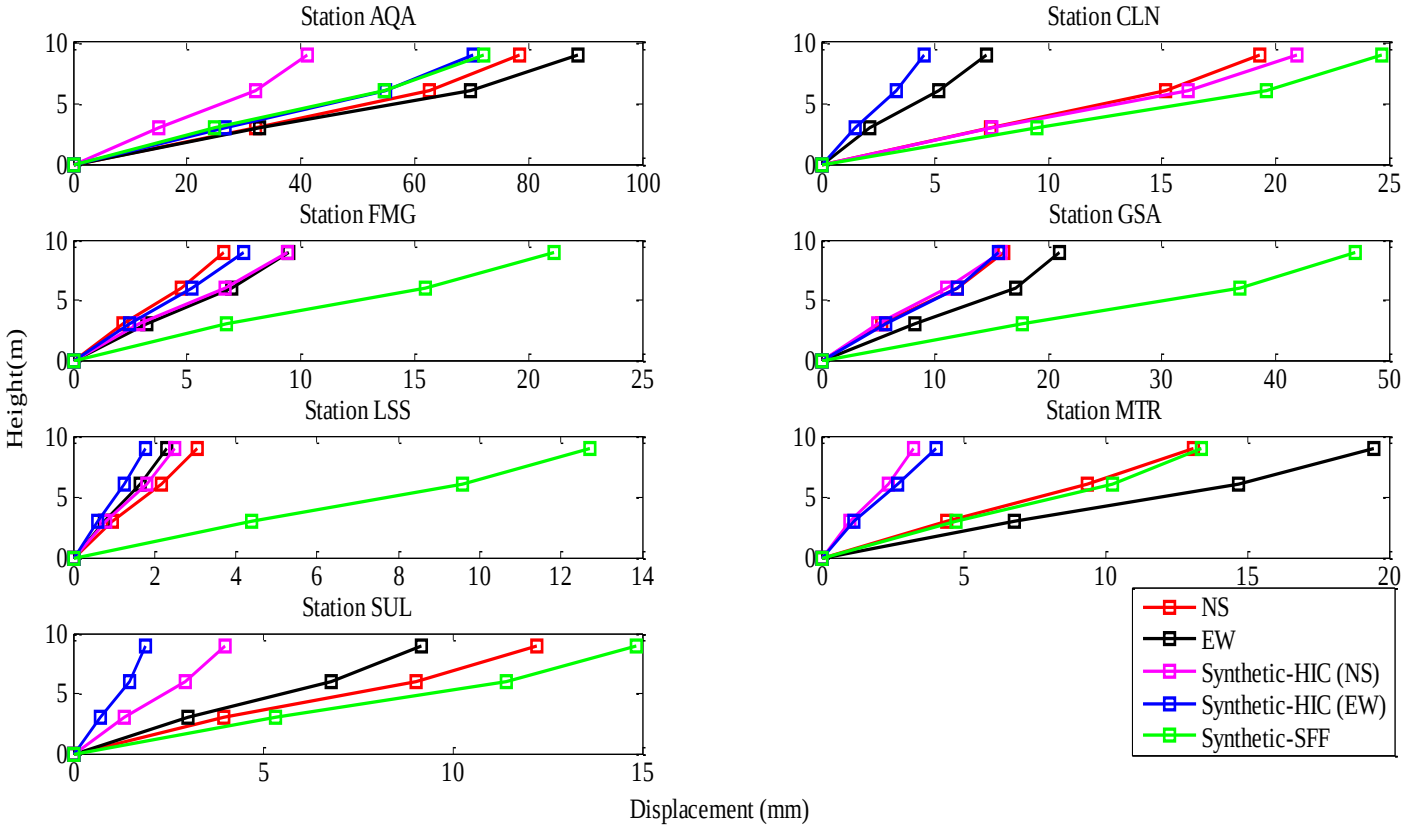


| Station | Real (mm) | $NR(roof)_{Synthetic\text{-}HIC}$ / $NR(roof)_{obs}$ | $NR(roof)_{Synthetic\text{-}SFF}$ / $NR(roof)_{obs}$ |
|---|---|---|---|
| AQA | 83.4356 | 0.6445 | 0.8636 |
| CLN | 11.8399 | 0.8217 | 2.0833 |
| FMG | 7.9211 | 1.0598 | 2.6653 |
| GSA | 18.3664 | 0.8525 | 2.5587 |
| LSS | 2.6454 | 0.7984 | 4.7990 |
| MTR | 15.9715 | 0.2278 | 0.8396 |
| SUL | 10.5884 | 0.2607 | 1.4028 |

# Distribution of maximum story displacements due to the real and simulated records– F6-5S2B

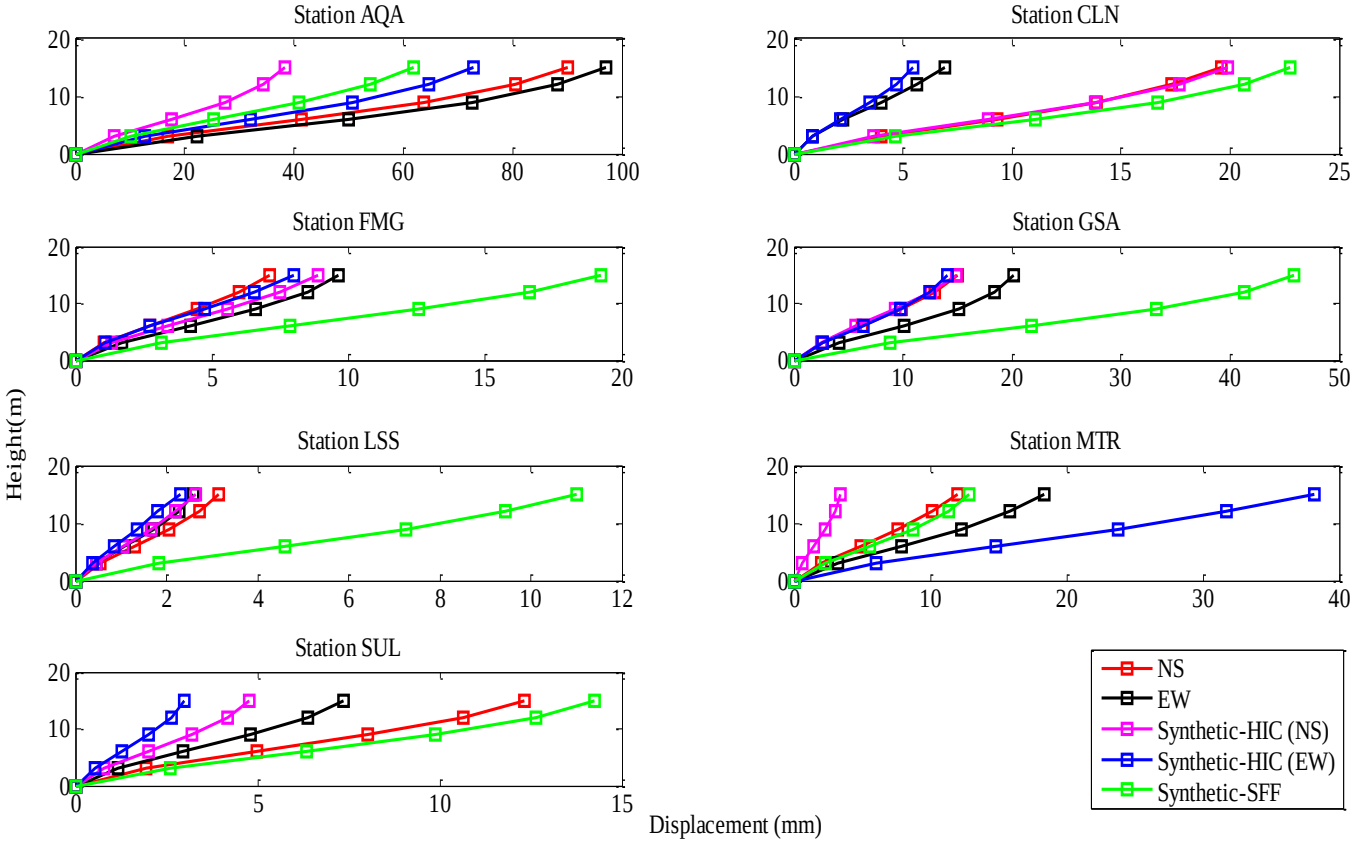


| Station | Real (mm) | $NR(roof)_{Synthetic\text{-}HIC} / NR(roof)_{obs}$ | $NR(roof)_{Synthetic\text{-}SFF} / NR(roof)_{obs}$ |
|---|---|---|---|
| AQA | 93.3877 | 0.5647 | 0.6599 |
| CLN | 11.7848 | 0.8747 | 1.9194 |
| FMG | 8.3229 | 1.0271 | 2.2956 |
| GSA | 17.0733 | 0.8500 | 2.6733 |
| LSS | 2.8434 | 0.9064 | 3.9042 |
| MTR | 15.0158 | 0.2407 | 0.8564 |
| SUL | 9.4576 | 0.3892 | 1.4966 |

# Distribution of maximum story displacements due to the real and simulated records– F9-8S3B

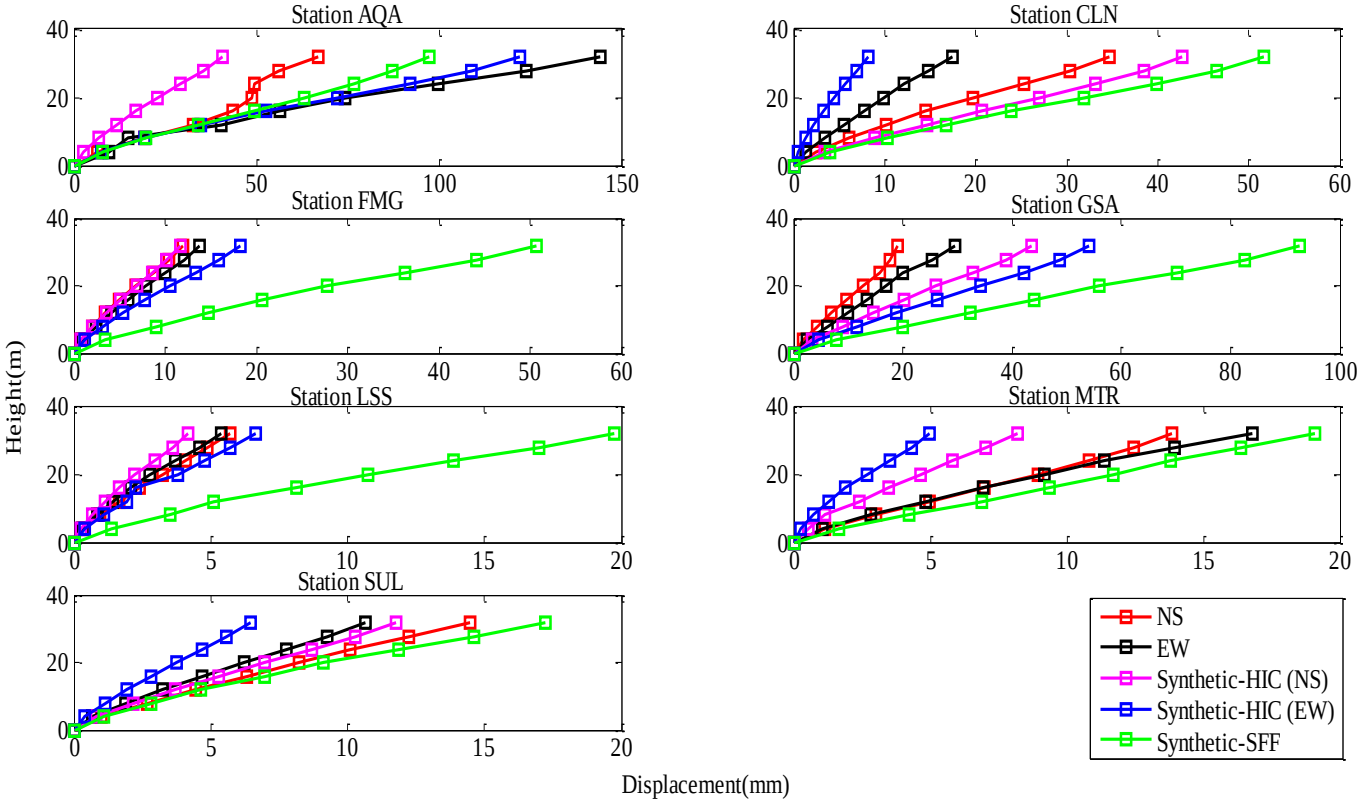


| Station | Real (mm) | $NR(roof)_{Synthetic\text{-}HIC}$ / $NR(roof)_{obs}$ | $NR(roof)_{Synthetic\text{-}SFF}$ / $NR(roof)_{obs}$ |
|---|---|---|---|
| AQA | 97.0789 | 0.7268 | 1.0035 |
| CLN | 24.5896 | 0.7599 | 2.1033 |
| FMG | 12.8187 | 1.1384 | 3.9559 |
| GSA | 23.6624 | 2.0547 | 3.9163 |
| LSS | 5.5325 | 0.9504 | 3.5644 |
| MTR | 15.2584 | 0.4192 | 1.2518 |
| SUL | 12.4225 | 0.7022 | 1.3886 |

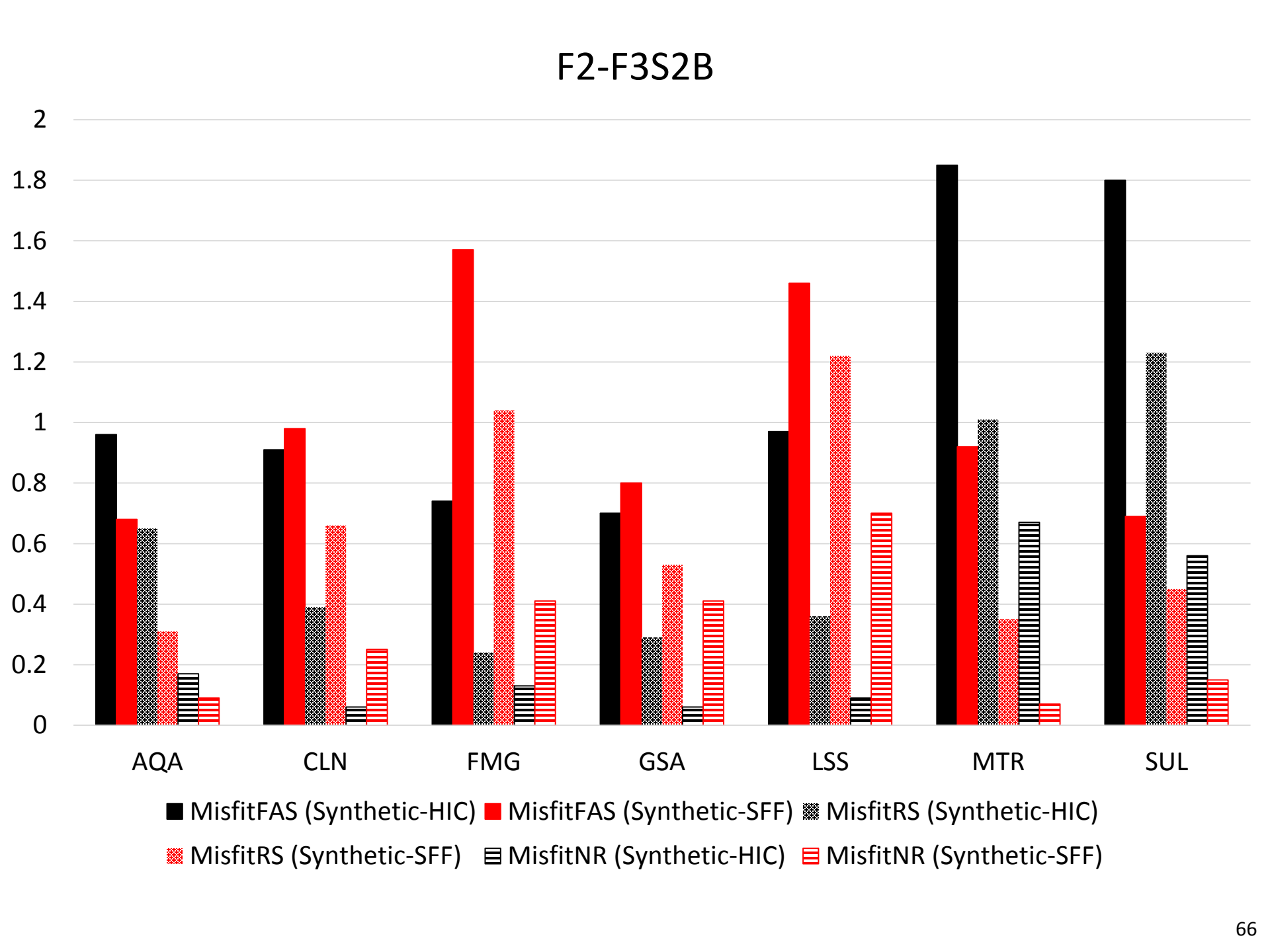
F2-F3S2B
2
1.8
1.6
1.4
1.2
1
0.8
0.6
0.4
0.2
0
AQA
CLN
FMG
GSA
LSS
MTR
SUL
MisfitFAS (Synthetic-HIC)
MisfitFAS (Synthetic-SFF)
MisfitRS (Synthetic-HIC)
MisfitRS (Synthetic-SFF)
MisfitNR (Synthetic-HIC)
MisfitNR (Synthetic-SFF)

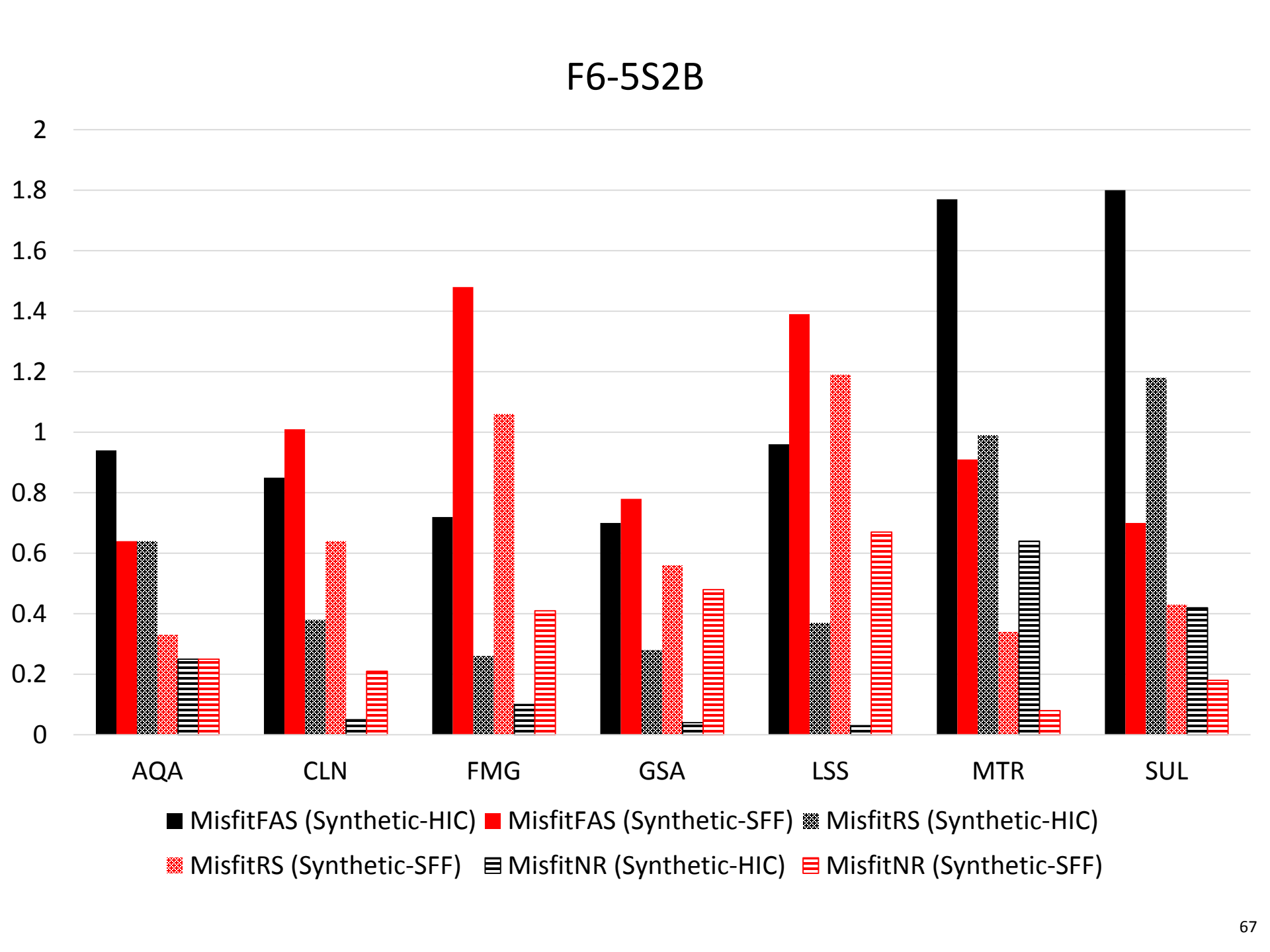
F6-5S2B
2
1.8
1.6
1.4
1.2
1
0.8
0.6
0.4
0.2
0
AQA
CLN
FMG
GSA
LSS
MTR
SUL
MisfitFAS (Synthetic-HIC)
MisfitFAS (Synthetic-SFF)
MisfitRS (Synthetic-HIC)
MisfitRS (Synthetic-SFF)
MisfitNR (Synthetic-HIC)
MisfitNR (Synthetic-SFF)

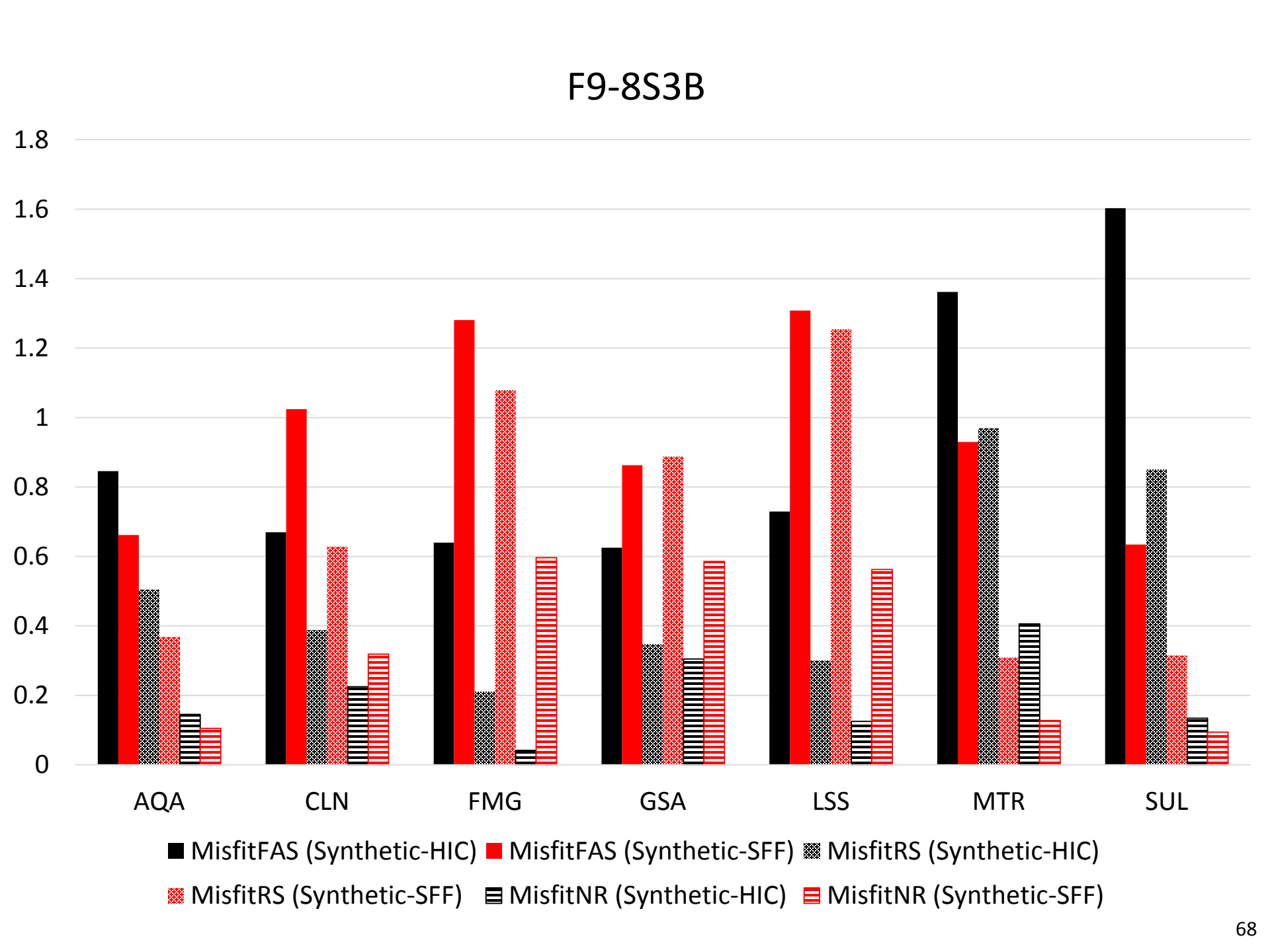
F9-8S3B
1.8
1.6
1.4
1.2
1
0.8
0.6
0.4
0.2
0
AQA
CLN
FMG
GSA
LSS
MTR
SUL
MisfitFAS (Synthetic-HIC)
MisfitFAS (Synthetic-SFF)
MisfitRS (Synthetic-HIC)
MisfitRS (Synthetic-SFF)
MisfitNR (Synthetic-HIC)
MisfitNR (Synthetic-SFF)

# Main findings of NLTHA of MDOF structures

- For Duzce, which is located on a shallow alluvial basin, simulated records are found to be efficient to predict the real MDOF responses.

- For L'Aquila mostly located on rock or stiff soil conditions:

1. Stochastic finite-fault model yields more conservative results.
2. Hybrid-integral-composite method mostly provides accurate results as it covers the broadband frequency range. However, in some cases underestimation of real responses are observed.

- For both cases, frequency-dependent misfits governed the accuracy of MDOF responses.

- Simulated records that overestimate the nonlinear response could be conservatively used for seismic design and assessment purposes of MDOF structures.

# Part 3:
# Distribution of seismic intensity maps (MMI) for the eastern part of the NAFZ (Turkey) using simulated records

# OBJECTIVE

MMI distributions of potential scenario events are studied on the eastern segments of NAFZ through ground motion simulations.

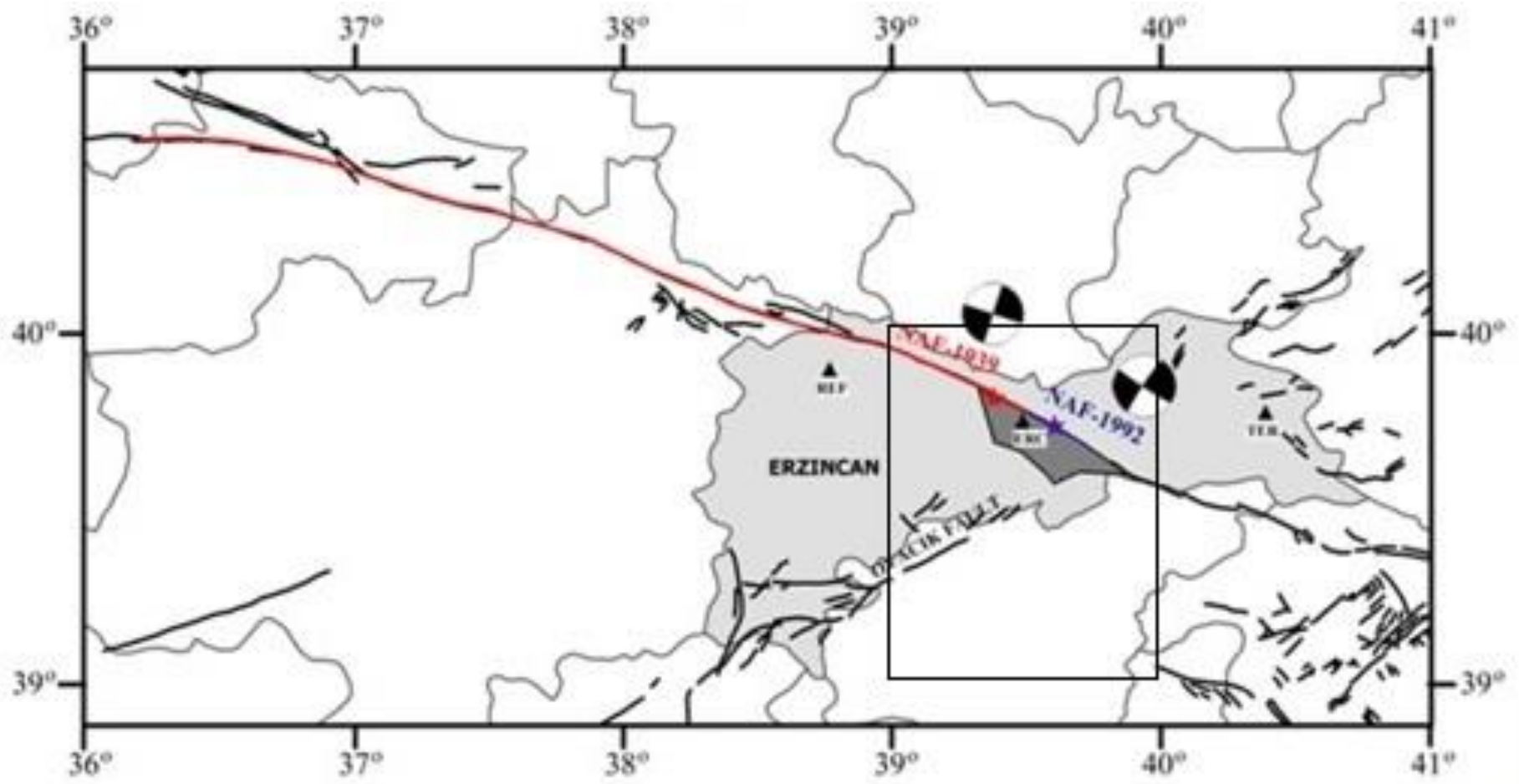


Askan, Karimzadeh and Bilal (2017), Chapter in a Book, AGU Book, Wiley

# Main Steps:

- Simulations along Eastern segments of NAFZ
- Relationships between peak ground motion parameters and felt intensity values
- Applications in the study region
- Conclusions

**Spatial distribution of the simulated (a) PGA, (b) PGV values of the 1992 Erzincan earthquake in Erzincan region. The rectangle shows the Erzincan city center.**

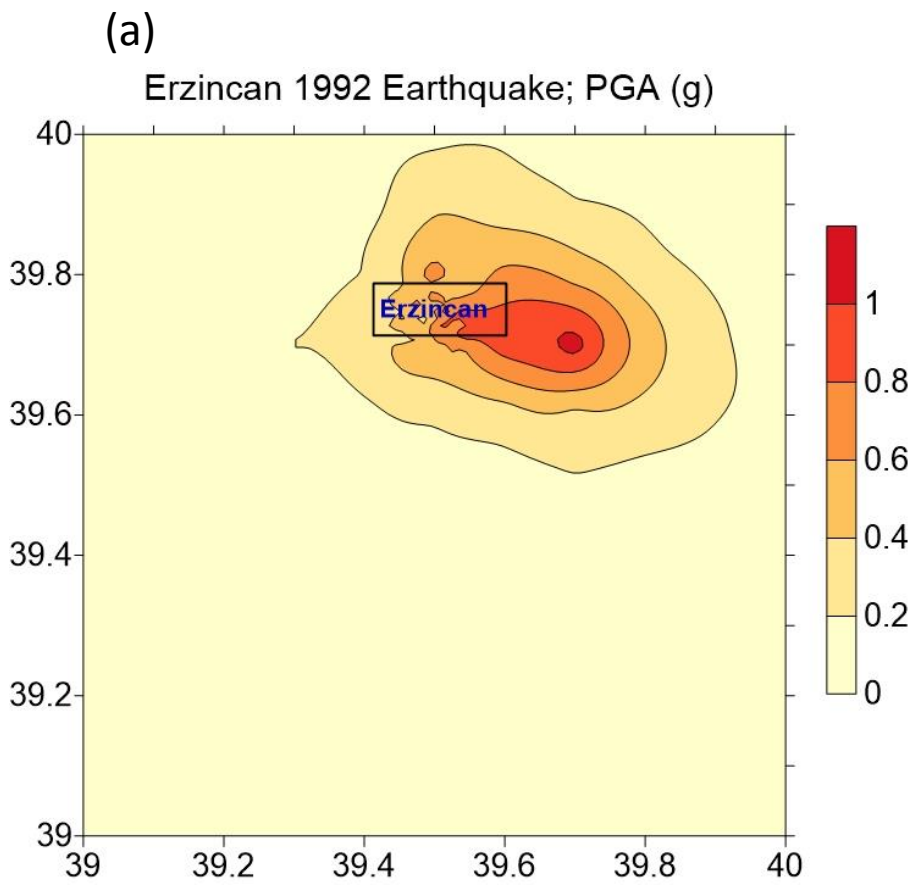


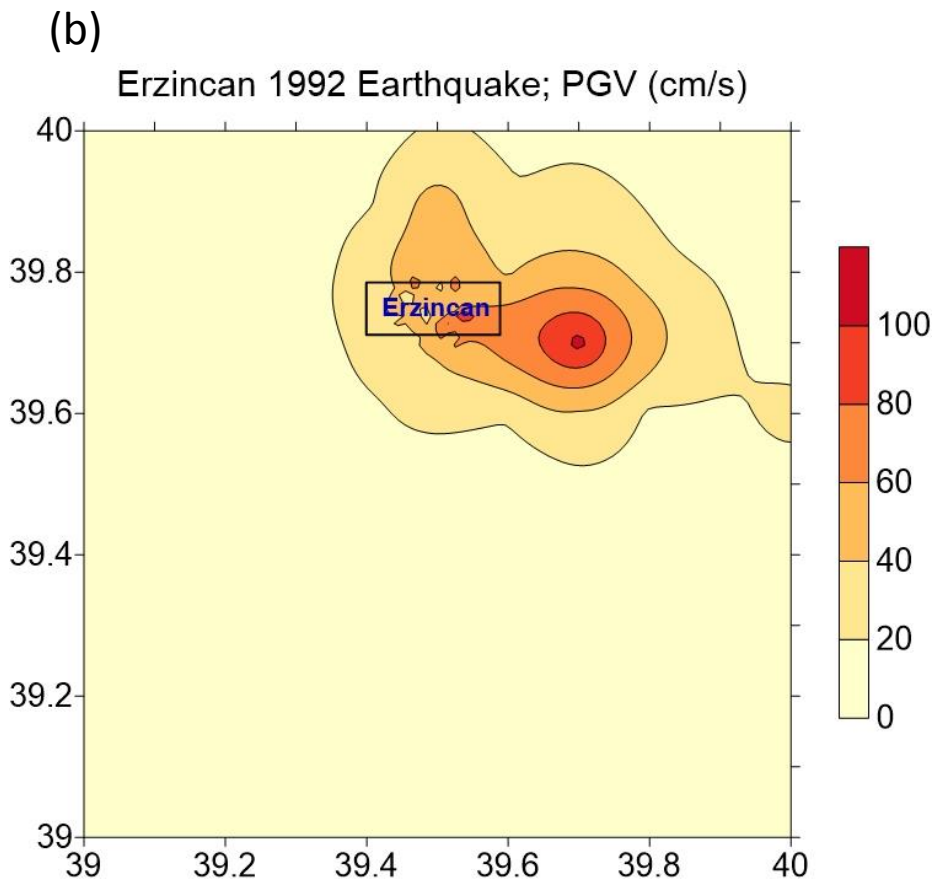

**Spatial distribution of the simulated (a) PGA, (b) PGV values of the scenario event Mw=7.0 in Erzincan region. The rectangle shows the Erzincan city center.**

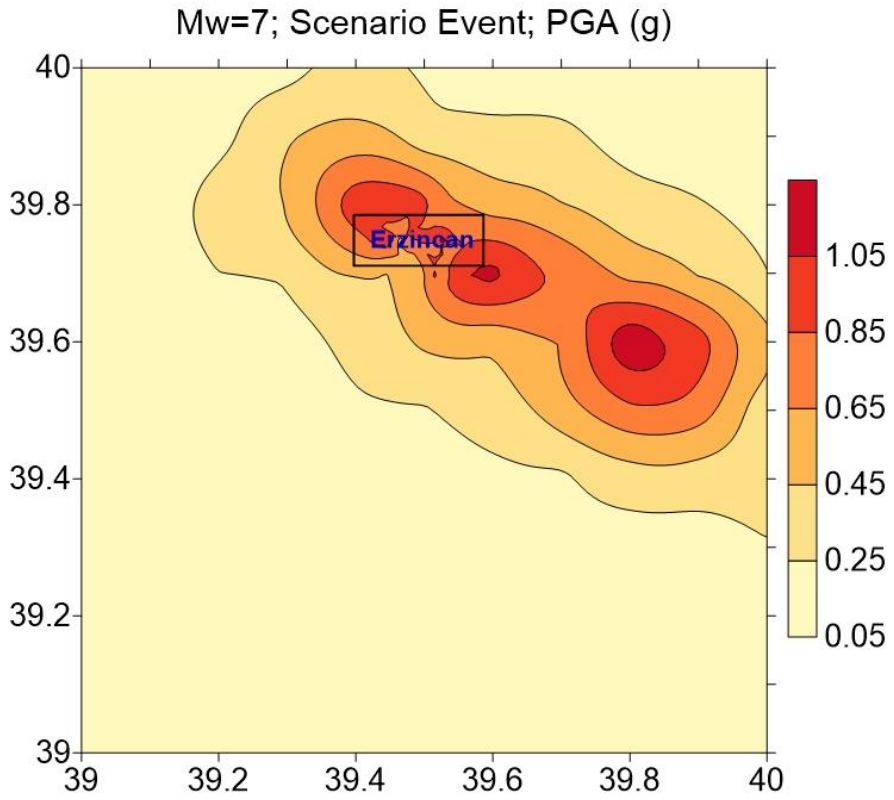


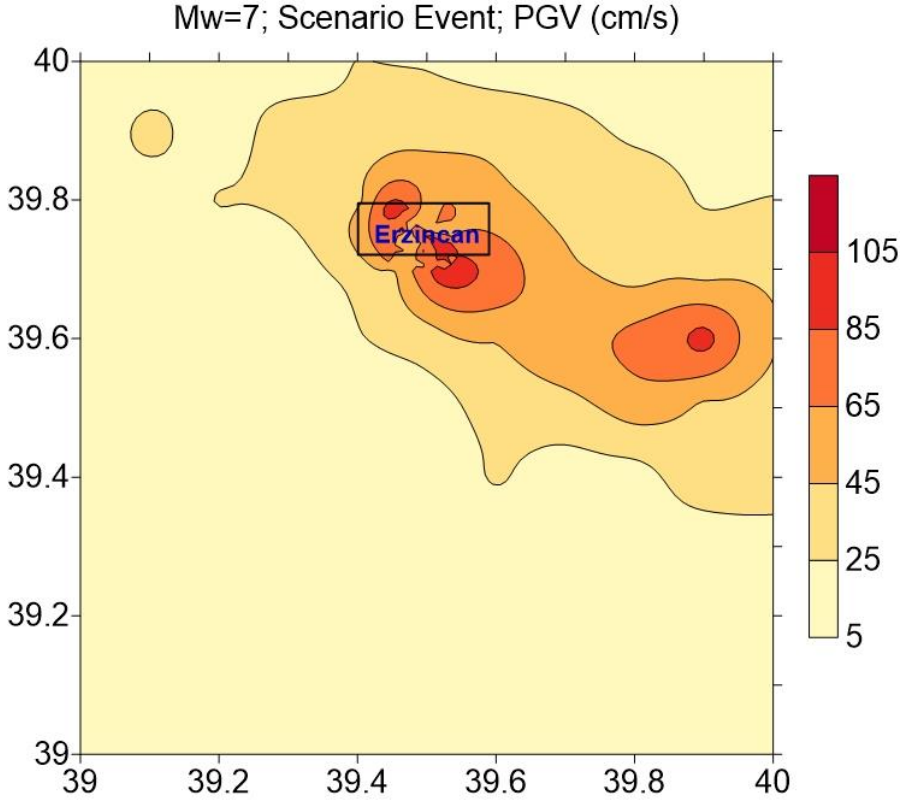

# Relationships between peak ground motion parameters and felt intensity values

- To assess the spatial distribution of potential seismic damage:

Using the local correlations of Bilal and Askan, (2014)

- Correlations between: measured ground motion parameters (PGA and PGV) and felt intensity values in terms of modified Mercalli (MMI) scale

$$MMI = 0.132 + 3.884 \log(PGA)$$

$$MMI = 2.673 + 4.340 \log(PGV)$$

**Seismic intensity map of the 1992 Erzincan earthquake in terms of MMI scale in Erzincan region using (a) the MMI-PGA correlation, the MMI-PGV correlation, (c) prepared by the USGS ShakeMap software, (d) prepared in the field by Turkish Ministry of Construction**

(a)

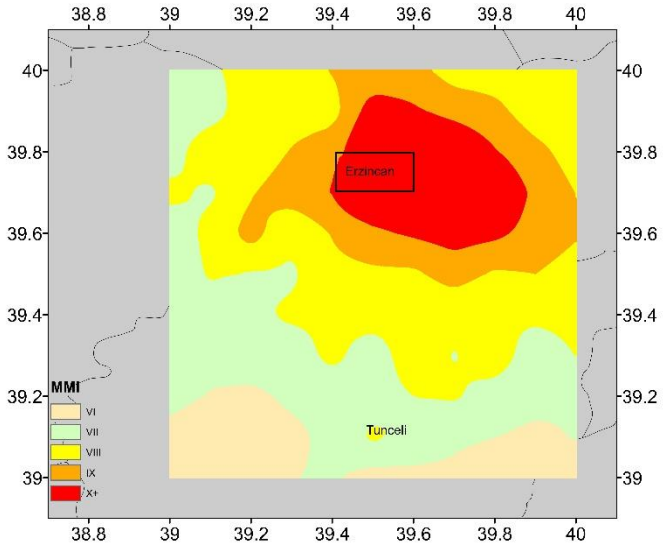


(b)

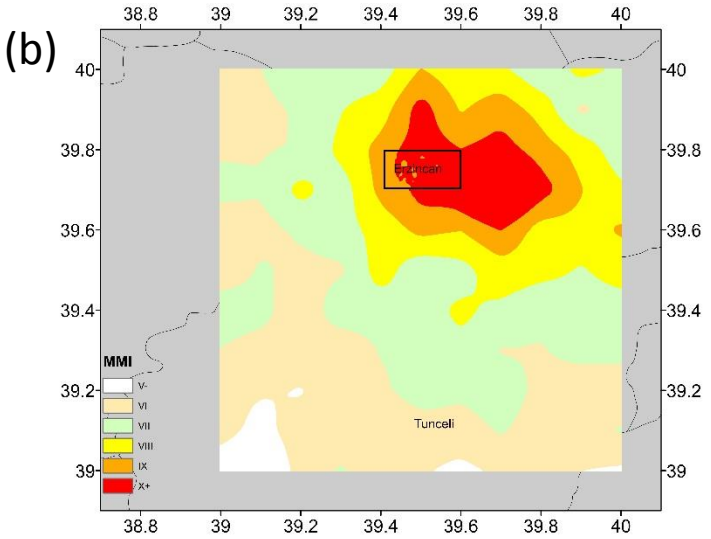


(c)

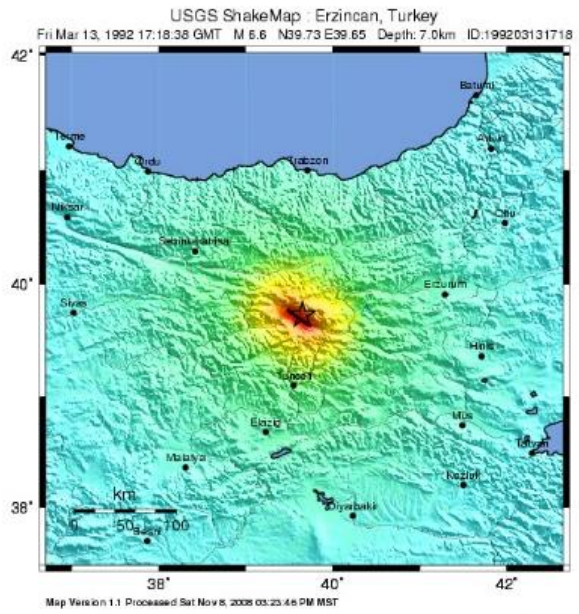


(d)

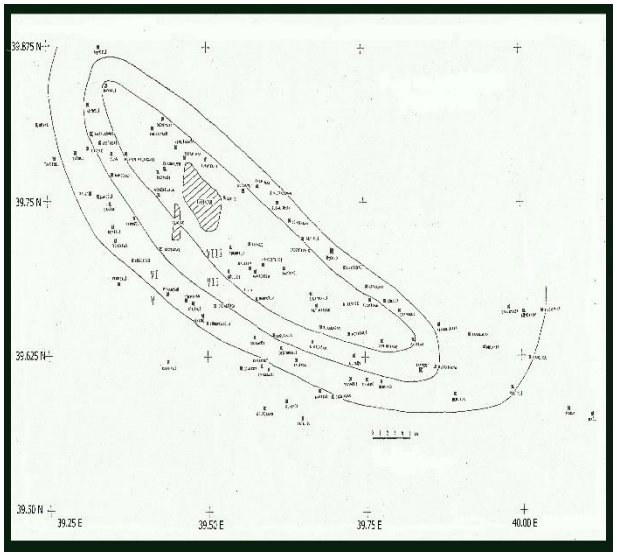

**Synthetic intensity map of the scenario event with Mw=7.0 in terms of MMI scale in Erzincan region using (a) PGA-MMI (b) PGV-MMI. The rectangle shows the Erzincan city center.**

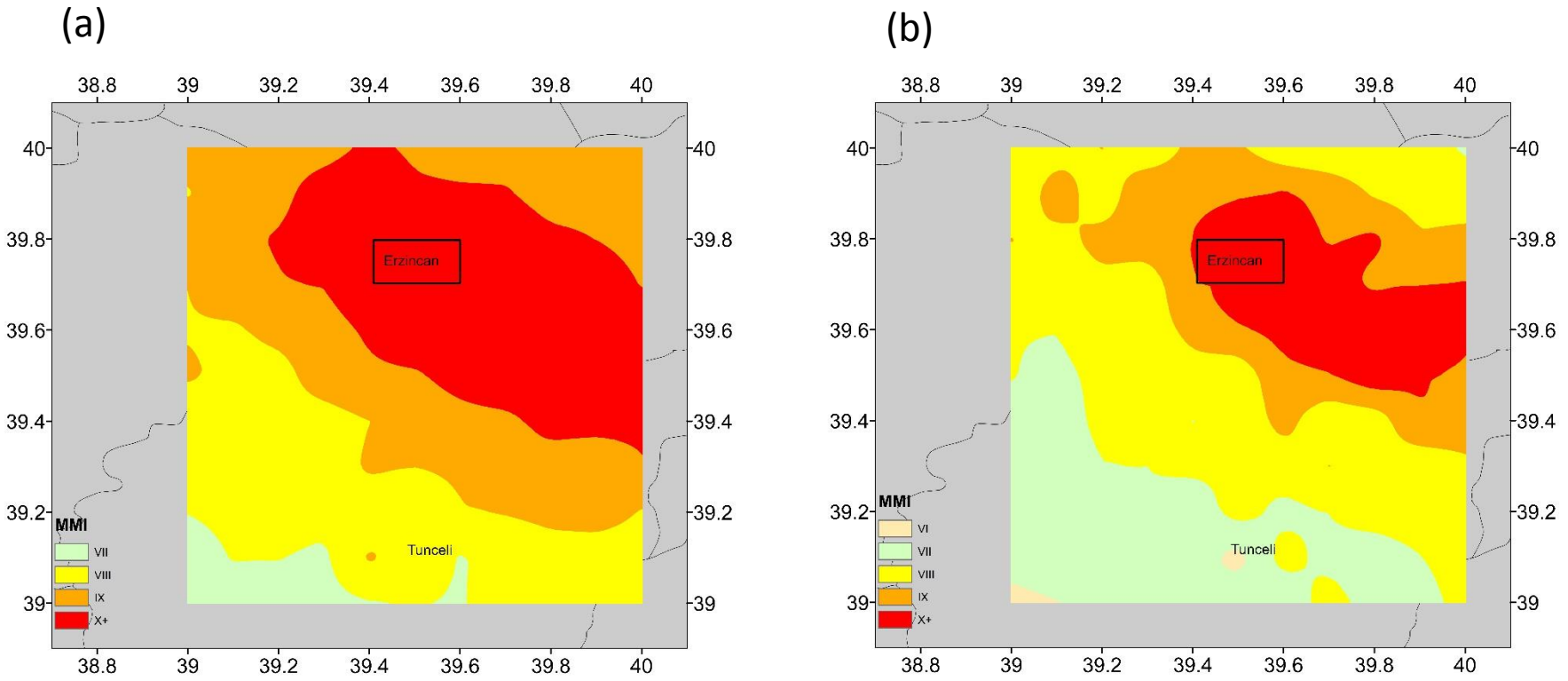

# Contributions, conclusions and future work

# Summary and What is next:

- When a poor fit is obtained from a seismological point of view, a similar outcome is observed from the engineering point of view.
- Simulated motions need to be carefully assessed for their frequency, amplitude, and energy content before practical and common use in earthquake engineering.
- It is important to simulate realistic amplitudes over the entire broadband frequency range of interest for earthquake engineering purposes in order to cover all types of structures with a range of fundamental periods.

- The accuracy of input parameters (fault models, source-time functions, and velocity models) for GM simulation can be increased.

- To simulate lower frequency content, hybrid methods that require complex source and wave velocity models are necessary.

- More investigations can be performed on the behavior of other structural types such as bridges, tanks, tall buildings, based isolated structures.

- Use of simulated motions in different aspects of the earthquake problem such as evacuation, casualty estimation, insurance premium calculations.

# References:


- Ameri, G., Gallovič, F., and Pacor, F., (2012), JOURNAL OF GEOPHYSICAL RESEARCH, VOL. 117, BXXXXX, doi:10.1029/2011JB008729.
- Askan, A. and Yucemen, M.S. (2010). Probabilistic methods for the estimation of potential seismic damage: Application to reinforced concrete buildings in Turkey. Structural Safety 32:4, 262-271.
- Askan, A., Sisman, F., and Ugurhan, B., (2013), Stochastic strong ground motion simulations in sparsely-monitored regions: A validation and sensitivity study on the 13 March 1992 Erzincan (Turkey) earthquake, Soil Dynamics and Earthquake Engineering 55 170–181.
- Erberik, M.A. (2008,a). Generation of fragility curves for Turkish masonry buildings considering in-plane failure modes. Earthquake Engineering & Structural Dynamics 37:3, 387-405.
- Erberik, M.A. (2008,b). Fragility-based assessment of typical mid-rise and low-rise RC buildings in Turkey. Engineering Structures 30:5, 1360-1374.
- Erdik, M., Yüzügüllü, O., Karakoc, Yilmaz, C.and Akkas, N. (1994). March 13, 1992 Erzincan (Turkey) earthquake, Earthquake Engineering, Tenth World Conference, Balkema, Rotterdam.
- Gürpinar, A., Abali, M., Yücemen, M. S. & Yesilcay, Y. (1978). Feasibility of Obligatory Earthquake Insurance in Turkey. Earthquake Engineering Research Center, Civil Engineering Department, Middle East Technical University, Report No. 78-05, Ankara (in Turkish).
- Ibarra, L.F., Medina, R.A. and Krawinkler, H. (2005). Hysteretic models that incorporate strength and stiffness deterioration. Earthquake Engineering and Structural Dynamics 34, 1489–1511.
- Kadaş, K., Influence of Idealized Pushover Curves on Seismic Response, (Sep. 2006), MS Theses.
- Motazedian, D. and Atkinson G.M. (2005). Stochastic finite-fault modeling based on a dynamic corner frequency. Bulletin of Seismological Society of America 95, 995–1010.
- Sucuoğlu H. and Tokyay M. (1992). 13 Mart 1992 Erzincan earthquake engineering report, civil engineering department, Ankara, pp: 102.
- Şengezer, B.S. (1993). The Damage Distribution during March 13, 1992 Erzincan Earthquake, proceedings, 2nd National Earthquake Engineering Conference, pp: 404-415.
- Ugurhan, B., Askan, A., (2010), Stochastic Strong Ground Motion Simulation of the 12 November 1999 Düzce (Turkey) Earthquake Using a Dynamic Corner Frequency Approach, Bull. Seism. Soc. Am. 100, 1498-1512.
- Ugurhan, B., Askan A., Akinci, A., and Malagnini, L., (2012), Strong-Ground-Motion Simulation of the 6 April 2009 L'Aquila, Italy, Earthquake, Bull. Seismol. Soc. Am 102 (4), 1429–1445.
- Yılmaz, H., (2007), I Correlation of Deformation Demands with Ground Motion Intensity, MS Theses.
- http://opensees.berkeley.edu/OpenSees/copyright.php

# Homework

Prepare a total of 1-page summary on:

a. Description of alternative ground motion simulation techniques. (Provide a brief explanation on the type of input parameters required for each method)
b. What are the limitations corresponding to alternative ground motion simulation techniques?
c. As an engineer for design of a tall building with a fundamental period of 3 seconds, which type of simulation technique do you offer to perform time history analysis? Why?

# Contact

Shaghayegh Karimzadeh

Middle East Technical University (METU)

shaghkn@gmail.com